UNIVERSITY OF COPENHAGEN
FACULTY OF SCIENCE

Master's Thesis

Cecilie Hermansen

Photon Absorption in Josephson Junctions

A linear response study

Supervisor: Jens Paaske

Handed in: March 27, 2021

Abstract

Subgap states in Josephson junctions have been proposed as qubit candidates because they form closed energy subspaces with distinct transition frequencies and are hence currently of great interest to the scientific community. Probing these states and inducing transitions between them requires knowledge of the photon absorption properties of the Josephson junctions, which is what we study in this thesis. Using the Green's function method, the linear response of the system to a harmonic voltage bias is calculated. This procedure reveals a result for the real part of the admittance which is related to the absorption rate of the junction. The different contributions to the admittance can be ascribed to excitation processes involving the creation of quasiparticles in the subgap states. We initially perform this calculation for the simple case of a QPC, and then move on to consider the more complicated Anderson model where approximations must be introduced to make the problem solvable. Firstly we consider the limit of $U \gg \Delta$ in the classical spin approximation. Here we derive the Green's functions for the system and obtain the YSR bound states. Calculating the admittance reveals a discrete absorption peak arising from the creation of two quasiparticles in the bound states which vanishes at the phase transition to a ground state where the impurity spin is no longer screened by a quasiparticle. The problem is also treated using perturbation theory in the scattering formalism, which provides a way of understanding the underlying reason for the constraints on the properties of quasiparticles created in absorption processes. To investigate whether the results for the classical spin approximation are also valid outside of this regime we proceed by studying the Anderson model in other limits; firstly we consider the noninteracting limit $U = 0$ with a magnetic field and subsequently the limit of infinite gap $\Delta \to \infty$. In both cases we regain the result from the classical spin approximation, and furthermore these approaches turn out to be useful for providing a more straightforward physical interpretation of the singlet and doublet states of the Anderson model and the absorption processes leading to transitions between them.

Acknowledgements

First and foremost I would like to express my gratitude towards Jens Paaske for his unceasing patience and interest in this project. Our many discussions have been extremely valuable and enjoyable as well - they taught me a lot of physics, have been a great source of inspiration and importantly never failed to spark my motivation. I am also thankful for the help I have received from Gorm Steffensen - his willingness to spend time discussing my project and patiently explain to me parts of his own research has improved my understanding of important topics. Lastly I would like to thank Amira, Anne, Asla, Bettina, Emilie, Freja, Louise, Rebekka and Silja for having entered my life during the course of this education. Studying with you has been absolutely great and has also improved my learning outcome of the many courses I have taken together with some or all of you.

Contents

List of Figures

Chapter 1

Introduction

When a Josephson junction is subject to a constant phase bias, Andreev bound states form at subgap energies. These states are receiving significant interest from the scientific community, not least because they have been proposed as platforms for quantum computation. This is due to the fact that Josephson junctions are nonlinear inductors where the bound states forms closed subspaces with distinct transition energies which can be manipulated coherently. An example is the transmon qubit exploiting the Andreev bound states in a superconducting quantum point contact (QPC) which is operated by inducing transitions between the states of even parity [1]. More complicated types of Josephson junctions such as the S-QD-S junction where tunneling between the leads happens across a quantum dot exhibit even richer non-degenerate subgap spectra. In order to gain knowledge about the properties of these subgap states and learn how they can be manipulated, it is necessary to investigate the ability of Josephson junctions to absorb microwave radiation when they are embedded in electrical circuits. Hence this thesis investigates the photon absorption properties of Josephson junctions with and without magnetic interactions. Our ultimate goal is to account for the absorption which is related to creation of quasiparticles in the spin-split YSR subgap states predicted by Yu, Shiba and Rusinov to exist in the presence of a magnetic impurity ([2], [3], [4]). To establish the necessary formalism, we start by considering the simpler case of a quantum point contact following the approach used by Kos and co-authors [5]. By means of a linear response calculation using the Green's function method, we calculate the real part of the admittance of a QPC subject to a small, time-dependent voltage bias. This quantity is related to the absorption rate of the junction and has distinct frequency-dependent features which can be ascribed to the creation of quasiparticles by photon absorption. The calculation is then repeated for an S-QD-S Josephson junction described by the Anderson model in the limit where the quantum dot is occupied by a single spin, which is assumed to be classical. To aid the physical interpretation of the results from this calculation and compare with the result for different kinds of approximations, we then continue by performing a similar calculation for a Josephson junction where tunneling between the leads happens through a single energy level subject to a magnetic field. We also provide an explanation for the excitation processes

which are possible by photon absorption using scattering theory. Finally, we consider the Anderson model in the limit of $\Delta \to \infty$ where it becomes exactly solvable and a particularly simple calculation reveals the way a change of ground state affects the absorption due to quasiparticle creation in the bound states.

1.1 Superconductivity

In order to understand the basic properties of superconducting systems which will be relevant throughout this thesis and to establish the necessary formalism, in this section we go through some of the most important results of BCS theory and calculate the Green's functions for a homogeneous BCS superconductor.

In a BCS-superconductor, the superconductivity is due to an attractive phonon-mediated interaction in the homogeneous electron gas. The interaction is attractive only for Cooper-pairs which consist of two time-reversed electrons $c^\dagger_{\mathbf{k}\uparrow}$ and $c^\dagger_{-\mathbf{k}\downarrow}$ (in the simplest case of s-wave superconductivity). In momentum-space the Hamiltonian for such a system can be written as

$$H = \sum_{\mathbf{k}\sigma} \xi_{\mathbf{k}} c^\dagger_{\mathbf{k}\sigma} c_{\mathbf{k}\sigma} + \sum_{\mathbf{k}\mathbf{k}'} V_{\mathbf{k}\mathbf{k}'} c^\dagger_{\mathbf{k}\uparrow} c^\dagger_{-\mathbf{k}\downarrow} c_{-\mathbf{k}'\downarrow} c_{\mathbf{k}'\uparrow}. \tag{1.1}$$

It is assumed that the interaction $V_{\mathbf{k}\mathbf{k}'}$ is a constant V for electrons with an energy within an interval of the Debye frequency around the Fermi surface and zero otherwise. To make the problem solvable one then performs a mean-field decoupling of the quartic term. When using the mean-field approximation we assume that the expectation values of the operators which create and annihilate a Cooper pair have a nonzero expectation value $\langle c^\dagger_{\mathbf{k}\uparrow} c^\dagger_{-\mathbf{k}\downarrow} \rangle \neq 0$, and that the fluctuations around the average value are small. This approximation is based on the assumption that in the superconducting ground state many Cooper pairs are present. The mean-field decoupling yields the Hamiltonian

$$H_{MF} = \sum_{\mathbf{k}\sigma} \xi_{\mathbf{k}} c^\dagger_{\mathbf{k}\sigma} c_{\mathbf{k}\sigma} - \sum_{\mathbf{k}} \Delta_{\mathbf{k}} c^\dagger_{\mathbf{k}\uparrow} c^\dagger_{-\mathbf{k}\downarrow} - \sum_{\mathbf{k}} \Delta^*_{\mathbf{k}} c_{-\mathbf{k}\downarrow} c_{\mathbf{k}\uparrow}, \tag{1.2}$$

where the pair-potential $\Delta_{\mathbf{k}} = -\sum_{\mathbf{k}'} V_{\mathbf{k}\mathbf{k}'} \langle c_{-\mathbf{k}'\downarrow} c_{\mathbf{k}'\uparrow} \rangle$ is to be determined self-consistently. $\Delta_{\mathbf{k}}$ is the superconducting order parameter which is nonzero only below the critical temperature T_c. The now bilinear Hamiltonian can easily be diagonalized by means of a Bogoliubov transformation. We will get back to this in chapter 4.

1.1.1 Matsubara Green's functions

In the Green's function formalism, the imaginary time Matsubara Green's functions are very essential, as from these we can obtain retarded and advanced Green's functions by analytic continuation. They will also be used frequently throughout this thesis. Generally the Matsubara Green's function is defined as

$$\mathcal{G}_{AB}(\tau, \tau') = -\langle T_\tau A(\tau) B(\tau') \rangle, \tag{1.3}$$

where T_τ is the time-ordering operator acting as

$$T_\tau A(\tau)B(\tau') = \theta(\tau-\tau')A(\tau)B(\tau') \pm \theta(\tau'-\tau)B(\tau')A(\tau). \tag{1.4}$$

The plus sign is for bosons and the minus is for fermions. We will now consider the Matsubara Green's functions for a homogeneous BCS-superconductor. Due to the expectation value of the Cooper pair operator being nonzero in the superconduting state, we anticipate that there will be anomalous Green's functions which are not always zero in the normal state. Hence we define two types of Green's functions: The normal Matsubara Green's function is defined as

$$\mathcal{G}_{\uparrow\uparrow}(\mathbf{k},\tau) = -\langle T_\tau c_{\mathbf{k}\uparrow}(\tau)c^\dagger_{\mathbf{k}\uparrow}(0)\rangle, \tag{1.5}$$

and the anomalous one is

$$\mathcal{F}_{\downarrow\uparrow}(\mathbf{k},\tau) = -\langle T_\tau c^\dagger_{-\mathbf{k}\downarrow}(\tau)c^\dagger_{\mathbf{k}\uparrow}(0)\rangle, \tag{1.6}$$

The Green's functions can be calculated using the equation of motion-technique. Starting from $\mathcal{G}_{\uparrow\uparrow}(\mathbf{k},\tau)$ we differentiate with respect to τ and use that in imaginary time we have $\partial_\tau A(\tau) = [H,A](\tau)$. We also assume that Δ is independent of $\mathbf{k}$.

$$\begin{aligned}
-\partial_\tau \mathcal{G}_{\uparrow\uparrow}(\mathbf{k},\tau) &= \delta(\tau)\langle\{c_{\mathbf{k}\uparrow}, c^\dagger_{\mathbf{k}\uparrow}\}\rangle \\
&\quad + \Big(\theta(\tau)\langle[H,c_{\mathbf{k}\uparrow}](\tau)c^\dagger_{\mathbf{k}\uparrow}(0)\rangle - \theta(-\tau)\langle c^\dagger_{\mathbf{k}\uparrow}(0)[H,c_{\mathbf{k}\uparrow}](\tau)\rangle\Big) \\
&= \delta(\tau) + \langle T_\tau[H,c_{\mathbf{k}\uparrow}](\tau)c^\dagger_{\mathbf{k}\uparrow}(0)\rangle \\
&= \delta(\tau) - \xi_{\mathbf{k}}\langle T_\tau c_{\mathbf{k}\uparrow}(\tau)c^\dagger_{\mathbf{k}\uparrow}(0)\rangle + \Delta\langle c^\dagger_{-\mathbf{k}\downarrow}(\tau)c^\dagger_{\mathbf{k}\uparrow}(\tau)\rangle \\
&= \delta(\tau) + \xi_{\mathbf{k}}\mathcal{G}_{\uparrow\uparrow}(\mathbf{k},\tau) - \Delta\mathcal{F}_{\downarrow\uparrow}(\mathbf{k},\tau)
\end{aligned} \tag{1.7}$$

From this we see that the normal and anomalous Green's functions are coupled so that we also have to find an equation for $\mathcal{F}_{\downarrow\uparrow}(\mathbf{k},\tau)$. We again take the time derivative

$$-\partial_\tau \mathcal{F}_{\downarrow\uparrow}(\mathbf{k},\tau) = -\xi_{\mathbf{k}}\mathcal{F}_{\downarrow\uparrow}(\mathbf{k},\tau) - \Delta^*\mathcal{G}_{\uparrow\uparrow}(\mathbf{k},\tau). \tag{1.8}$$

Here there is no term arising from the derivative of $\theta(\tau)$ because $\{c^\dagger_{-\mathbf{k}\downarrow}, c^\dagger_{\mathbf{k}\uparrow}\} = 0$. By Fourier transforming eqs. 1.7 and 1.8 we obtain a closed set of algebraic equations which are readily solved

$$\begin{aligned}
(i\omega_l - \xi_{\mathbf{k}})\mathcal{G}_{\uparrow\uparrow}(\mathbf{k},i\omega_l) &= 1 - \Delta\mathcal{F}_{\downarrow\uparrow}(\mathbf{k},i\omega_l) \\
-(i\omega_l + \xi_{\mathbf{k}})\mathcal{F}_{\downarrow\uparrow}(\mathbf{k},i\omega_l) &= \Delta^*\mathcal{G}_{\uparrow\uparrow}(\mathbf{k},i\omega_l).
\end{aligned} \tag{1.9}$$

The solution is

$$\mathcal{G}_{\uparrow\uparrow}(\mathbf{k},i\omega_l) = \frac{\xi_{\mathbf{k}} + i\omega_l}{(i\omega_l)^2 - |\Delta|^2 - \xi^2_{\mathbf{k}}} \tag{1.10}$$

$$\mathcal{F}_{\downarrow\uparrow}(\mathbf{k},i\omega_l) = -\frac{\Delta^*}{(i\omega_l)^2 - |\Delta|^2 - \xi^2_{\mathbf{k}}} \tag{1.11}$$

We will later need the local (**k**-summed) versions of these Green's functions, so we calculate those here:

$$\begin{aligned}\mathcal{G}_{\uparrow\uparrow}(i\omega_l) &= \sum_{\mathbf{k}} \mathcal{G}_{\uparrow\uparrow}(\mathbf{k}, i\omega_l) = \sum_{\mathbf{k}} \frac{\xi_{\mathbf{k}} + i\omega_l}{(i\omega_l)^2 - |\Delta|^2 - \xi_{\mathbf{k}}^2} \\ &= \nu_F \int_{-\infty}^{\infty} d\xi \, \frac{\xi + i\omega_l}{(i\omega_l)^2 - |\Delta|^2 - \xi^2} = -\pi\nu_F \frac{i\omega_l}{\sqrt{|\Delta|^2 - (i\omega_l)^2}}\end{aligned} \tag{1.12}$$

and

$$\mathcal{F}_{\downarrow\uparrow}(i\omega_l) = \pi\nu_F \frac{\Delta^*}{\sqrt{|\Delta|^2 - (i\omega_l)^2}} \tag{1.13}$$

1.1.2 Nambu basis

In superconducting condensed matter systems it is customary to work in the so-called Nambu basis. That is, one defines the two-spinor $\psi_{\mathbf{k}}^\dagger = (c_{\mathbf{k}\uparrow}^\dagger, c_{-\mathbf{k}\downarrow})$. This is useful because we can then cast the Hamiltonian in a particularly simple form

$$H = \sum_{\mathbf{k}} (c_{\mathbf{k}\uparrow}^\dagger \, c_{-\mathbf{k}\downarrow}) \begin{pmatrix} \xi_{\mathbf{k}} & -\Delta \\ -\Delta^* & -\xi_{\mathbf{k}} \end{pmatrix} \begin{pmatrix} c_{\mathbf{k}\uparrow} \\ c_{-\mathbf{k}\downarrow}^\dagger \end{pmatrix} + \text{const.} = \sum_{\mathbf{k}} \psi_{\mathbf{k}}^\dagger \mathbf{m}_{\mathbf{k}}^{SC} \psi_{\mathbf{k}}. \tag{1.14}$$

The Matsubara Green's function in the Nambu basis is defined as

$$\mathcal{G}(\tau) = -\sum_{\mathbf{k}} \left\langle T_\tau \psi_{\mathbf{k}}(\tau) \psi_{\mathbf{k}}^\dagger(0) \right\rangle = \begin{pmatrix} \mathcal{G}_{\uparrow\uparrow}(\mathbf{k}, \tau) & \mathcal{F}_{\downarrow\uparrow}^*(\mathbf{k}, \tau) \\ \mathcal{F}_{\downarrow\uparrow}(\mathbf{k}, \tau) & \mathcal{G}_{\uparrow\uparrow}^*(\mathbf{k}, \tau) \end{pmatrix}. \tag{1.15}$$

The local Nambu Green's function in frequency space is then

$$\mathcal{G}(i\omega_l) = \frac{\pi\nu_F}{\sqrt{|\Delta|^2 - (i\omega_l)^2}} \begin{pmatrix} -i\omega_l & \Delta \\ \Delta^* & -i\omega_l \end{pmatrix}. \tag{1.16}$$

1.2 Josephson junctions

In order to set the stage for the calculations that follow, we will start by presenting some results from the early seminal work on Josephson junctions carried out by Josephson and others, and for which Josephson was awarded the Nobel Prize in 1973. He predicted the Josephson effect which is the phenomenon where a dissipationsless supercurrent runs across a Josephson junction even in the absence of a voltage bias. A Josephson junction consists of two superconducting leads connected by a region of some other material. Examples of Josephson junctions are SIS-junctions where the leads are separated by a piece of insulating material, SNS-junctions where they are separated by a normal metal and S-QD-S-junctions where tunneling between the leads happens through the energy levels of a quantum dot.

Naively one might anticipate that no current can run across such a junction unless a voltage bias $V > 2\Delta$ is applied due to the superconducting energy gap. However, by studying an SIS-junction Josephson showed [6] that a current flows across the junction if there is a finite phase difference ϕ between the leads

$$I = I_c \sin(\phi(t)), \tag{1.17}$$

where I_c is the critical current, which is the maximum supercurrent that the junction can sustain. This is the first Josephson relation. The fact that this current runs without an applied bias tells us that it can't be carried by electrons. Instead it is due to Cooper pairs tunneling across the junction. The second Josephson relation gives the relation between the time evolution of the phase and the applied voltage bias [7]

$$\dot{\phi} = \frac{2eV}{\hbar}. \tag{1.18}$$

Combining the two Josephson relations we see that when applying a DC voltage the phase grows linearly with time, which gives rise to a current oscillating in time. This is known as the AC Josephson effect. Throughout the past 60 years, the field of research involving Josephson junctions has become very rich, both experimentally and theoretically. Especially in the recent years experimental techniques have improved, which has allowed for the implementation of Josephson junctions in circuits where they can be probed with microwave radiation in order to examine their properties.

1.3 Quantum electric circuits

This section follows the derivations of [8] and [9].
In this section we provide an elemental description of a Josehpson junction embedded in an electrical circuit. This is a necessary foundation for our later studies, where we investigate Josephson junctions subject to a harmonic voltage bias. When implementing Josephson junctions in electrical circuits, the simplest type of circuit one can have is the LC-circuit. We can imagine it as consisting of two distinct elements: a capacitor and an inductor. In practice the circuit usually consists of many devices all contributing to an effective capacitance and inductance, but for our purposes this simplistic description suffices. To gain knowledge about such a circuit, we find the energy associated with it and write up the Lagrangian. The energy related to the current flow through the inductor is $T = LI^2/2 = L\dot{q}^2/2$, which can be interpreted as a kinetic energy as it arises from the motion of the charges. The system also has a potential energy, which is the charging energy of the capacitor. It is given by $V = q^2/2C$. This gives the Lagrangian

$$\mathcal{L} = \frac{L\dot{q}^2}{2} - \frac{q^2}{2C}. \tag{1.19}$$

We find the conjugate momentum

$$\frac{\partial \mathcal{L}}{\partial \dot{q}} = L\dot{q} = LI = \Phi, \tag{1.20}$$

where Φ is the flux through the inductor. The resulting Hamiltonian is

$$H = \dot{q}\frac{\partial \mathcal{L}}{\partial \dot{q}} - \mathcal{L} = \frac{L\dot{q}^2}{2} + \frac{q^2}{2C} = \frac{\Phi^2}{2L} + \frac{q^2}{2C}. \tag{1.21}$$

This is the well-known Hamiltonian for a harmonic oscillator with eigenfrequency $\omega = 1/\sqrt{LC}$ where q is the generalized position coordinate and Φ is as mentioned the generalized momentum. Motivated by this, we define the quantum mechanical flux and charge operators which satisfy the canonical commutation relation $[\hat{q}, \hat{\Phi}] = i\hbar$. Furthermore we define the reduced flux operator $\hat{\phi} = 2\pi\Phi/\Phi_0$ given in terms of the flux quantum $\Phi_0 = h/2e$. An operator which gives the number of Cooper pairs is also defined as $\hat{n} = -\hat{q}/2e$. In terms of these operators we can rewrite the Hamiltonian as

$$H = 4E_c\hat{n}^2 + E_L\frac{\hat{\phi}^2}{2}, \tag{1.22}$$

where $E_c = e^2/2C$ is the charging energy of adding one electron to the capacitor and $E_L = (\Phi_0/2\pi)^2/L$ is the inductive energy per (reduced) flux quantum. Following the standard approach we can now introduce the annihilation and creation operators

$$\hat{a} = \frac{1}{\sqrt{2\hbar C\omega}}\hat{q} + i\frac{1}{\sqrt{2\hbar L\omega}}\hat{\phi} \quad \text{and} \quad \hat{a}^\dagger = \frac{1}{\sqrt{2\hbar C\omega}}\hat{q} - i\frac{1}{\sqrt{2\hbar L\omega}}\hat{\phi}. \tag{1.23}$$

In terms of these operators the Hamiltonian is quadratic $H = \hbar\omega(\hat{a}^\dagger\hat{a} + 1/2)$. As the energy levels of a quantum mechanical harmonic oscillator are equidistant, such a system is fundamentally unsuitable as a qubit. To construct a qubit one must have a subspace of two states with distinct energies, so that they can be manipulated without unintentionally and unknowingly exciting any other states. Essentially the equidistance of the energy levels is due to the fact that the potential of the LC-circuit is quadratic in ϕ. By using instead a nonlinear inductor with an inductance which depends on ϕ, a level structure with distinct transition frequencies can be created, allowing for creation of systems which can potentially be utilized as qubits. A Josephson junction is such a nonlinear inductor. We see this even for the simplest type of Josephson junction in the tunnel limit, which satisfies the first Josephson relation in eq. 1.17. From eq. 1.18, we can find the inductance as

$$V = -L_J\frac{dI_J}{dt} = \dot{\phi}\frac{\hbar}{2e} \Rightarrow \frac{1}{L_J} = -\frac{2e}{\hbar}\left(\frac{d\phi}{dt}\right)^{-1}\frac{dI_J}{dt} \Rightarrow \frac{1}{L_J} = -\frac{2e}{\hbar}\frac{dI_J}{d\phi}. \tag{1.24}$$

In the simple case of weakly coupled leads (eq. 1.17) we find that the inductance is $L_J = -2eI_c/\hbar\cos(\phi)$. Inserting this in eq. 1.22 yields the Hamiltonian

$$H = 4E_c\hat{n}^2 - E_J\cos\left(\hat{\phi}\right), \tag{1.25}$$

where the characteristic scale of the Josephson energy is $E_J = \Phi_0 I_c/2\pi$. From this it is clear that the Hamiltonian is no longer quadratic in ϕ and hence we no longer have a

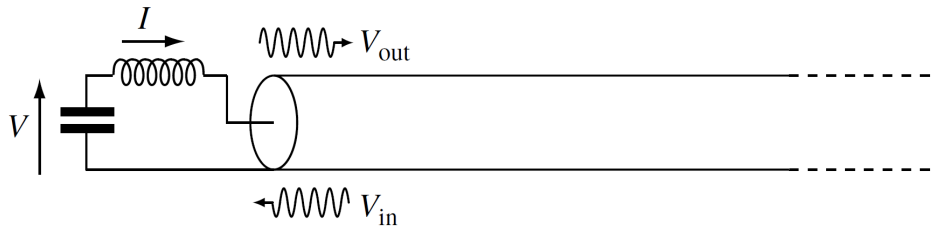

Figure 1.1: Simple sketch of a circuit which allows for a measurement of the power absorbed by an inductor such as a Josephson junction. Figure taken from [10].

harmonic potential with equidistant energy levels. Up to this point we have only dealt with the general case of a purely inductive Josephson junction carrying dissipationsless current. However, our main interest is the dissipative properties when an AC voltage is applied. To find the absorption rate we use the relation for dissipated power in an AC-circuit which is given by

$$\langle P \rangle = \frac{V^2}{2|Z|} \cos(\theta), \tag{1.26}$$

where V is the amplitude of the applied voltage and θ is the phase difference between current and voltage. Using that $\cos(\theta) = R/|Z|$ where $Z = R + iX$ is the impedance we obtain an average absorbed power of

$$\langle P \rangle = \frac{V_0^2 R}{2|Z|^2} = \frac{V_0^2}{2} \operatorname{Re} Y \tag{1.27}$$

where we introduced the admittance $Y = Z^{-1} = (R - iX)/|Z|^2$, which relates voltage and current as $I(\omega) = Y(\omega)V(\omega)$. Hence we see that the absorption can be determined by calculating the real part of the admittance. This quantity will play a major role in the rest of the thesis. To experimentally measure the power absorbed by a Josephson junction embedded in a circuit one can use reflectometry. Here the LC-resonator described above is connected to the inner and outer conductor of a coaxial cable constituting the transmission line of the setup and an oscillating voltage bias is applied to the coaxial cable, which supplies microwaves that can be absorbed by the inductor. The circuit is sketched in fig. 1.1. The reflection coefficient which directly yields the dissipated power can then be determined by measuring the difference between the characteristic impedance of the cable Z_c and that of the resonator $Z(\omega)$ from the relation [10]

$$r = \frac{Z(\omega) - Z_c}{Z(\omega) + Z_c}. \tag{1.28}$$

Chapter 2

Superconducting quantum point contact

2.1 Green's functions

In the first part of this thesis we study the type of Josephson junction which is a superconducting quantum point contact, where the two leads are connected by a weak link. Generally, a point contact is a narrow constriction connecting two leads and in the ballistic regime where the elastic scattering length of the electrons is much larger than the length of the constriction, the normal state zero-temperature conductance of the point contact is quantized in units of $G_0 = 2e^2/h$ and given by the famous Landauer formula $G = G_0\tau$ [11] (for a single channel of transmission probability τ). See appendix A for a derivation of the normal-state conductance. When the leads are superconducting the situation is more complicated, and in this section we will study the implications of this. As we subsequently wish to follow the approach presented in ref. [5] and calculate the linear response of the system to a small voltage bias using the Green's function method, we start by deriving and solving the equations of motion for the Green's functions. This will also yield information about the subgap states and equilibrium current. The system of our interest is described by the Hamiltonian

$$\begin{aligned} H &= H_{LR} + H_T \\ H_{LR} &= \sum_{\alpha k\sigma} \xi_k c^\dagger_{\alpha k\sigma} c_{\alpha k\sigma} - \sum_{\alpha k} \left(\Delta_\alpha c^\dagger_{\alpha k\uparrow} c^\dagger_{\alpha -k\downarrow} + \Delta^*_\alpha c_{\alpha -k\downarrow} c_{\alpha k\uparrow} \right) \\ H_T &= w \sum_{kp\sigma} (c^\dagger_{Lk\sigma} c_{Rp\sigma} + c^\dagger_{Rp\sigma} c_{Lk\sigma}) + w \sum_{kk'\sigma} c^\dagger_{Lk\sigma} c_{Lk'\sigma} + w \sum_{pp'\sigma} c^\dagger_{Rp\sigma} c_{Rp'\sigma}, \end{aligned} \tag{2.1}$$

where H_T includes both tunneling between the leads and backscattering at the interface and $\alpha \in \{L, R\}$ refers to the left and right leads. The transmission coefficient is given by $\tau = (2\pi\nu_F w)^2/(1 + (2\pi\nu_F w)^2)$ (see appendix A). The order parameter contains the phase dependence $\Delta_{L/R} = \Delta e^{i\phi_{L/R}}$. Throughout the thesis we will be using units

where $\hbar = 1$ and reinstate it when necessary. The phase difference across the junction is $\phi = \phi_R - \phi_L$. We can let $\phi_R = 0$ without loss of generality so that $\Delta_R = \Delta$ and $\Delta_L = \Delta e^{-i\phi}$, with Δ real. We can also remove the phase dependence from the order parameter by performing a gauge transformation $c^\dagger_{Lk\sigma} \to c^\dagger_{Lk\sigma} e^{i\phi/2}$. The phase dependence is then transferred to the tunneling term which becomes

$$H_T = w \sum_{kp\sigma} (e^{i\phi/2} c^\dagger_{Lk\sigma} c_{Rp\sigma} + e^{-i\phi/2} c^\dagger_{Rp\sigma}) + w \sum_{kk'} c^\dagger_{Lk\sigma} c_{Lk'\sigma} + w \sum_{pp'} c^\dagger_{Rp\sigma} c_{Rp'\sigma} \tag{2.2}$$

We will now calculate the Green's functions using the equation of motion-technique for the time-ordered Matsubara Green's function. Subsequently the retarded and advanced Green's functions can be obtained by performing an analytical continuation. The calculations will be performed in Nambu space. In terms of the Nambu spinors defined for each lead as

$$\psi^\dagger_{\alpha k} = \begin{pmatrix} c^\dagger_{\alpha k\uparrow}, & c_{\alpha -k\downarrow} \end{pmatrix} \quad \text{and} \quad \psi_{\alpha k} = \begin{pmatrix} c_{\alpha k\uparrow} \\ c^\dagger_{\alpha -k\downarrow} \end{pmatrix}, \tag{2.3}$$

the Hamiltonian is given by

$$\begin{aligned} H = &\sum_{\alpha k} \psi^\dagger_{\alpha k} \mathbf{m}^{SC}_k \psi_{\alpha k} + \sum_{kp} (\psi^\dagger_{Lk} \mathbf{w}_T \psi_{Rp} + h.c.) \\ &+ \sum_{kk'} \psi^\dagger_{Lk} \mathbf{w}_R \psi_{Lk'} + \sum_{pp'} \psi^\dagger_{Rp} \mathbf{w}_R \psi_{Rp'}, \end{aligned} \tag{2.4}$$

where

$$\mathbf{m}^{SC}_k = \begin{pmatrix} \xi_k & -\Delta \\ -\Delta & -\xi_k \end{pmatrix}, \quad \mathbf{w}_R = \begin{pmatrix} w & 0 \\ 0 & -w \end{pmatrix}, \quad \mathbf{w}_T = \begin{pmatrix} we^{i\phi/2} & 0 \\ 0 & -we^{-i\phi/2} \end{pmatrix}. \tag{2.5}$$

We will start by considering the equation of motion for the local Matsubara Nambu Green's function for the left lead

$$\mathcal{G}_{LL}(\tau - \tau') = -\sum_{kk'} \langle T_\tau \psi_{Lk}(\tau) \psi^\dagger_{Lk'}(\tau') \rangle. \tag{2.6}$$

However, it turns out to be easier to work with $\mathcal{G}_{kL}(\tau - \tau') = -\sum_{k'} \langle T_\tau \psi_{Lk}(\tau) \psi^\dagger_{Lk'}(\tau') \rangle$, and perform the sum over k at a later time. To find the time derivative of the Green's function we use the Heisenberg equation of motion for imaginary time [12]

$$\partial_\tau \hat{O}(\tau) = \left[H, \hat{O} \right](\tau), \tag{2.7}$$

so we need to calculate the commutators of the Hamiltonian with the Nambu spinors. They are given by:

$$
\begin{aligned}
\Big[H, \psi_{Lk,\mu}\Big] &= -\sum_{\mu'} \mathbf{m}^{SC}_{k,\mu\mu'}\psi_{Lk,\mu'} - \sum_{p,\mu'} \mathbf{w}_{T,\mu\mu'}\psi_{Rp,\mu'} - \sum_{k',\mu'} \mathbf{w}_{R,\mu\mu'}\psi_{Lk',\mu'} \\
\Big[H, \psi^\dagger_{Lk,\mu}\Big] &= \sum_{\mu'} \mathbf{m}^{SC}_{k,\mu'\mu}\psi^\dagger_{Lk,\mu'} + \sum_{p,\mu'} \mathbf{w}^*_{T,\mu\mu'}\psi^\dagger_{Rp',\mu'} + \sum_{k',\mu'} \mathbf{w}_{R,\mu\mu'}\psi^\dagger_{Lk',\mu'} \\
\Big[H, \psi_{Rp,\mu}\Big] &= -\sum_{\mu'} \mathbf{m}^{SC}_{p,\mu\mu'}\psi_{Rp,\mu'} - \sum_{k,\mu'} \mathbf{w}^*_{T,\mu'\mu}\psi_{Lk,\mu'} - \sum_{p',\mu'} \mathbf{w}_{R,\mu\mu'}\psi_{Rp',\mu'} \\
\Big[H, \psi^\dagger_{Rp,\mu}\Big] &= \sum_{\mu'} \mathbf{m}^{SC}_{p,\mu'\mu}\psi^\dagger_{Rp,\mu'} + \sum_{k,\mu'} \mathbf{w}_{T,\mu'\mu}\psi^\dagger_{Lk',\mu'} + \sum_{p',\mu'} \mathbf{w}_{R,\mu\mu'}\psi^\dagger_{Rp',\mu'},
\end{aligned}
\tag{2.8}
$$

where the indices μ refer to Nambu space. From this we find the equation of motion for the left lead Matsubara Green's function

$$
\begin{aligned}
-\partial\tau\mathcal{G}_{kL,\mu\mu'}(\tau-\tau') &= \delta(\tau)\delta_{\mu\mu'} - \sum_{k',\mu''} \mathbf{m}^{SC}_{k,\mu\mu''}\langle T_\tau \psi_{Lk,\mu''}(\tau)\psi^\dagger_{Lk',\mu'}(\tau')\rangle \\
-\sum_{k'p',\mu''} \mathbf{w}_{T,\mu\mu''}\langle T_\tau \psi_{Rp',\mu''}(\tau)\psi^\dagger_{Lk',\mu'}(\tau')\rangle &- \sum_{k'k'',\mu''} \mathbf{w}_{R,\mu\mu''}\langle T_\tau \psi_{Lk'',\mu''}(\tau)\psi^\dagger_{Lk',\mu'}(\tau')\rangle.
\end{aligned}
\tag{2.9}
$$

Introducing $\mathcal{G}_{LR}(\tau,\tau') = -\sum_{kp}\langle T_\tau \psi_{Lk}(\tau)\psi^\dagger_{Rp}(\tau')\rangle$ which couples the two leads, we can write this on matrix form in Nambu space as

$$
-\partial_\tau \mathcal{G}_{kL}(\tau,\tau') = \delta(\tau)\sigma_0 + \mathbf{m}^{SC}_k \mathcal{G}_{kL}(\tau,\tau') + \mathbf{w}_R\mathcal{G}_{LL}(\tau,\tau') + \mathbf{w}_T\mathcal{G}_{RL}(\tau,\tau'), \tag{2.10}
$$

where σ_0 is the (identity) Pauli matrix. We Fourier transform

$$
(i\omega_l - \mathbf{m}^{SC}_k)\mathcal{G}_{kL}(i\omega_l) = \sigma_0 + \mathbf{w}_R\mathcal{G}_{LL}(i\omega_l) + \mathbf{w}_T\mathcal{G}_{RL}(i\omega_l) \tag{2.11}
$$

and perform the momentum sum to obtain

$$
\begin{aligned}
\mathcal{G}_{LL}(i\omega_l) &= \sum_k \mathcal{G}_{kL}(i\omega_l) \\
&= \sum_k (i\omega_l\sigma_0 - \mathbf{m}^{SC}_k)^{-1}(1 + \mathbf{w}_R\mathcal{G}_{LL}(i\omega_l) + \mathbf{w}_T\mathcal{G}_{RL}(i\omega_l)) \\
&= \mathcal{G}_0(i\omega_l)(\sigma_0 + \mathbf{w}_R\mathcal{G}_{LL}(i\omega_l) + \mathbf{w}_T\mathcal{G}_{RL}(i\omega_l)) \\
\implies \mathcal{G}_{LL}(i\omega_l) &= (\sigma_0 - \mathcal{G}_0(i\omega_l)\mathbf{w}_R)^{-1}\mathcal{G}_0(i\omega_l)(\sigma_0 + \mathbf{w}_T\mathcal{G}_{RL}(i\omega_l)) \\
&= \tilde{\mathcal{G}}_0(i\omega_l) + \tilde{\mathcal{G}}_0(i\omega_l)\mathbf{w}_T\mathcal{G}_{RL}(i\omega_l).
\end{aligned}
$$

Here we identified the bare k-summed Nambu Green's function $\mathcal{G}_0(\omega) = \sum_k (i\omega_l\sigma_0 - \mathbf{m}^{SC}_k)^{-1}$ which we calculated in eq. 1.16. Furthermore in the last step a modified bare Green's function containing also the backscattering processes in the separate leads was defined as

$$
\tilde{\mathcal{G}}_0(i\omega_l) = (\mathcal{G}_0(i\omega_l)^{-1} - \mathbf{w}_R)^{-1}. \tag{2.12}
$$

The bare Green's function has no lead index as it is diagonal in lead space, $\tilde{\mathcal{G}}_{0,LR}(i\omega_l) = \tilde{\mathcal{G}}_{0,RL}(i\omega_l) = 0$ and $\tilde{\mathcal{G}}_{0,LL}(i\omega_l) = \tilde{\mathcal{G}}_{0,RR}(i\omega_l)$. We see that the equations of motion for

$\mathcal{G}_{LL}(i\omega_l)$ and $\mathcal{G}_{RL}(i\omega_l)$ are coupled, and a completely similar calculation of the equation of motion for $\mathcal{G}_{RL}(i\omega_l)$, yields the following equation:

$$\mathcal{G}_{RL}(i\omega_l) = \tilde{\mathcal{G}}_0(i\omega_l)\mathbf{w}_T^\dagger \mathcal{G}_{LL}(i\omega_l) \tag{2.13}$$

A similar set of coupled equations is obtained for $\mathcal{G}_{RR}(i\omega_l)$ and $\mathcal{G}_{LR}(i\omega_l)$, and we can write this total set of four coupled equations as a Dyson equation in the combined Nambu and lead space

$$\mathcal{G}(i\omega_l) = \tilde{\mathcal{G}}_0(i\omega_l) + \tilde{\mathcal{G}}_0(i\omega_l)\mathbf{\Sigma}\mathcal{G}(i\omega_l), \tag{2.14}$$

where all the quantities are $4 \times 4-$matrices in lead space

$$\mathcal{G}(i\omega_l) = \begin{pmatrix} \mathcal{G}_{LL}(i\omega_l) & \mathcal{G}_{LR}(i\omega_l) \\ \mathcal{G}_{RL}(i\omega_l) & \mathcal{G}_{RR}(i\omega_l) \end{pmatrix},$$

and each element is a 2×2 Nambu matrix. The self-energy is independent of frequency so that $\mathbf{\Sigma}^R = \mathbf{\Sigma}^A$ and is given by

$$\mathbf{\Sigma} = \begin{pmatrix} 0 & \mathbf{w}_T \\ \mathbf{w}_T^\dagger & 0 \end{pmatrix}. \tag{2.15}$$

From eq. 2.14 we can obtain all necessary Matsubara Green's functions for the system. Performing the analytical continuation then yields the retarded and advanced Green's functions as well

$$G^{R,A}(\omega) = \mathcal{G}(i\omega_l \to \omega \pm i\eta). \tag{2.16}$$

In particular, for the retarded Green's function obtained as

$$G^R(\omega + i\eta) = \left((\tilde{G}_0^R(\omega + i\eta))^{-1} - \mathbf{\Sigma}\right)^{-1} \tag{2.17}$$

the $LL-$sector describing the left lead is

$$G_{LL}^R(\omega) = \begin{pmatrix} -\frac{\pi\nu\sqrt{\Delta^2-(\omega+i\eta)^2}\left((1+2\pi^2\nu^2w^2)\omega+\pi\nu w\sqrt{\Delta^2-(\omega+i\eta)^2}\right)}{D(\omega+i\eta)} & \frac{\pi\Delta\nu\left(\left(1+e^{i\phi}\right)\pi^2w^2\nu^2+1\right)\sqrt{\Delta^2-(\omega+i\eta)^2}}{D(\omega+i\eta)} \\ \frac{e^{-i\phi}\pi\Delta\nu\left(\pi^2w^2\nu^2+e^{i\phi}\left(\pi^2w^2\nu^2+1\right)\right)\sqrt{\Delta^2-(\omega+i\eta)^2}}{D(\omega+i\eta)} & \frac{\pi\nu\sqrt{\Delta^2-(\omega+i\eta)^2}\left(-(1+2\pi^2\nu^2w^2)\omega+\pi\nu w\sqrt{\Delta^2-(\omega+i\eta)^2}\right)}{D(\omega+i\eta)} \end{pmatrix}, \tag{2.18}$$

and the $LR-$sector which accounts for tunneling between the leads is

$$G^R_{LR}(\omega) =$$
$$\begin{pmatrix} \frac{e^{-i\phi/2}\pi^2 w\nu^2\left(e^{i\phi}\omega\left(\omega+2\pi w\nu\sqrt{\Delta^2-(\omega+i\eta)^2}\right)-\Delta^2\right)}{D(\omega+i\eta)} & -\frac{e^{-i\phi/2}\pi^2 w\Delta\nu^2\left(\left(-1+e^{i\phi}\right)\omega+\left(1+e^{i\phi}\right)\pi w\nu\sqrt{\Delta^2-(\omega+i\eta)^2}\right)}{D(\omega+i\eta)} \\ -\frac{e^{-i\phi/2}\pi^2 w\Delta\nu^2\left(\left(-1+e^{i\phi}\right)\omega+\left(1+e^{i\phi}\right)\pi w\nu\sqrt{\Delta^2-(\omega+i\eta)^2}\right)}{D(\omega+i\eta)} & \frac{e^{-i\phi/2}\pi^2 w\nu^2\left(e^{i\phi}\Delta^2+\left(2\pi w\nu\sqrt{\Delta^2-(\omega+i\eta)^2}-\omega\right)\omega\right)}{D(\omega+i\eta)} \end{pmatrix}. \tag{2.19}$$

The two remaining parts of the Green's function are related to those by $G^R_{RR}(\omega,\phi) = G^R_{LL}(\omega,-\phi)$ and $G^R_{RL}(\omega,\phi) = G^R_{LR}(\omega,-\phi)$. The denominator $D(\omega+i\eta)$ of the Green's functions is equal to the determinant of the inverse retarded Green's function. By letting $\eta \to 0$ and solving the equation $D(\omega) = \det G^R(\omega)^{-1} = 0$ we find the poles of the Green's function which are the bound state energies

$$\begin{aligned} 0 &= \Delta^2(1+2\pi^2w^2\nu^2) - (1+4\pi^2w^2\nu^2)\omega^2 + 2\pi^2w^2\nu^2\Delta^2\cos\phi \\ &\Rightarrow E_A(\phi) = \pm\Delta\sqrt{1-\tau\sin^2(\phi/2)}. \end{aligned} \tag{2.20}$$

We have now arrived at an expression for the well-known Andreev bound states forming inside the superconducting gap due to a process called Andreev reflections, which can be described as follows [13] (for the case of a spin-up electron):

At an interface between a supeconductor and a normal metal, a spin-up electron in the normal lead which impinges on the interface can't tunnel to the superconductor as there are no available states due to the energy gap. Instead a hole with opposite spin and momentum is retroreflected from the interface and a Cooper pair is transferred to the superconductor. In an SNS-junction as studied here (in the short-junction limit), the Andreev reflections can happen repeatedly, as when the spin-down hole reaches the opposite interface, it can be reflected back as a spin-up electron in combination with a Cooper pair being annihilated in the other superconductor. In this way the quasiparticles which are superpositions of spin-up electrons and spin-down holes can become trapped in the normal region. In addition to this process there is an equivalent one where the electrons and holes move in the opposite direction which also transports Cooper pairs in the opposite direction. These two processes are responsible for the formation of the two Andreev levels with energy $\pm E_A$. In fig. 2.1 the bound state energies are plotted as a function of phase difference ϕ for different values of the transmission coefficient. For perfect transmission $\tau = 1$ the two bound states $\pm E_A$ meet at zero energy for $\phi = \pi$, whereas for non-perfect transmission an avoided crossing is seen. This is because $\tau < 1$ corresponds to the presence of a scattering mechanism which couples the two Andreev reflection processes described above.

From the above explanation it is also clear why the Andreev levels carry supercurrent, as they are responsible for the transport of Cooper pairs across the junction. In the next section we will calculate an expression for this current. Of course we are here considering the limit where the length of the normal region is zero, but the physical

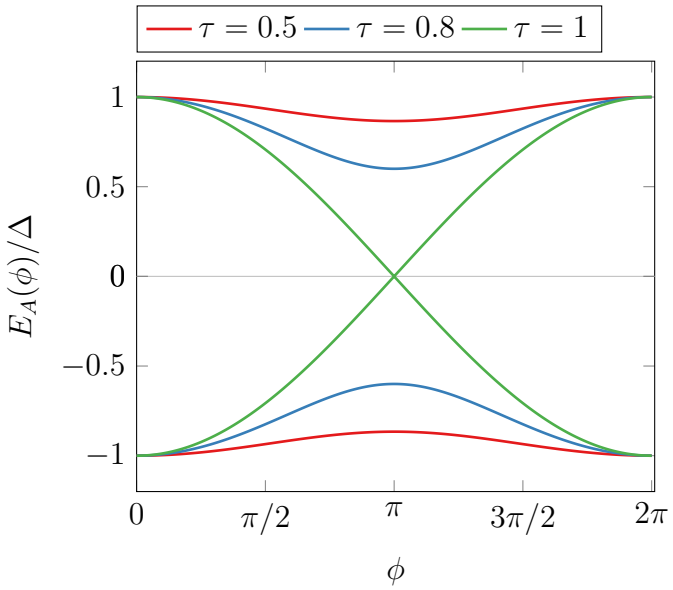

Figure 2.1: Energies of the bound states as a function of phase difference ϕ for different values of the transmission coefficient.

picture is nevertheless correct. We will see this more explicitly later when treating the QPC using the scatterting formalism.

From the retarded Green's function we can also find the spectral function which is given by

$$A(\omega) = -2\,\mathrm{Im}(G^R(\omega)). \tag{2.21}$$

In our case this is of course also a 4×4 matrix which has a number of different entries. In fig. 2.2 the normal components of the spectral function for the left lead are shown. We see that the familiar divergence of the density of states at the gap edge has disappeared, while discrete peaks form inside the gap at position of the bound state energy E_A.

2.2 Equilibrium current

We will now calculate the current across the junction as a function of the constant phase difference ϕ. We will need the current operator in terms of both Nambu and electron operators later, so we derive both of them here. The current operator is defined as

$$\hat{I}(t) = e\dot{N}_L(t) = ie[H, N_L](t), \quad N_L = \sum_{k\sigma} c^\dagger_{k\sigma} c_{k\sigma}. \tag{2.22}$$

With the Hamiltonian in eq. 2.1 we obtain (after performing the gauge transformation)

$$\hat{I}(t) = 2ie\Delta \sum_k \left(c^\dagger_{Lk\uparrow} c^\dagger_{L-k\downarrow} - c_{L-k\downarrow} c_{Lk\uparrow} \right) - iew \sum_{kp\sigma} (e^{i\phi/2} c^\dagger_{Lk\sigma} c_{Rp\sigma} - e^{-i\phi/2} c^\dagger_{Rp\sigma} c_{Lk\sigma}). \tag{2.23}$$

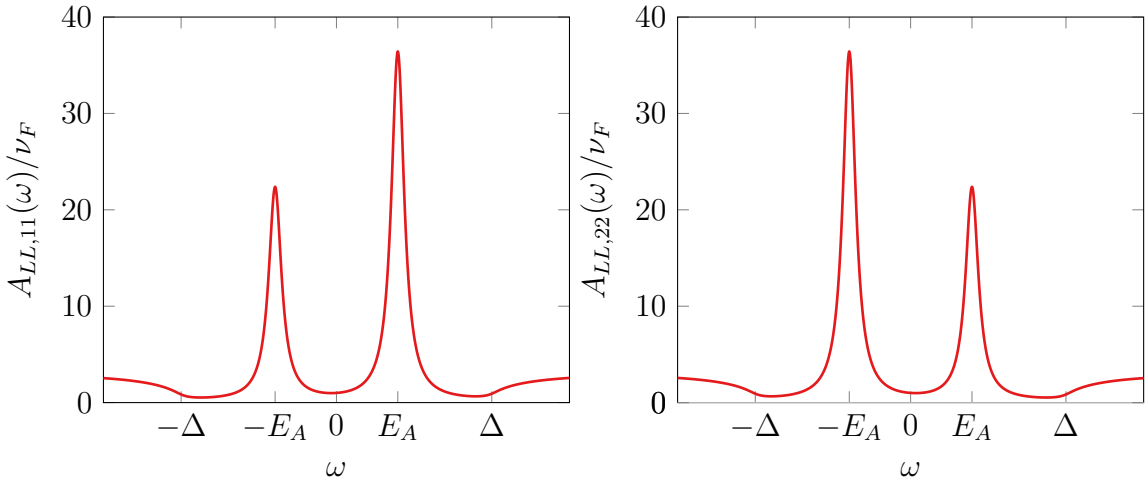

Figure 2.2: Normal (diagonal) components of the spectral function for the left lead. Discrete peaks (which acquire a width as $\eta = 0.05$ has a finite value for plotting purposes) appear at the bound state energies. The parameters are $\phi = 3\pi/4$ and $\tau = 0.99$.

The first two terms arise from the commutator with the BCS part of the Hamiltonian and are an artefact of the mean-field expansion where the number of electrons isn't a conserved quantity, so we will discard those. In equilibrium the current can have a time-independent nonzero expectation value even without a voltage bias, which is given by

$$\langle I(t)\rangle_0 = \langle I(0)\rangle = 2ew\,\mathrm{Im}\sum_{kp\sigma}\langle e^{i\phi/2}c^\dagger_{Lk\sigma}c_{Rp\sigma}\rangle. \tag{2.24}$$

To express the current operator in terms of the Nambu spinors, we write the number operator as

$$N_L = \sum_k \psi^\dagger_{Lk}\sigma_3\psi_{Lk} = \sum_k\sum_{\mu\mu'}\psi^\dagger_{Lk\mu}\sigma_{3,\mu\mu'}\psi_{Lk\mu'}.$$

The commutator with the Hamiltonian (in Nambu basis) is found to be:

$$\begin{aligned}[H,N_L] &= \sum_{kp}\Big(\,\mathrm{Tr}\,\sigma_3(\mathbf{w}_T^*\psi^\dagger_{Rp}\psi_{Lk} - \mathbf{w}_T\psi^\dagger_{Lk}\psi_{Rp}) + 2\,\mathrm{Tr}\,\psi^\dagger_{Lk}\mathbf{m}^\Delta_k\psi_{Lk}\Big),\\ &\text{where}\quad \mathbf{m}^\Delta_k = \begin{pmatrix}0 & -\Delta_L\\ -\Delta_L^* & 0\end{pmatrix}.\end{aligned} \tag{2.25}$$

Again the last term is the BCS-contribution which we discard. Identifying the lesser Green's function $G^<_{LR}(t-t') = i\sum_{kp}\langle\psi^\dagger_{Rp}(t')\psi_{Lk}(t)\rangle$, which depends only on the time difference $t-t'$, the equilibrium expectation value of the current can be written as

$$\begin{aligned}\langle\hat{I}(t)\rangle_0 &= -ie\sum_{kp}\mathrm{Tr}\left(\sigma^3(\mathbf{w}_T\langle\psi^\dagger_{Lk}(t)\psi_{Rp}(t)\rangle - \mathbf{w}_T^*\langle\psi^\dagger_{Rp}(t)\psi_{Lk}(t)\rangle)\right)\\ &= -e\,\mathrm{Tr}\left(\sigma^3(\mathbf{w}_T G^<_{RL}(t) - \mathbf{w}_T^* G^<_{LR}(t))\right).\end{aligned} \tag{2.26}$$

By considering now $\langle \hat{I}(t=0)\rangle_0$ and Fourier transforming we find that the expectation value of the current in frequency space is given by

$$\langle \hat{I}(0)\rangle_0 = -e\int_{-\infty}^{\infty}\frac{d\omega}{2\pi}\,\mathrm{Tr}\Big[\sigma^3(\mathbf{w}_T G^<_{RL}(\omega) - \mathbf{w}_T^* G^<_{LR}(\omega))\Big]. \tag{2.27}$$

In the case of a constant phase difference (no voltage bias) the problem can be treated using equilibrium methods. We will see that in this case we obtain the same result both when using the Keldysh nonequilibrium method [14] and the equilibrium method to calculate the lesser Green's functions. In equilibrium the fluctuation-dissipation theorem applies and the lesser Green's function is obtained as

$$G^<(\omega) = -n_F(\omega)(G^R(\omega) - G^A(\omega)). \tag{2.28}$$

Out of equilibrium the lesser Green's function can be determined in the Keldysh formalism from the following equation (where all quantites are matrices in Nambu- and LR-space)

$$G^<(\omega) = (1 + G^R(\omega)\Sigma^R)G_0^<(1 + \Sigma^A G^A(\omega)) + G^R(\omega)\Sigma^< G^A(\omega), \tag{2.29}$$

where in this case the second term vanishes because $\Sigma^< = 0$ as there is no scattering between the two branches on the Keldysh contour, and where $\Sigma^A = \Sigma^R = \Sigma$ is independent of frequency. Both when using eq. 2.28 and eq. 2.29 we obtain the following expression for the current in eq. 2.27 (at $T = 0$ where $n_F(\omega) = \theta(-\omega)$):

$$\langle \hat{I}_0(t)\rangle = -e\int_{-\infty}^{0}\frac{d\omega}{2\pi}\Delta^2\sin(\phi)\tau\frac{\eta}{(E_A^2/2\omega - \omega/2)^2 + \eta^2}. \tag{2.30}$$

Taking the limit $\eta \to 0$ and using that $\delta(f(x)) = \sum_i \delta(x - x_i)/|f'(x_i)|$, eq. 2.30 becomes very simple

$$\langle \hat{I}_0(0)\rangle = -\frac{e}{2}\tau\sin(\phi)\Delta^2\int_{-\infty}^{0} d\omega\,\frac{1}{\omega}(\delta(\omega - E_A) + \delta(\omega + E_A)) = \frac{e\tau\Delta^2\sin(\phi)}{2E_A(\phi)} = G\frac{\pi\Delta^2\sin(\phi)}{2eE_A(\phi)}, \tag{2.31}$$

where in the last step the normal-state conductance $G = e^2\tau/\pi$ was identified. Fig. 2.3 shows the current as a function of phase difference across the junction for different values of τ. We see that the current has a sinusoidal dependence on the phase similar to the first Jospehson relation, but modified by the phase dependence of the bound state energy. The pure sine form of the current-phase relation is only obtained in the tunnel limit $\tau \ll 1$. We can now find the contribution to the admittance related to the equilibrium current I_0 using eq. 1.24 and that the admittance of an ideal inductor is given by $Y = i/\omega L$

$$\begin{aligned} Y_0 = \frac{i}{\omega L_J} &= -\frac{2ie}{\omega}\frac{\partial I_0}{\partial \phi} = -\frac{2ie}{\omega}\frac{\partial}{\partial\phi}\left(\frac{G\pi\Delta\sin(\phi)}{2e\sqrt{1 - \tau\sin^2(\phi/2)}}\right) \\ &= -i\frac{\pi\Delta G}{\omega}\frac{\cos(\phi) + \tau\sin^4(\phi/2)}{(1 - \tau\sin^2(\phi/2))^{3/2}}. \end{aligned} \tag{2.32}$$

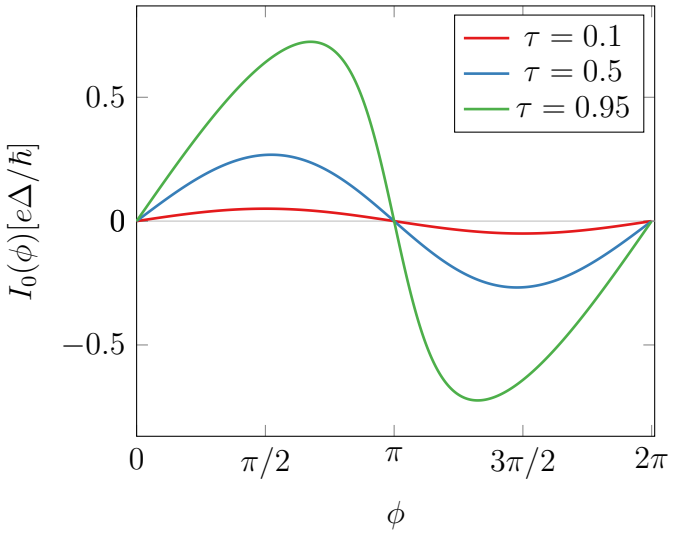

Figure 2.3: Equilibrium current as a function of phase difference across the junction for different transmission probabilities.

The admittance in equilibrium is purely imaginary and does not contribute to the dissipation. This is in accordance with the fact that the supercurrent is dissipationless.

We conclude this section by noting that the current-phase relation can also be obtained by taking the derivative of the free energy which can be related to the ground state energy in the so-called single-particle picture described elaborately by Bretheau [13] and originally by Datta [15]. Then $I_0 = -2e\partial E_A(\phi)/\partial\phi$, which again yields the result of eq. 2.31. This indicates that in equilibrium the current is carried solely by the bound states so that there is no contribution from the continuum even though we are considering finite Δ. This has been found by others to be exactly true in the short-junction limit ([16], [17]). Generally there is also a contribution to the current from the continuum states.

2.3 Linear response

We will now investigate the effect of perturbing a QPC as described in the previous section with a small AC voltage bias. This will be done using linear response theory following the approach used in ref. [5]. As we wish to determine the ability of the junction to absorb photons, the quantity of our interest is the real part of the admittance. The Hamiltonian for the system is given by eq. 2.1. Applying a voltage bias across the junction amounts to shifting the chemical potential of the left lead, whereby the Hamiltonian is modified as

$$H_0 \to H(t) = H_0 - eV(t)\hat{N}_L, \quad \hat{N}_L = \sum_{k\sigma} c^\dagger_{Lk\sigma} c_{Lk\sigma}. \tag{2.33}$$

Furthermore we know from the second Josephson relation (eq. 1.18) that the applied votage bias gives rise to a time dependent phase difference across the junction. Hence in the Hamiltonian we must also make the substitution $\phi_L \to \phi_L + 2\phi_1(t)$, which modifies the phase of the order parameter in the left lead, and where the factor of two is chosen for convenience later on. We use a harmonic voltage bias of the form $V(t) = V_0(e^{i\omega t} - e^{-i\omega t}) = 2V_0 \sin(\omega t)$, which yields the phase difference

$$\phi_1(t) = 2eV_0 \int_0^t dt' \sin\Big(\omega t'\Big) = -\frac{2e}{\omega} V_0 \cos(\omega t). \tag{2.34}$$

In the regime where linear response theory is valid the amplitude of the perturbation satisfies $|\phi_1| = |\frac{2eV_0}{\omega}| \ll 1$. The current operator expressed in terms of the electron creation and annihilation operators is given by eq. 2.23 which we repeat here

$$\hat{I} = e\dot{N}_L = -iew \sum_{kp\sigma} (e^{i\phi/2} c^\dagger_{Lk\sigma} c_{Rp\sigma} - e^{-i\phi/2} c^\dagger_{Rp\sigma} c_{Lk\sigma}). \tag{2.35}$$

In the absence of a voltage difference the expectation value of the current is given by eq. 2.24. Before calculating the linear response of the current to the applied voltage it is convenient to perform a gauge transformation $c_{Lk\sigma} \to c_{Lk\sigma} e^{i\phi_1(t)}$, which as shown in appendix B moves the dependence of $\phi_1(t)$ from Δ to the tunneling term. Furthermore, it generates an additional term in the transformed Hamiltonian which exactly cancels the time-dependent term in eq. 2.33. This simplifies the following calculations significantly. In terms of the transformed operators the Hamiltonian is found to be

$$\begin{aligned} H(t) &= H_0 + H_T(t) \\ H_0 &= \sum_{\alpha k\sigma} \xi_{\alpha k} c^\dagger_{\alpha k\sigma} c_{\alpha k\sigma} - \Delta\Big(\sum_{\alpha k} c^\dagger_{\alpha k\uparrow} c^\dagger_{\alpha -k\downarrow} + \sum_{\alpha k} c_{\alpha k\downarrow} c_{\alpha -k\uparrow} \Big) + w \sum_{kk'\alpha\sigma} c^\dagger_{\alpha k\sigma} c_{\alpha k'\sigma} \\ H_T(t) &= w \sum_{kp\sigma} (e^{-i(\phi_1(t) - \phi/2)} c^\dagger_{Lk\sigma} c_{Rp\sigma} + e^{i(\phi_1(t) - \phi/2)} c^\dagger_{Rp\sigma} c_{Lk\sigma}) \end{aligned} \tag{2.36}$$

The exponential functions in the tunneling terms contain infinite powers of ϕ_1, so to perform the linear response calculation we expand H_T to linear order in the phase

$$H_T(t) \approx w \sum_{kp\sigma} (e^{i\phi/2}(1 - i\phi_1(t)) c^\dagger_{Lk\sigma} c_{Rp\sigma} + e^{-i\phi/2}(1 + i\phi_1(t)) c^\dagger_{Rp\sigma} c_{Lk\sigma}). \tag{2.37}$$

Extracting the part which depends on ϕ_1 we can define:

$$\delta H(t) \equiv -iw\phi_1(t) \sum_{kp\sigma} (e^{i\phi/2} c^\dagger_{Lk\sigma} c_{Rp\sigma} - e^{-i\phi/2} c^\dagger_{Rp\sigma} c_{Lk\sigma}) = \frac{\phi_1(t)}{e} \hat{I}_0 \tag{2.38}$$

The Kubo formula gives the linear response of the current as [12]

$$\langle \hat{I}(t) \rangle = I_0 - i \int_{-\infty}^{\infty} dt'\, \theta(t - t') \Big\langle [\hat{I}(t), \delta H(t')] \Big\rangle_0. \tag{2.39}$$

However, before proceeding with the Kubo formula it should be noted that there is also a contribution to the current to linear order in ϕ_1 arising from the current operator itself, which in the presence of a voltage difference has the expectation value

$$\begin{aligned}\langle \hat{I}(t)\rangle_0 &= -iew\sum_{kp\sigma}\langle e^{-i(\phi_1(t)+\phi/2)}c^\dagger_{Lk\sigma}c_{Rp\sigma} - e^{i(\phi_1(t)+\phi/2)}c^\dagger_{Rp\sigma}c_{Lk\sigma}\rangle_0 \\ &\approx I_0 - 2ew\phi_1(t)\sum_{kp\sigma}\mathrm{Re}\langle e^{i\phi/2}c^\dagger_{Lk\sigma}c_{Rp\sigma}\rangle_0.\end{aligned} \tag{2.40}$$

The first term is just the equilibrium Josephson current which has previously been accounted for and the second term is already to linear order in ϕ_1.

To calculate the linear response of the system, we see in eq. 2.39 that we have to calculate the correlation function

$$\begin{aligned}\chi(t-t') = iew^2\theta(t-t')\sum_{k_1p_1\sigma}\sum_{k_2p_2\sigma'}\Big\langle &[e^{i\phi/2}c^\dagger_{Lk_1\sigma}(t)c_{Rp_1\sigma}(t) - e^{-i\phi/2}c^\dagger_{Rp_1\sigma}(t)c_{Lk_1\sigma}(t), \\ &e^{i\phi/2}c^\dagger_{Lk_2\sigma'}(t')c_{Rp_2\sigma'}(t') - e^{-i\phi/2}c^\dagger_{Rp_2\sigma'}(t')c_{Lk_2\sigma'}(t')]\Big\rangle_0 \\ &- 2ew\delta(t-t')\,\mathrm{Re}\left\langle e^{i\phi/2}\sum_{kp\sigma}c^\dagger_{Lk\sigma}c_{Rp\sigma}\right\rangle_0\end{aligned} \tag{2.41}$$

in terms of which we can write the linear response of the current as

$$\langle \hat{I}(t)\rangle = I_0 + \int_{-\infty}^{\infty} dt'\,\chi(t-t')\phi_1(t'). \tag{2.42}$$

The first term in eq. 2.42 is time-independent and gives the purely inductive contribution to the current discussed above (eq. 2.32). Fourier transforming the second term in eq. 2.42 is easy as this is just a convolution and yields the product of the Fourier transforms. We obtain

$$I(\omega) = \chi(\omega)\phi_1(\omega) = \frac{ie}{\omega}\chi(\omega)V(\omega). \tag{2.43}$$

From this we see that the response function $\chi(\omega)$ is related to the admittance as

$$Y(\omega) = \frac{ie}{\omega}\chi(\omega). \tag{2.44}$$

Hence from the response function obtained through the linear response calculation we can obtain the admittance, and by taking the real part we gain knowledge about the dissipated power. This allows us to determine the frequencies at which photons can be absorbed by the junction. We note that the second term in the response function is real, which means that it gives an imaginary contribution to the admittance, and hence doesn't contribute to the dissipation. For this reason we will not consider it in what follows. As the Hamiltonian is noninteracting, we can use Wick's theorem to evaluate

the first part of the correlation function which consists of a sum of two-particle Green's functions

$$\begin{aligned}\chi(t,0) =& iew^2\theta(t)\sum_{k_1p_1\sigma}\sum_{k_2p_2\sigma'}\langle[e^{i\phi/2}c^\dagger_{Lk_1\sigma}(t)c_{Rp_1\sigma}(t) - e^{-i\phi/2}c^\dagger_{Rp_1\sigma}(t)c_{Lk_1\sigma}(t)\\ & e^{i\phi/2}c^\dagger_{Lk_2\sigma'}(0)c_{Rp_2\sigma'}(0) - e^{-i\phi/2}c^\dagger_{Rp_2\sigma'}(0)c_{Lk_2\sigma'}(0)]\rangle_0.\end{aligned} \tag{2.45}$$

The first term evaluates to

$$\begin{aligned}&\sum_{k_1p_1\sigma}\sum_{k_2p_2\sigma'} e^{i\phi}\langle[c^\dagger_{Lk_1\sigma}(t)c_{Rp_1\sigma}(t), c^\dagger_{Lk_2\sigma'}(0)c_{Rp_2\sigma'}(0)]\rangle =\\ &\sum_{k_1p_1}\sum_{k_2p_2} e^{i\phi}\Big[- \langle c^\dagger_{Lk_1\uparrow}(t)c^\dagger_{Lk_2\downarrow}(0)\rangle\langle c_{Rp_1\uparrow}(t)c_{Rp_2\downarrow}(0)\rangle - \langle c^\dagger_{Lk_1\downarrow}(t)c^\dagger_{Lk_2\uparrow}(0)\rangle\langle c_{Rp_1\downarrow}(t)c_{Rp_2\uparrow}(0)\rangle\\ &+ \langle c^\dagger_{Lk_1\uparrow}(t)c_{Rp_2\uparrow}(0)\rangle\langle c_{Rp_1\uparrow}(t)c^\dagger_{Lk_2\uparrow}(0)\rangle + \langle c^\dagger_{Lk_1\downarrow}(t)c_{Rp_2\downarrow}(0)\rangle\langle c_{Rp_1\downarrow}(t)c^\dagger_{Lk_2\downarrow}(0)\rangle\\ &+ \langle c^\dagger_{Lk_2\uparrow}(0)c^\dagger_{Lk_1\downarrow}(t)\rangle\langle c_{Rp_2\uparrow}(0)c_{Rp_1\downarrow}(t)\rangle + \langle c^\dagger_{Lk_2\downarrow}(0)c^\dagger_{Lk_1\uparrow}(t)\rangle\langle c_{Rp_2\downarrow}(0)c_{Rp_1\uparrow}(t)\rangle\\ &- \langle c^\dagger_{Lk_2\uparrow}(0)c_{Rp_1\uparrow}(t)\rangle\langle c_{Rp_2\uparrow}(0)c^\dagger_{Lk_1\uparrow}(t)\rangle - \langle c^\dagger_{Lk_2\downarrow}(0)c_{Rp_1\downarrow}(t)\rangle\langle c_{Rp_2\downarrow}(0)c^\dagger_{Lk_1\downarrow}(t)\rangle\Big],\end{aligned} \tag{2.46}$$

where the sums over spin were performed and where it was used that $\langle c^\dagger_{i\sigma}c_{j\bar{\sigma}}\rangle = \langle c^\dagger_{i\sigma}c^\dagger_{j\sigma}\rangle = 0$. The remaining terms in eq. 2.45 yield similar contributions. Using the momentum summed greater and lesser Nambu Green's functions the correlation function can be cast in a more compact form

$$\begin{aligned}\chi(t) = iew^2\theta(t)\,\mathrm{Tr}\Big[&- \hat{t}^*G^<_{LL}(-t)\hat{t}G^>_{RR}(t) - \hat{t}G^<_{RR}(-t)\hat{t}^*G^>_{LL}(t)\\ &+\hat{t}^*G^<_{LL}(t)\hat{t}G^>_{RR}(-t) + \hat{t}G^<_{RR}(t)\hat{t}^*G^>_{LL}(-t)\\ &+\hat{t}G^<_{RL}(-t)\hat{t}G^>_{RL}(t) - \hat{t}G^<_{RL}(t)\hat{t}G^>_{RL}(-t)\\ &+\hat{t}^*G^<_{LR}(-t)\hat{t}^*G^>_{LR}(t) - \hat{t}^*G^<_{LR}(t)\hat{t}^*G^>_{LR}(-t)\Big],\end{aligned} \tag{2.47}$$

where a matrix containing the constant phase $\hat{t} = \begin{pmatrix} e^{i\phi/2} & 0 \\ 0 & e^{-i\phi/2}\end{pmatrix}$ was defined and where the local lesser Nambu Green's function is

$$G^<_{\alpha\beta}(t) = i\sum_{kp}\begin{pmatrix}\langle c^\dagger_{\beta p\uparrow}(0)c_{\alpha k\uparrow}(t)\rangle & \langle c_{\beta p\downarrow}(0)c_{\alpha k\uparrow}(t)\rangle\\ \langle c^\dagger_{\beta p\uparrow}(0)c^\dagger_{\alpha k\downarrow}(t)\rangle & \langle c_{\beta p\downarrow}(0)c^\dagger_{\alpha k\downarrow}(t)\rangle\end{pmatrix}, \tag{2.48}$$

with $(\alpha,\beta)\in\{L,R\}$. We now wish to Fourier transform eq. 2.47. As this is not entirely straightforward the calculation will be presented in some detail here. All terms in $\chi(t)$ are of the form $i\theta(t)G^<(t)G^>(-t)$, and as we know that $\chi(t)$ is a retarded Green's function its Fourier transform is defined as [12]

$$\chi^R(\omega) = \int_{-\infty}^{\infty} dt\, e^{-i\omega t-\eta t}\chi^R(t) \tag{2.49}$$

where η is a positive infinitesimal. Using also that

$$G^<(\pm t) = \frac{1}{2\pi}\int_{-\infty}^{\infty} d\omega\, e^{\mp i\omega t}G^<(\omega), \tag{2.50}$$

we can write

$$\begin{aligned}\mathcal{F}\left[i\theta(t)G^<(t)G^>(-t)\right] &= i\theta(t)\frac{1}{(2\pi)^2}\int_{-\infty}^{\infty}d\omega'\int_{-\infty}^{\infty}d\omega''\int_{-\infty}^{\infty}dt\,e^{-i\omega t-\eta t}e^{-i\omega' t}e^{i\omega'' t}G^<(\omega')G^>(\omega'')\\ &= i\frac{1}{(2\pi)^2}\int_{-\infty}^{\infty}d\omega'\int_{-\infty}^{\infty}d\omega''\int_{0}^{\infty}dt\,e^{i(\omega-\omega'+\omega'')t-\eta t}G^<(\omega')G^>(\omega'')\\ &= \frac{1}{(2\pi)^2}\int_{-\infty}^{\infty}d\omega'\int_{-\infty}^{\infty}d\omega''\frac{1}{\omega'-\omega''-\omega-i\eta}G^<(\omega')G^>(\omega'').\end{aligned} \tag{2.51}$$

Taking the limit $\eta\to 0$ and using the Sokhotski–Plemelj theorem which states that

$$\lim_{\eta\to 0^+}\int_{-\infty}^{\infty}dx\,\frac{f(x)}{x-x_0\pm i\eta} = \mp i\pi f(x_0)\delta(x-x_0)+\text{P.V.}\int_{-\infty}^{\infty}dx\,\frac{f(x)}{x-x_0} \tag{2.52}$$

by evaluating the integral over ω'' we obtain

$$\begin{aligned}\mathcal{F}\left[i\theta(t)G^<(t)G^>(-t)\right] &= \frac{1}{(2\pi)^2}\int_{-\infty}^{\infty}d\omega'\int_{-\infty}^{\infty}d\omega''\,i\pi G^<(\omega')G^>(\omega'')\delta(\omega'-\omega''-\omega)\\ &+\frac{1}{(2\pi)^2}\int_{-\infty}^{\infty}d\omega'\,\text{P.V.}\int_{-\infty}^{\infty}d\omega''\frac{1}{\omega'-\omega''-\omega}G^<(\omega')G^>(\omega'')\\ &= \frac{i}{4\pi}\int_{-\infty}^{\infty}d\omega'\,G^<(\omega')G^>(\omega'-\omega)\\ &+\frac{1}{(2\pi)^2}\int_{-\infty}^{\infty}d\omega'\,\text{P.V.}\int_{-\infty}^{\infty}d\omega''\,\frac{1}{\omega'-\omega''-\omega}G^<(\omega')G^>(\omega'').\end{aligned} \tag{2.53}$$

As mentioned above our aim is to calculate the real part of the admittance from the response function using eq. 2.44. When using the result of eq. 2.53 in eq. 2.47 we find that the contribution from the first term in eq. 2.53 to the admittance is purely real due to the form of the Green's functions (which we will see more explicitly later) whereas the second term gives a purely imaginary contribution. Hence we need to consider only the first term. Using the result for the Fourier transformation and the relation between correlation function and admittance, we find that the real part of the admittance in frequency space is given by

$$\begin{aligned}\text{Re}\,Y(\omega) = \frac{e^2w^2}{4\pi\omega}\int d\epsilon\ \text{Tr}\big[&-\hat{t}^*G^<_{LL}(\epsilon-\omega)\hat{t}G^>_{RR}(\epsilon)-\hat{t}G^<_{RR}(\epsilon-\omega)\hat{t}^*G^>_{LL}(\epsilon)\\ &+\hat{t}^*G^<_{LL}(\epsilon)\hat{t}G^>_{RR}(\epsilon-\omega)+\hat{t}G^<_{RR}(\epsilon)\hat{t}^*G^>_{LL}(\epsilon-\omega)\\ &+\hat{t}G^<_{RL}(\epsilon-\omega)\hat{t}G^>_{RL}(\epsilon)-\hat{t}G^<_{RL}(\epsilon)\hat{t}G^>_{RL}(\epsilon-\omega)\\ &+\hat{t}^*G^<_{LR}(\epsilon-\omega)\hat{t}^*G^>_{LR}(\epsilon)-\hat{t}^*G^<_{LR}(\epsilon)\hat{t}^*G^>_{LR}(\epsilon-\omega)\big].\end{aligned} \tag{2.54}$$

As the Green's functions are evaluated using the unperturbed Hamiltonian we can find the greater and lesser Green's functions using the fluctuation-dissipation theorem

$$G^<_{ij}(\omega) = -(G^R_{ij}(\omega)-G^A_{ij}(\omega))n_F(\omega)\quad G^>_{ij}(\omega) = (G^R_{ij}(\omega)-G^A_{ij}(\omega))(1-n_F(\omega)). \tag{2.55}$$

Defining the spectral function $A_{ij}(\omega,\phi) = i(G^R_{ij}(\omega,\phi) - G^A_{ij}(\omega,\phi))$ (stating explicitly the ϕ-dependence), $A_r(\omega,\phi) = A_{LL}(\omega,\phi)$ and $A_t(\omega,\phi) = A_{LR}(\omega,\phi)$, and exploiting that $A_{RR}(\omega,\phi) = A_r(\omega,-\phi)$ and $A_{RL}(\omega,\phi) = A_t(\omega,-\phi)$, we can write

$$\begin{aligned}
\mathrm{Re}\, Y(\omega) &= \frac{e^2w^2}{4\pi\omega}\int_{-\infty}^{\infty} d\epsilon\, \mathrm{Tr}\Big[\hat{t}^* A_r(\epsilon,\phi)\hat{t}A_r(\epsilon-\omega,-\phi) + \hat{t}^* A_r(\epsilon-\omega,\phi)\hat{t}A_r(\epsilon,-\phi) \\
&- \hat{t}A_t(\epsilon-\omega,-\phi)\hat{t}A_t(\epsilon,-\phi) - \hat{t}^* A_t(\epsilon-\omega,\phi)\hat{t}^* A_t(\epsilon,\phi)\Big](n_F(\epsilon-\omega) - n_F(\epsilon)) \\
&= \frac{e^2w^2}{4\pi\omega}\int_{0}^{\omega} d\epsilon\, \mathrm{Tr}\Big[\hat{t}^* A_r(\epsilon,\phi)\hat{t}A_r(\epsilon-\omega,-\phi) + \hat{t}^* A_r(\epsilon-\omega,\phi)\hat{t}A_r(\epsilon,-\phi) \\
&- \hat{t}A_t(\epsilon-\omega,-\phi)\hat{t}A_t(\epsilon,-\phi) - \hat{t}^* A_t(\epsilon-\omega,\phi)\hat{t}^* A_t(\epsilon,\phi)\Big].
\end{aligned} \tag{2.56}$$

In the last equality sign we used that the Fermi functions are Heaviside step functions at zero temperature. We also restrict ourselves to considering $\omega > 0$. The real part of the admittance is an even function as it arises from the imaginary part of the response function, and one can obtain the result for $\omega < 0$ using this property. In this expression all quantities are known as the retarded and advanced Green's functions have already been evaluated using the Dyson equation. Plugging these into the above expression yields a sum of terms which all have the same analytic structure. The whole expression takes up several pages so it will not be presented here in its entirety. Instead it will suffice to study the first two terms of the integrand in detail. They are given by

$$\begin{aligned}
&\pi\nu w\Delta\Bigg(-\frac{\sqrt{\Delta^2-(\epsilon+i\eta)^2}\left(\pi^2w^2\nu^2(1+e^{i\phi})+e^{i\phi}\right)}{(E_A-\epsilon+i\eta)(E_A+\epsilon-i\eta)} + \\
&\frac{\sqrt{\Delta^2-(\epsilon-i\eta)^2}\left(\pi^2w^2\nu^2(1+e^{i\phi})+e^{i\phi}\right)}{(E_A-\epsilon-i\eta)(E_A+\epsilon+i\eta)}\Bigg)\cdot\Big(\epsilon\leftrightarrow\epsilon-\omega\Big) + \\
&\pi\nu w\Delta\Bigg(-\frac{\sqrt{\Delta^2-(\epsilon+i\eta)^2}\left(\pi^2w^2\nu^2(1+e^{-i\phi})+e^{-i\phi}\right)}{(E_A-\epsilon+i\eta)(E_A+\epsilon-i\eta)} + \\
&\frac{\sqrt{\Delta^2-(\omega-i\eta)^2}\left(\pi^2w^2\nu^2(1+e^{-i\phi})+e^{-i\phi}\right)}{(E_A-\epsilon-i\eta)(E_A+\epsilon+i\eta)}\Bigg)\cdot\Big(\epsilon\leftrightarrow\epsilon-\epsilon\Big).
\end{aligned} \tag{2.57}$$

Here we used that the denominators which originate from the retarded and advanced Green's functions can be written as products of two simple poles because they are second order polynomials. To leading order in η the square roots can be expanded as

$$\sqrt{\Delta^2-(\epsilon\pm i\eta)} = \theta(\Delta-|\epsilon|)\sqrt{\Delta^2-\epsilon^2} \mp i\mathrm{sign}(\epsilon)\theta(|\epsilon|-\Delta)\sqrt{\epsilon^2-\Delta^2}. \tag{2.58}$$

Everywhere else in the numerator we can let $\eta = 0$. The two terms in eq. 2.57 are identical apart from the sign of the phase ϕ, and the rest of the terms appear in similar

pairs. Considering the first factor in each term of $\mathrm{Re}\, Y(\omega)$, they can all be written on the form

$$B(\epsilon) \equiv \frac{z_1(\epsilon) z_2}{(E_A - \epsilon + i\eta)(E_A + \epsilon - i\eta)} - \frac{z_1(\epsilon)^* z_2}{(E_A - \epsilon - i\eta)(E_A + \epsilon + i\eta)}, \tag{2.59}$$

where $z_1(\epsilon) = z'(\epsilon) + iz''(\epsilon)$ is a complex function of ϵ and z_2 is a (possibly complex) common factor. Using

$$\frac{1}{ab} = \frac{1}{(b-a)} \left(\frac{1}{a} - \frac{1}{b} \right), \tag{2.60}$$

we can split up the denominators as

$$\begin{aligned} B(\epsilon, \omega) &= z_2 \frac{z' + iz''}{2\epsilon} \left(\frac{1}{E_A - \epsilon + i\eta} - \frac{1}{E_A + \epsilon - i\eta} \right) - z_2 \frac{z' - iz''}{2\epsilon} \left(\frac{1}{E_A - \epsilon - i\eta} - \frac{1}{E_A + \epsilon + i\eta} \right) \\ &= \frac{z_2}{2\epsilon} \left(\frac{z' + iz''}{E_A - \epsilon + i\eta} - \frac{z' - iz''}{E_A - \epsilon - i\eta} \right) - \frac{z_2}{2\epsilon} \left(\frac{z' + iz''}{E_A + \epsilon - i\eta} - \frac{z' - iz''}{E_A + \epsilon + i\eta} \right). \end{aligned} \tag{2.61}$$

The first term in the last line becomes

$$\begin{aligned} &\frac{z_2}{2\epsilon} \left(\frac{z' + iz''}{E_A - \epsilon + i\eta} - \frac{z' - iz''}{E_A - \epsilon - i\eta} \right) \\ &= \frac{z_2}{2\epsilon} \frac{(z' + iz'')(E_A - \epsilon - i\eta) - (z' - iz'')(E_A - \epsilon + i\eta)}{(E_A - \epsilon)^2 + \eta^2} \\ &= \frac{2z_2}{2\epsilon} \frac{-i\eta z' + iz''(E_A - \epsilon)}{(E_A - \epsilon)^2 + \eta^2} = \frac{z_2}{\epsilon} \left(-i\pi z' \delta(E_A - \epsilon) + \frac{iz''}{E_A - \epsilon} \right), \end{aligned} \tag{2.62}$$

where in the last step the limit $\eta \to 0$ was taken. The other term gives a similar contribution so that we finally obtain

$$B(\epsilon, \omega) = \frac{z_2}{\epsilon} \left(-i\pi z' \delta(E_A - \epsilon) + \frac{iz''}{E_A - \epsilon} \right) - \frac{z_2}{\epsilon} \left(-i\pi z' \delta(E_A + \epsilon) + \frac{iz''}{E_A + \epsilon} \right). \tag{2.63}$$

As the limits on the integral in eq. 2.56 imply that we are only considering $0 < \epsilon < \omega$ we can discard the term with $\delta(E_A + \epsilon)$. Hence

$$\begin{aligned} B(\epsilon, \omega) &= \frac{z_2}{\epsilon} \left(-i\pi z' \delta(E_A - \epsilon) + \frac{iz''}{E_A - \epsilon} - \frac{iz''}{E_A + \epsilon} \right) \\ &= \frac{z_2}{\epsilon} \left(-i\pi z' \delta(E_A - \epsilon) + \frac{4iz''\epsilon}{E_A^2 - \epsilon^2} \right). \end{aligned} \tag{2.64}$$

Reinstating the frequency dependence of z' and z'' and multiplying this term by the

contribution from $B(\epsilon-\omega)$ yields

$$\begin{aligned}B(\epsilon)B(\epsilon-\omega) = \frac{z_2^2}{\epsilon(\epsilon-\omega)}\Big(&- \frac{4\epsilon(\epsilon-\omega)z''(\epsilon)z''(\epsilon-\omega)}{(\epsilon^2-E_A^2)((\epsilon-\omega)^2-E_A^2)} \\ &+ 2\pi\frac{\epsilon z''(\epsilon)z'(\epsilon-\omega)}{\epsilon^2-E_A^2}\delta(E_A+\epsilon-\omega) + 2\pi\frac{(\epsilon-\omega)z''(\epsilon-\omega)z'(\epsilon)}{(\epsilon-\omega)^2-E_A^2}\delta(E_A-\epsilon) \\ &- \pi^2 z'(\epsilon)z'(\epsilon-\omega)\delta(E_A-\epsilon)\delta(E_A+\epsilon-\omega)\Big) \\ &= ① + ② + ③ + ④.\end{aligned} \tag{2.65}$$

For each term with a given z_2 there is an identical term with z_2^* multiplied by the same factor (also seen in eq. 2.57), so when adding them we do get a real number as postulated earlier. The four terms in the above expression give rise to different contributions to the admittance which all have a physical interpretation.

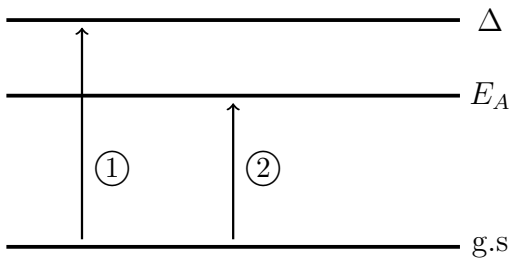

Figure 2.4: Single-particle excitation spectrum of the QPC in the absence of quasiparticles. The Andreev level is spin-degenerate and two quasiparticles of opposite spin can hence occupy this state.

Adding all terms with the structure ① we get

$$\begin{aligned}\mathrm{Re}\, Y_1(\omega) = \frac{e^2\tau}{\pi\omega}\int_0^\omega d\epsilon\, \frac{\sqrt{\epsilon^2-\Delta^2}}{\epsilon^2-E_A^2}\frac{\sqrt{(\omega-\epsilon)^2-\Delta^2}}{(\omega-\epsilon)^2-E_A^2}\epsilon(\omega-\epsilon)\left(1-\frac{\Delta^2\cos(\phi)+\Delta^2-E_A^2}{\epsilon(\omega-\epsilon)}\right) \\ \theta(|\epsilon|-\Delta)\theta(|\epsilon-\omega|-\Delta) \\ = G\frac{\theta(\omega-2\Delta)}{\omega}\int_\Delta^{\omega-\Delta} d\epsilon\, \rho(\epsilon)\rho(\omega-\epsilon)|z_{\epsilon,\omega}|^2,\end{aligned} \tag{2.66}$$

where following ref. [5] we defined the quantities $\rho(\epsilon) = \epsilon\sqrt{\epsilon^2-\Delta^2}/(\epsilon^2-E_A^2)$ and $|z_{\epsilon,\omega}|^2 = 1-(\Delta^2\cos(\phi)+\Delta^2-E_A^2)/\epsilon(\omega-\epsilon)$ which are reminiscent of an occupation factor (or density of states) and a transition matrix element. The second contribution comes from ② and ③

$$\mathrm{Re}\, Y_2(\omega) = \pi G\frac{\theta(\omega-E_A-\Delta)}{\omega}\sqrt{\Delta^2-E_A^2}\rho(\omega-E_A)|z_{E_A,\omega}|^2, \tag{2.67}$$

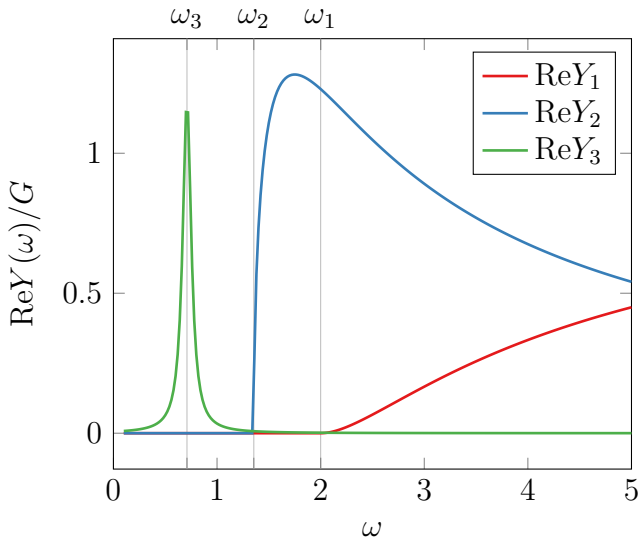

Figure 2.5: The three terms contributing to $\mathrm{Re}\, Y(\omega)$ for $\tau = 0.9$, $\Delta = 1$ and $\phi = 2.8$. The $\delta-$function in Y_3 has been given a finite width to make it visible by using a finite value of η. This also means that the height of the peak is arbitrary. The gridlines are located at frequencies $\omega_3 = 2E_A$, $\omega_2 = E_A + \Delta$ and $\omega_1 = 2\Delta$.

and from terms of the form ④ we obtain

$$\mathrm{Re}\, Y_3(\omega) = \pi^2 G \frac{(\Delta^2 - E_A^2)(E_A^2 - \Delta^2\cos(\phi))}{2E_A^3}\delta(\omega - 2E_A). \tag{2.68}$$

This concludes our calculation of the real part of the admittance and a plot of the three different contributions can be seen in fig. 2.5. If needed, the corresponding imaginary part can be determined using equation 2.53 or from eqs. 2.66-2.68 by invoking the Kramers-Kronig relations because the admittance is analytic in the upper complex half plane (as it arises from a retarded Green's function which has poles in the lower half plane).

Using eq. 1.27 we can directly relate $\mathrm{Re}\, Y$ to the absorbed power by inserting that $\phi_1 = eV_0/\omega$

$$\langle P\rangle = \frac{\phi_1^2}{2e^2}\omega^2\, \mathrm{Re}\, Y. \tag{2.69}$$

The related transition rate which is also the absorption rate of photons is obtained as $\Gamma = \langle P\rangle/\hbar\omega$, so that (reinstating $\hbar$)

$$\Gamma = \frac{\phi_1^2}{2e^2}\hbar|\omega|\, \mathrm{Re}\, Y. \tag{2.70}$$

We can now give an estimate of the order of magnitude of the absorption rate. The frequency is $\hbar\omega \sim \Delta$ where taking Al as an example $\Delta = 3.4{\cdot}10^{-4}eV$. The contributions

to $\mathrm{Re}\, Y$ are on the order of $G_0 = 2e^2/h$, and we are studying the regime of linear response where $\phi_1 \ll 1$, so taking $\phi_1 = 10^{-2}$ we obtain

$$\Gamma \sim \phi_1^2 \frac{\Delta}{h} \sim 8 \cdot 10^6 \mathrm{s}^{-1}. \tag{2.71}$$

The different contributions to the admittance can be interpreted as arising from processes where the absorption of a photon causes the creation of a pair of quasiparticles whereby the system ends up in an excited state. The excitation spectrum is schematically depicted in fig. 2.4. Y_1 has threshold frequency $\omega = 2\Delta$ and arises from the process where two quasiparticles are created in the superconducting continuum. This corresponds to two of the process denoted ① in fig. 2.4.

Y_2 has threshold frequency $\omega = \Delta + E_A$ and arises from the creation of one quasiparticle in the bound state and one in the continuum; ①+② in fig. 2.4. Finally, Y_3 which is only nonzero for $\omega = 2E_A$ is associated with the creation of two quasiparticles of opposite spin in the bound state. In fig. 2.6 we plot the magnitude of $\mathrm{Re}\, Y_3$ for $\omega = 2E_A$, and from this we see that the absorption due to this excitation process increases as the bound states move deeper into the gap and approach zero energy.

In later chapters we will get back to the reason why all absorption processes are related to creation of quasiparticle pairs and never single quasiparticles. But in this simple system it is not surprising, as in the BCS-ground state (which is modified by the negative energy Andreev level), quasiparticles can only be provided by splitting a Cooper pair which results in the creation of two quasiparticles. Having established a formalism which allows us to calculate and interpret the admittance of a Josephson junction when the Green's functions are known, we are now ready to tackle more complicated models, and in the next chapter we will proceed by studying an S-QD-S junction.

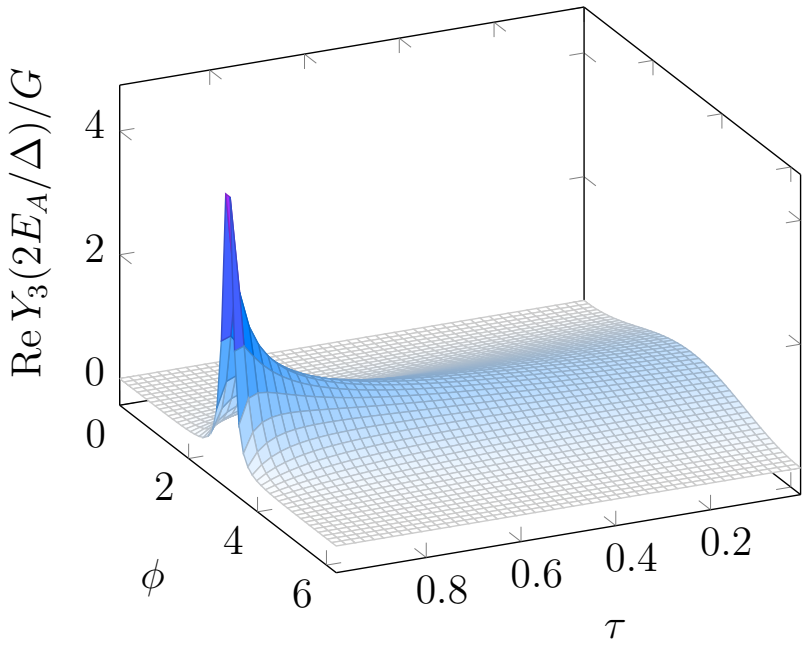

Figure 2.6: Magnitude of $\mathrm{Re}\, Y_3(\omega = 2E_A/\Delta)$. It is clear that the contribution to the dissipative admittance arising from the creation of two quasiparticles in the Andreev bound state increases drastically as the bound state approaches zero energy, which happens for $\tau = 1$ and $\phi = \pi$. We thus expect the absorption to be largest when the bound states are deep inside the gap.

Chapter 3

Magnetic impurity

In this chapter we calculate the response function for a Josephson junction described by the Anderson model using the method of the previous chapter. This reveals information about the photon absorption properties of an S-QD-S junction which has a bound state spectrum exhibiting richer features compared to the simple, spin-degenerate Andreev bound states. Prior to this, we will calculate the Green's functions and study the subgap states in some detail to gain insight into the most important properties of the system.

3.1 Green's functions

We consider a Josephson junction with an interacting quantum dot between the two superconducting leads described by the Anderson model with Hamiltonian [18]

$$\begin{aligned} H &= H_{LR} + H_T + H_d \\ H_{LR} &= \sum_{\alpha k\sigma} \xi_{k\sigma} c^\dagger_{\alpha k\sigma} c_{\alpha k\sigma} - \sum_{\alpha k} \left(\Delta_\alpha c^\dagger_{\alpha k\uparrow} c^\dagger_{\alpha -k\downarrow} + \Delta^*_\alpha c_{\alpha -k\downarrow} c_{\alpha k\uparrow} \right) \\ H_T &= \sum_{\alpha k\sigma} (t_\alpha c^\dagger_{\alpha k\sigma} d_\sigma + t^*_\alpha d^\dagger_\sigma c_{\alpha k\sigma}) \\ H_d &= \sum_\sigma \xi_d d^\dagger_\sigma d_\sigma + U n_{d\uparrow} n_{d\downarrow}. \end{aligned} \tag{3.1}$$

Due to the quartic interaction term, this problem is not exactly solvable. To simplify it sufficiently to allow for an analytic treatment, we restrict ourselves to considering the Coulomb diamond where the dot is occupied by a single electron. This is a good approximation in the case where the doubly occupied states are well separated in energy from the singly occupied ones, which requires $\Delta/U \ll 1$, where U is the strength of the Coulomb interaction. By performing a Schrieffer-Wolff transformation, one can then describe the system in terms of an effective cotunneling model. In the cotunneling regime transport across the quantum dot due to sequential tunneling is blocked and only higher-order cotunneling processes couple the dot and leads. We will not go

through the Schrieffer-Wolff transformation here as detailed treatments are already given elsewhere, see [19] and [20]. The resulting Hamiltonian is $H = H_{LR} + H_J + H_W$ with H_{LR} given in eq. 3.1 and

$$H_J = \sum_{\substack{i=x,y,x \\ \alpha k\sigma, \alpha' k'\sigma'}} J_{\alpha\alpha'} S^i c^\dagger_{\alpha k\sigma} \tau^i_{\sigma\sigma'} c_{\alpha' k'\sigma'} \tag{3.2}$$

$$H_W = \sum_{\alpha k\sigma, \alpha' k'} W_{\alpha\alpha'} c^\dagger_{\alpha k\sigma} c_{\alpha' k'\sigma}. \tag{3.3}$$

Here τ^i are the Pauli matrices, and $\alpha \in (L, R)$ is the lead index. H_J describes the exchange interaction with the impurity spin, (which acts as a magnetic impurity) and H_W gives the potential scattering. To simplify the model further, we will employ the classical spin approximation where the spin of the magnetic impurity is assumed to be fixed in the $\hat{z}-$direction, and is hence treated as a classical variable. In this case H_J becomes

$$H_J = \sum_{\alpha k\sigma, \alpha' k'} J_{\alpha\alpha'} S\sigma c^\dagger_{\alpha k\sigma} c_{\alpha' k'\sigma}. \tag{3.4}$$

We use the results of ref. [18] to parametrize the couplings $J_{\alpha\alpha'}$ and $W_{\alpha\alpha'}$ by an angle θ which determines the coupling asymmetry between the leads. Furthermore we will as in the last chapter perform a gauge transformation to transfer the (constant) phase dependence from the superconducting order parameter to the coupling constants t_α. Hence the matrices $\mathbf{W} = W\mathbf{\Theta}$ and $\mathbf{J} = J\mathbf{\Theta}$ in lead space are given by

$$\mathbf{\Theta} = \begin{pmatrix} \cos^2(\theta) & \sin(\theta)\cos(\theta)e^{i\phi/2} \\ \sin(\theta)\cos(\theta)e^{-i\phi/2} & \sin^2(\theta) \end{pmatrix}. \tag{3.5}$$

For $\theta = \pi/4$ the coupling is symmetric and small angles $\theta \ll 1$ correspond to a dot which is strongly coupled to the left lead and weakly coupled to the right lead. With these definitions the interaction strengths arising from the Schrieffer-Wolff transformation are given by

$$J = \frac{4}{1-x^2}\frac{t_L^2 + t_R^2}{U} \quad \text{and} \quad W = \frac{2x}{1-x^2}\frac{t_L^2 + t_R^2}{U}. \tag{3.6}$$

The parameter $x \in (-1, 1)$ is given by $x = 1 + 2\xi_d/U$ and is to be understood as the gate voltage determining the displacement from the particle-hole-symmetric point in the middle of the oddly occupied Coulomb diamond. In the Green's functions we wish to express the strength of the potentials in terms of a dimensionless parameter. Hence we define the dimensionless quantitites $g = \pi\nu_F JS$ and $w = \pi\nu_F W$ so that

$$w = c\frac{2x}{1-x^2}, \quad g = c\frac{4}{1-x^2} \quad \text{with} \quad c = \pi\nu_F\frac{t_L^2 + t_R^2}{U}. \tag{3.7}$$

Physically c is the dimensionless strength of the exchange interaction in the particle-hole symmetric point where $w = 0$.

As was the case for the weak-link junction, we wish to do the calculations in Nambu space. However, it turns out (quite subtlely) that we can no longer use the same two-Nambu spinor as was used previously, $\psi^\dagger_{\alpha k} = \begin{pmatrix} c^\dagger_{\alpha k\uparrow} & c_{\alpha -k\downarrow}\end{pmatrix}$. Even though it is possible to write the Hamiltonian in this basis, it limits us to consider only spin up-quasiparticles, and hence we would not find the full solution to the problem. This was not an issue in the QPC due to the Andreev bound states being spin-degenerate. To remedy this we use the spin-indexed Nambu-spinors

$$\psi^\dagger_{\alpha k\sigma} = \begin{pmatrix} c^\dagger_{\alpha k\sigma}, & c_{\alpha -k\bar{\sigma}}\end{pmatrix} \quad \text{and} \quad \psi_{\alpha k\sigma} = \begin{pmatrix} c_{\alpha k\sigma} \\ c^\dagger_{\alpha -k\bar{\sigma}}\end{pmatrix}. \tag{3.8}$$

In spin-dependent problems, four-Nambu spinors are often used, as this is necessary if spin-flip processes are to be considered, eg. if one wishes to go beyond the classical-spin approximation and consider a quantum mechanical treatment of the impurity spin (see [18]). However, in the classical spin approximation, even if four-spinors are used the Green's functions turn out to be spin-diagonal as our Hamiltonian contains no spin-flip terms. Using the classical spin-approximation enables us to use two-spinors and find an exact solution to the problem at the cost of loosing the ability to describe the effects of the quantum mechanical nature of the impurity spin. In this basis the superconducting part of the Hamiltonian has the same form as what we have previously seen, whereas H_J contributes with a spin-dependent interaction (as is already visible from the Hamiltonian above), but apart from that the form of the Hamiltonian is similar to what we have previously studied and is given by

$$H = \frac{1}{2}\sum_{\alpha k\sigma} \psi^\dagger_{\alpha k\sigma}\mathbf{m}^{SC}_{k\sigma}\psi_{\alpha k\sigma} + \frac{1}{2}\sum_{kk'\sigma} \psi^\dagger_{Lk\sigma}\mathbf{w}^R_{L\sigma}\psi_{Lk'\sigma} + \tag{3.9}$$

$$\frac{1}{2}\sum_{kk'\sigma} \psi^\dagger_{Rk\sigma}\mathbf{w}^R_{R\sigma}\psi_{Rk'\sigma} + \frac{1}{2}\sum_{kk'\sigma} (\psi^\dagger_{Lk\sigma}\mathbf{w}^T_{\sigma}\psi_{Rk'\sigma} + h.c.). \tag{3.10}$$

Where

$$\mathbf{m}^{SC}_{k\sigma} = \begin{pmatrix} \xi_k & -\sigma\Delta \\ -\sigma\Delta & -\xi_k\end{pmatrix}. \tag{3.11}$$

The backscattering (reflection) in the indidvidual leads is described by

$$\mathbf{w}^R_{L\sigma} = \begin{pmatrix} JS\sigma + W & 0 \\ 0 & JS\sigma - W\end{pmatrix}\cos^2(\theta) \tag{3.12}$$

and

$$\mathbf{w}^R_{R\sigma} = \begin{pmatrix} JS\sigma + W & 0 \\ 0 & JS\sigma - W\end{pmatrix}\sin^2(\theta). \tag{3.13}$$

Furthermore

$$\mathbf{w}^T_{\sigma} = \begin{pmatrix} (JS\sigma + W)e^{i\phi/2} & 0 \\ 0 & (JS\sigma - W)e^{-i\phi/2}\end{pmatrix}\cos(\theta)\sin(\theta) \tag{3.14}$$

describes tunneling between the leads. We should now determine an equation for the Matsubara Green's functions which are diagonal in spin space and defined as

$$\mathcal{G}_{\alpha\alpha',\sigma}(\tau-\tau') = -\sum_{kk'}\langle T_\tau \psi_{\alpha k\sigma}(\tau)\psi^\dagger_{\alpha' k'\sigma}(\tau')\rangle. \tag{3.15}$$

There is a complication due to the use of spin-dependent Nambu spinors which means that we can't directly generalize the Dyson equation for the QPC to this case even though the form of the Hamiltonian is very similar. Namely that they don't obey the ordinary fermionic commutation relations. Instead we find that

$$\{\psi^\dagger_{\alpha k\sigma}, \psi_{\beta k'\sigma'}\} = \delta_{\alpha,\beta}\delta_{k,k'}\delta_{\sigma,\sigma'}\tau_0 \quad \{\psi_{\alpha k\sigma}, \psi_{\beta k'\sigma'}\} = \delta_{\alpha,\beta}\delta_{k,-k'}\delta_{\sigma,\bar{\sigma}'}\tau_x. \tag{3.16}$$

In the equation of motion for the Green's function we are calculating the quantity $[H,\psi_{\alpha k\sigma}](\tau)\psi^\dagger_{\alpha k'\sigma'}(\tau')$, so we follow ref. [20] and evaluate the commutator with the Hamiltonian using the modified commutation relations given above. To this end we also note that we can write the Hamiltonian compactly as

$$H = \frac{1}{2}\sum_{\alpha\alpha',kk',\sigma}\psi^\dagger_{\alpha k\sigma}\mathbf{m}_{\alpha\alpha',kk',\sigma}\psi_{\alpha' k'\sigma}. \tag{3.17}$$

The commutator is then

$$\begin{aligned}\Big[H,\psi_{\alpha k\sigma}\Big] &= \frac{1}{2}\sum_{\beta\beta',pp',\sigma'}\Big(\psi^\dagger_{\beta p\sigma'}\mathbf{m}_{\beta\beta',pp',\sigma'}\psi_{\beta' p'\sigma'}\psi_{\alpha k\sigma} - \psi_{\alpha k\sigma}\psi^\dagger_{\beta p\sigma'}\mathbf{m}_{\beta\beta',pp',\sigma'}\psi_{\beta' p'\sigma'}\Big)\\ &= \frac{1}{2}\sum_{\beta\beta',pp',\sigma'}\Big(\psi^\dagger_{\beta p\sigma'}\mathbf{m}_{\beta\beta',pp',\sigma'}(\delta_{\alpha,\beta'}\delta_{k,-p'}\delta_{\sigma\bar{\sigma}'}\tau_x - \psi_{\alpha k\sigma}\psi_{\beta' p'\sigma'})-\\ &(\delta_{\alpha,\beta}\delta_{k,p}\delta_{\sigma\sigma'}\tau_0 - \psi^\dagger_{\beta p\sigma'}\psi_{\alpha k\sigma})\mathbf{m}_{\beta\beta',pp',\sigma'}\psi_{\beta' p'\sigma'}\Big).\end{aligned} \tag{3.18}$$

We use that

$$\tau_x\mathbf{m}_{\beta\beta',pp',\sigma} = -\mathbf{m}_{\beta\beta',pp',\bar{\sigma}}\tau_x,$$
$$\psi_{\alpha k\sigma}\tau_x = \psi_{\alpha -k\bar{\sigma}}$$

and

$$\mathbf{m}_{\beta\beta',pp',\sigma} = \mathbf{m}_{\beta'\beta,p'p,\sigma} = \mathbf{m}_{\beta\beta',-pp',\sigma} = \mathbf{m}_{\beta\beta',-p-p',\sigma}$$

to obtain

$$\begin{aligned}\Big[H,\psi_{\alpha k\sigma}\Big] &= -\frac{1}{2}\sum_{\beta p}\Big(\psi_{\beta p\bar{\sigma}}\sigma_x\mathbf{m}_{\beta\alpha,p-k,\sigma} + \mathbf{m}_{\alpha\beta,kp',\sigma}\psi_{\beta p'\sigma}\Big)\\ &= -\sum_{\beta p}\mathbf{m}_{\alpha\beta,kp,\sigma}\psi_{\beta p\sigma}.\end{aligned} \tag{3.19}$$

This has the characteristic form which we expect to see in the equation of motion for a bilinear Hamiltonian and is what we would have obtained if the Nambu spinors

had obeyed the usual fermionic commutation relations. Hence we can immediately generalize our result from the equation of motion-calculations for the QPC to find that in the full, combined lead and Nambu space the Dyson equation for the Matsubara Green's function is given by:

$$\mathcal{G}_\sigma(i\omega_l) = \tilde{\mathcal{G}}_{0\sigma}(i\omega_l) + \tilde{\mathcal{G}}_{0\sigma}(i\omega_l)\mathbf{\Sigma}_\sigma\mathcal{G}_\sigma(i\omega_l), \tag{3.20}$$

where $\tilde{\mathcal{G}}_{0,\alpha\alpha'\sigma}(i\omega_l) = \tilde{\mathcal{G}}_{0,\alpha\sigma}(i\omega_l) = (1 - \mathcal{G}_{0\sigma}(i\omega_l)\mathbf{w}^R_{\alpha\sigma})^{-1}\mathcal{G}_{0\sigma}(i\omega_l)$ is diagonal in lead space and $\mathcal{G}_{0\sigma}(i\omega_l)$ is the bare Nambu Green's function for the BCS-Hamiltonian which is now spin-dependent ($\Delta \to \sigma\Delta$). The spin-dependent self-energy is

$$\mathbf{\Sigma}_\sigma = \begin{pmatrix} 0 & \mathbf{w}^T_\sigma \\ (\mathbf{w}^T_\sigma)^\dagger & 0 \end{pmatrix}. \tag{3.21}$$

From the Matsubara Green's function we can then as usual obtain the retarded and advanced Green's functions by analytical continuation. We are also interested in the bound state energies which are obtained as the poles of the Green's function. The denominator of the retarded Green's function is given by

$$D_\sigma(\omega + i\eta) = (1 + \chi u)\Delta^2 - (1 + u)(\omega + i\eta)^2 + 2g\sigma\omega\sqrt{\Delta^2 - (\omega + i\eta)^2}, \tag{3.22}$$

where $u = w^2 - g^2$ and $\chi = 1 - \sin^2(2\theta)\sin^2(\phi/2)$. We find the bound state energies by letting $\eta \to 0$ in the denominator, equating it to zero and solving for ω

$$0 = (1 + \chi u)\Delta^2 - (1 + u)\omega^2 + 2g\sigma\omega\sqrt{\Delta^2 - \omega^2} \tag{3.23}$$

$$\Rightarrow -(1 + \chi u)\Delta^2 + (1 + u)\omega^2 = 2g\sigma\omega\sqrt{\Delta^2 - \omega^2} \tag{3.24}$$

$$\Rightarrow ((1 + \chi u)\Delta^2 - (1 + u)\omega^2)^2 = 4g^2\omega^2(\Delta^2 - \omega^2). \tag{3.25}$$

Solving the last equation in the expression above for ω^2 yields

$$E^2_\pm = \Delta^2\frac{2g^2 + (1 + u)(1 + \chi u) \pm 2g\sqrt{g^2 + u(1 - \chi)(1 + \chi u)}}{4g^2 + (1 + u)^2}. \tag{3.26}$$

In order to find the solutions for E we must fix the signs so that eq. 3.24 is also satisfied, which introduces a spin-dependency of the bound state energies. Dividing both sides of eq. 3.24 by Δ^2 reveals that the sign of the left hand side for $E_\pm$ is determined by the quantity

$$s_\pm = \text{sign}\Big(g(u - 1 - 2u\chi) \pm (1 + u)\sqrt{g^2 + u(1 - \chi)(1 + u\chi)}\Big). \tag{3.27}$$

A graphical analysis reveals that this is the same as

$$s_- = -\text{sign}(1 + \chi u) \quad \text{and} \quad s_+ = \text{sign}(u) \tag{3.28}$$

for $g > 0$. We can then write the bound state energies as

$$E_{\pm\sigma} = \frac{s_\pm \sigma \Delta}{\sqrt{(1+u)^2+4g^2}} \left(2g^2 + (1+\chi u)(1+u) \pm 2g\sqrt{g^2 + u(1-\chi)(1+\chi u)} \right)^{1/2}. \quad (3.29)$$

We now see that adding a spin-dependent potential to our model breaks the spin degeneracy of the bound states, and we get four distinct bound state energies which can each be occupied by a single quasiparticle of a specific spin. We remind ourselves that the origin of the potential scattering term w is the Coulomb repulsion on the quantum dot. For this reason, whenever $w \neq 0$ ($x \neq 0$) particle-hole symmetry is broken. In fig. 3.1 we plot some of the normal (diagonal) components of the spectral function $A(\omega) = -2\,\mathrm{Im}\, G^R(\omega + i\eta)$. Here we see how the divergence of the density of states at the superconducting gap is removed and that the spectral function exhibits discrete peaks at the bound state energies. The breaking of particle-hole symmetry for $x \neq 0$ is seen in the spectral function getting asymmetric. It should be noted, that even though particle-hole symmetry is broken, there is still a well-defined equivalence between the creation of a spin-up quasiparticle at positive energy, and the removal of a spin-down quasiparticle (creation of a spin-up hole) at negative energies. We will elaborate on this in section 4.1.

We will now study the bound states in some detail to understand how they should be interpreted. If we allow w and g to vary freely instead of using the parametrization in eq. 3.7 in terms of the displacement from the particle-hole symmetric point, we can gain some intuition about the nature of the bound states. By setting $g = 0$ and $\theta = \pi/4$ in eq. 3.29 the subgap states reduce to the Andreev bound states $E_{\pm\sigma} = \pm\sigma\Delta\sqrt{1 - \tau\sin^2(\phi/2)}$ with $\tau = w^2/(1+w^2)$. If we then add a small exchange coupling $g \ll w$, we see that the effect of this is to split the spin-degenerate Andreev level into two bound states with different spin. This is seen in fig. 3.2, and as expected the states with spin-up are pushed up in energy and those with spin-down are pushed down in energy by the exchange interaction. We will see later that a similar result is obtained when applying a magnetic field in the $+\hat{z}-$direction to a noninteracting quantum dot. Note that strictly speaking this regime is not included in our model, as to reach the oddly occupied regime where the effective cotunneling model is valid, one has to use the correct parametrization in terms of the displacement from the particle-hole symmetric point $x = 0$. Hence we can not by varying x go continously from the case of spin-split ABS for weak exchange interaction to the effective cotunneling model. However, we will see later that when treating interaction with the magnetic impurity as a scattering problem, we can reach both regimes when varying the strength of the magnetic and non-magnetic parts of the scattering potential.

Our model exhibits two different branches of bound states - $E_{+\sigma}$ and $E_{-\sigma}$. This is related to the fact that what we are studying is a two-channel problem, where for $\phi \neq 0$ the two channels are coupled which is shown in appendix C. The two channels arise from the even and odd combinations of electrons in the left and right lead. After a diagonalization of the cotunneling part of the Hamiltonian, only the even sector

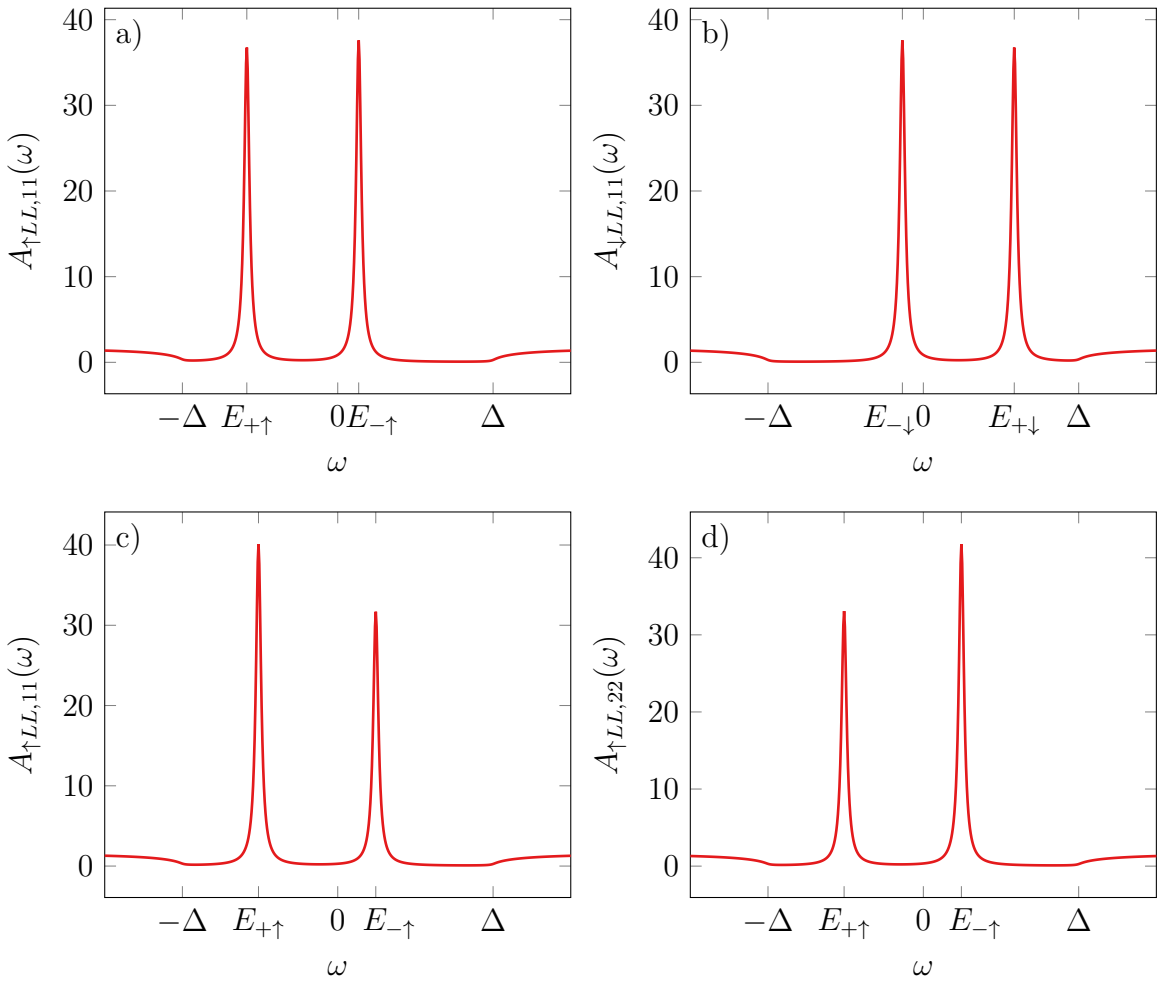

Figure 3.1: Normal components of the spectral function for the left lead for the parameters $c = 1$, $\phi = 3\pi/4$, $\eta = 0.02$ and $\theta = \pi/4$. In a) and b) in the particle-hole symmetric point $x = 0$ and in c) and d) for $x = 0.7$. The spectral functions exhibit peaks at the bound state energies, and we see that the divergence of the density of states at Δ characteristic for homogeneous superconductors is no longer present. In c) and d) particle-hole symmetry is broken, which is seen in the asymmetry of the spectral function where peaks from the electron- and hole-sector of the spectral function have different heights.

appears here. As we will see shortly the bound states $E_{+\sigma}$ are absent for $\phi = 0$, and we can conclude that they arise from the odd sector and require a coupling between the two sectors to form. In this sense they are reminiscent of the Andreev bound states, which also require two superconductors with non-zero phase bias which are coupled by a tunneling mechanism. In contrast, the bound states $E_{-\sigma}$ are present even for $\phi = 0$ and arise from the even sector. These states can cross zero energy as the phase or the strength of the exchange interaction are varied.

To understand the YSR-state and the meaning of the zero-energy crossing, we consider the case of $\phi = 0$ and $x = 0$. Here only the YSR-state with energy $E_{-\sigma} = -\Delta\sigma\frac{1-g^2}{1+g^2}$ is present. This is the expression first obtained by Yu, Shiba and Rusinov ([2], [3] and [4]). The bound state energies are plotted in fig. 3.4 a) as a function of coupling strength. At $g = 0$, the impurity spin is unscreened and the ground state is a BCS state where all electrons are bound in Cooper pairs. If we had been studying a quantum mechanical impurity spin and not a classical one, this state would have been a doublet state with a single unpaired electron [18]. As the coupling is increased, a spin-down subgap state forms and its energy decreases towards zero. This happens because the energy gained by having a single quasiparticle in the system which screens the impurity spin increases with increasing coupling strength. The same happens for a subgap state at $E < 0$ related to the removal of a quasiparticle of opposite spin. At some point ($g = g_{crit}$) the exchange coupling gets so large that the energy gained by screening the impurity with a quasiparticle of opposite spin exceeds the energy cost of having an unpaired quasiparticle in the lead (which is the pairing energy Δ). At this value of $g = g_{crit}$ the YSR-states cross zero energy, and this crossing signifies a change of ground state. For strong coupling the ground state has a single unpaired quasiparticle localized near the impurity. For a classical spin, the screening can only be partial, but in a quantum mechanical treatment, this would be a fully screened singlet state. This is shown in ref. [18] for a perturbative expansion in the exchange interaction.

For a classical spin Balatsky, Vekhter and Zhu [21] write the wave functions for these two states in terms of the BCS ground state (excluding the classical spin which just acts as a local magnetic field in their description). For $g < g_{crit}$ the ground state can be written as a product of states with zero and one Cooper pair

$$|\Phi_0\rangle = \prod_i (u_i + v_i c_i^\dagger c_{-i}^\dagger)\,|0\rangle\,. \tag{3.30}$$

Here $i > 0$ is the basis which diagonalizes the Hamiltonian (we will later see explicitly what this basis is), and a state with $-i$ is a time-reversed state, which for the bound states just has opposite spin. The state labelled $i = 1$ is the excited state with the lowest energy, which is the screened state. This is as mentioned the state with a single spin-down quasiparticle residing near the dot which screens the impurity spin so that they form a singlet-like bound state, namely

$$|\Phi_1\rangle = \gamma_{-1}^\dagger\,|\Phi_0\rangle\,, \tag{3.31}$$

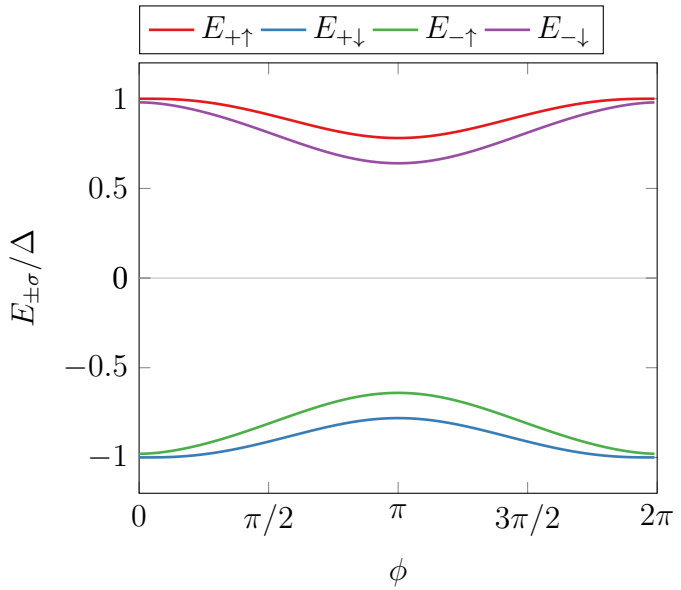

Figure 3.2: For a finite $w = 1$ and small exchange coupling $g = 0.2$ the Andreev bound states become spin-split. We have used $\theta = \pi/4$.

where $\gamma_i^\dagger$ is the Bogoliubov quasiparticle creation operator. At $g > g_{crit}$ where the subgap states cross zero energy, the ground state changes so that $|\Phi_1\rangle$ is the new ground state, and $|\Phi_0\rangle$ becomes an excited state. The ground state changes parity at the phase transition, as the number of unpaired electrons changes.

For a finite value of ϕ all four bound states are present. In fig. 3.3 we show the bound state energies as a function of phase difference for two different coupling strengths in the particle-hole symmetric point $x = 0$. In fig. 3.3 a) the exchange coupling is weak ($c = 0.1$), and bound the states with spin down (up) remain above (below) zero energy for all values of ϕ in accordance with the description given above. When increasing the coupling strength to $c > c_{crit}$, as seen in fig. 3.3 b) ($c = 0.3$,) the screened state is the groundstate for $\phi = 0$. The excited YSR-state $E_{-\uparrow}$ is related to the creation of a spin-up quasiparticle or equivalently the removal of one with spin-down (due to particle-hole symmetry). That is, in the first excited state the impurity is unscreened. The YSR-states approach zero from above and below and eventually cross. The value of ϕ where this happens approaches π if the coupling strength is increased. From this we see that we can also obtain the change of ground state mentioned above by keeping the coupling strength constant and varying the phase. Increasing the value of x to move away from the particle-hole symmetric point has the effect of breaking the degeneracy at $\phi = \pi$ and increasing the phase where the ground state changes towards $\phi = \pi$, see fig. 3.4 b). This can also be achieved by adding a coupling asymmetry $\theta \neq \pi/4$.

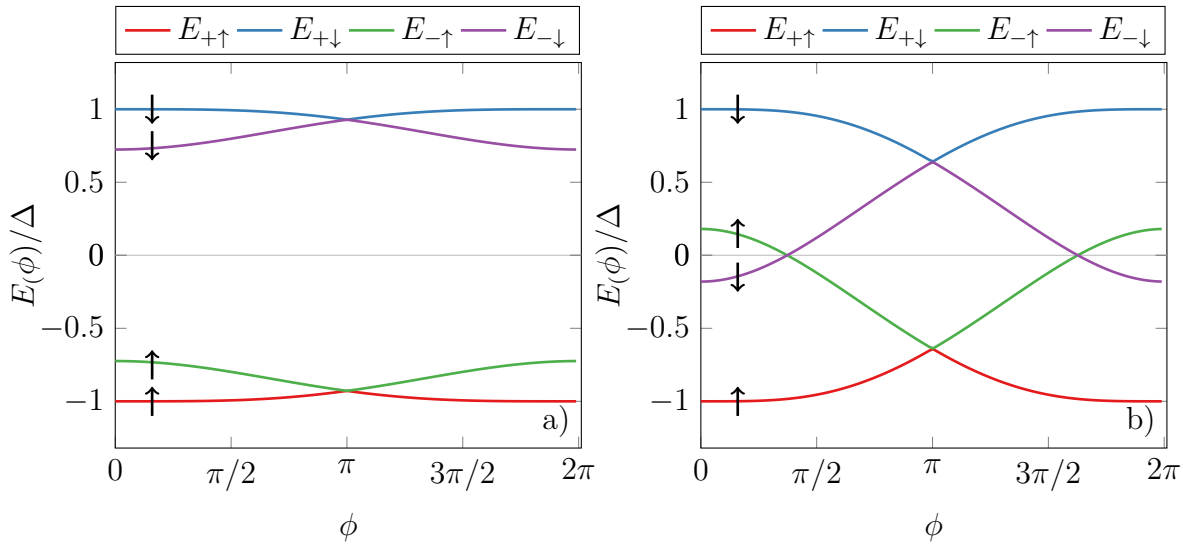

Figure 3.3: Bound state energies as a function of phase difference in the particle-hole symmetric point $x = 0$. We also consider symmetric coupling between the leads and the dot $\theta = \pi/4$. In a) the exchange coupling is weak, $c = 0.1$. In b) we see that when the coupling strength is increased ($c = 0.9$) the state $E_{-\downarrow}$ ($E_{-\uparrow}$) is pushed down (up) in energy at $\phi = 0$, and that the states $E_{-\sigma}$ cross zero energy at approximately $\phi \simeq \pi/2$ where the ground state changes.

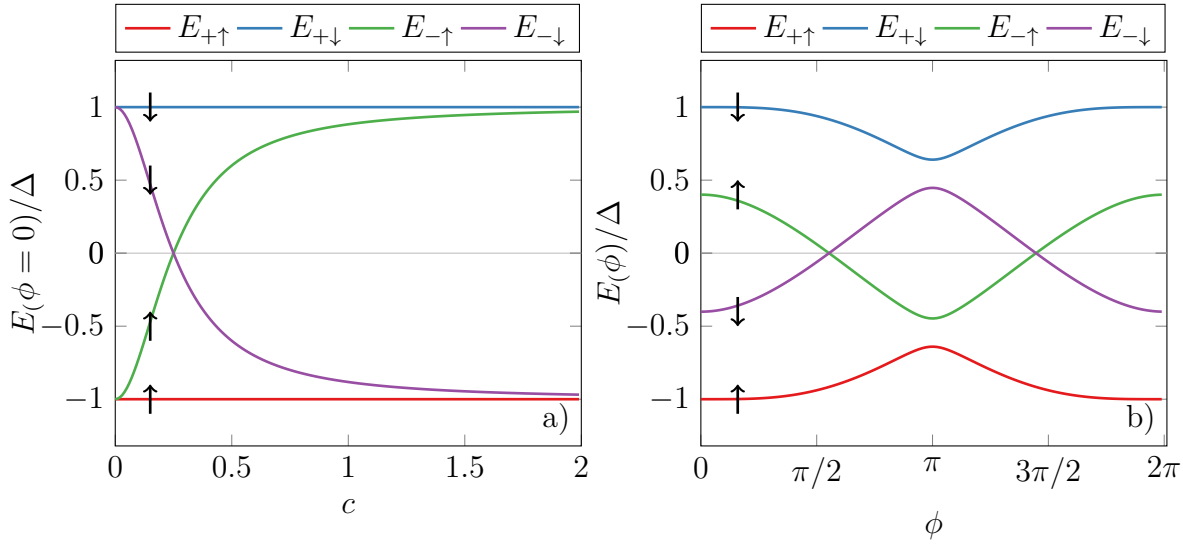

Figure 3.4: a) Bound state energies as a function of coupling strength for $x = 0$, $\phi = 0$ and $\theta = \pi/4$. At the critical coupling strength $c = c_{crit}$ the excited state with a single quasiparticle with spin down screening the impurity spin crosses zero energy an becomes the new ground state. b) Bound state energies as a function of phase difference for intermediate coupling ($c = 0.3$ and $\theta = \pi/4$) away from the particle-hole symmetric point ($x = 0.5$). This breaks the degeneracy of the subgap states at $\phi = \pi$.

3.2 Josephson current

We will start by considering the current across the junction in the case where there is a constant phase difference between the leads. We have already derived an expression for the expectation value of the current in a QPC in eq. 2.27, and the result is readily generalized to the present case where the Green's functions are spin-dependent

$$\langle \hat{I}(t)\rangle_0 = -\frac{e}{2}\sum_\sigma \int_{-\infty}^{\infty}\frac{d\omega}{2\pi}\,\mathrm{Tr}\Big[\tau^3(\mathbf{w}_\sigma^T G^<_{RL,\sigma}(\omega) - (\mathbf{w}_\sigma^T)^* G^<_{LR,\sigma}(\omega))\Big] \tag{3.32}$$

where the factor of $1/2$ in front accounts for double-counting introduced by the spin sum. We will here consider only the current carried by the bound states. Using the fluctuation-dissipation theorem, at zero temperature we obtain

$$\begin{aligned}
\langle \hat{I}(t)\rangle_0 &= -\sum_\sigma \int_{-\Delta}^{0} d\omega\,\frac{i}{4\pi} e\Delta^2(w^2-g^2)\sin^2(2\theta)\sin(\phi)\frac{D_\sigma(\omega-i\eta)-D_\sigma(\omega+i\eta)}{D_\sigma(\omega+i\eta)D_\sigma(\omega-i\eta)} \\
&= -\sum_\sigma \int_{-\Delta}^{0} d\omega\,\frac{i}{4\pi} e\Delta^2(w^2-g^2)\sin^2(2\theta)\sin(\phi)2i\,\mathrm{Im}\left(\frac{1}{D_\sigma(\omega-i\eta)}\right) \\
&= \sum_\sigma \int_{-\Delta}^{0} d\omega\,\frac{1}{2} e\Delta^2(w^2-g^2)\sin^2(2\theta)\sin(\phi)\left(\frac{\delta(\omega-E_{+\sigma})}{D'_\sigma(E_{+\sigma})}+\frac{\delta(\omega-E_{-\sigma})}{D'_\sigma(E_{-\sigma})}\right) \\
&= \frac{e\Delta^2(w^2-g^2)}{2}\sin^2(2\theta)\sin(\phi)\sum_\sigma\left(\frac{\theta(-E_{+\sigma})}{D'_\sigma(E_{+\sigma})}+\frac{\theta(-E_{-\sigma})}{D'_\sigma(E_{-\sigma})}\right).
\end{aligned} \tag{3.33}$$

The Josephson current is plotted in fig. 3.5 as a function of phase difference ϕ for the different values of θ and c in the particle-hole symmetric case $w = 0$. We see that depending on the parameters the junction can exhibit both $0-$ and $\pi-$junction behaviour. To understand the difference between the two types of Josephson junctions, we consider a junction in the tunnel limit with a simple sinusoidal current-phase relation $I = I_c\sin(\phi)$, where I_c is the ciritical current. The energy stored in the Josephson junction (Josephson energy) as a function of phase difference is the time-integral of the power $P = IV$ [9]. We find that

$$\begin{aligned}
E(\phi) &= \int_0^t dt\, IV = \frac{I_c\hbar}{2e}\int_0^t dt\,\sin(\phi)\dot{\phi} \\
&= \frac{I_c\hbar}{2e}\int_0^\phi d\phi\,\sin(\phi) = -E_J\cos(\phi).
\end{aligned} \tag{3.34}$$

When this relation applies, we easily see that the Josephson energy has a single minimum for $\phi = 0$ as long as the critical current is positive. At this minimum of the Josephson energy the junction is in the ground state and the current across it is $I = 0$. The current is also zero for $\phi = \pi$, but this is a local maximum of the Josephson energy. In this case the slope of the current will be positive for $\phi = 0$ and negative for $\phi = \pi$. However, in some cases the critical current can be negative, which corresponds to a shift of π of the phase in the relations above, so that $I = |I_c|\sin(\phi+\pi)$. We refer to

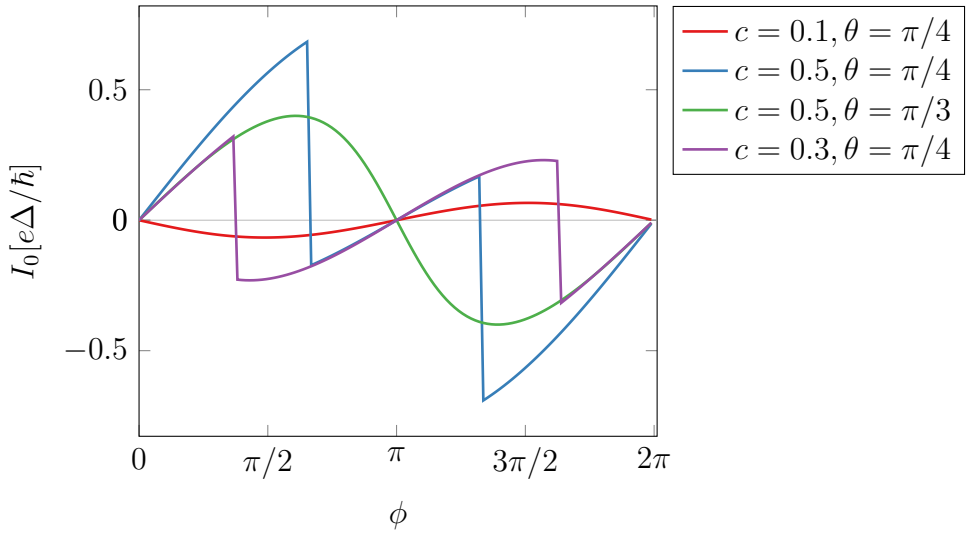

Figure 3.5: Equilibrium current for $x = 0$ and different values of c and θ. The green curve corresponds to a $0-$junction, the red curve a $\pi-$junction, the blue curve a $0'-$junction and the purple curve a $\pi'-$junction.

this as a $\pi-$junction. Then $\phi = 0$ is a maximum of the Josephson energy and $\phi = \pi$ is the ground state. The slope of the current will then be negative for $\phi = 0$ and positive for $\phi = \pi$.

It is also possible to have a junction with energy minima at both 0 and π, in which case the slope of the current is positive in both points and I is a discontinuous function of the phase. These are denoted $0'-$junctions (global minimum at $\phi = 0$ and local minimum at $\phi = \pi$) and $\pi'-$junctions (vice versa). All four types of junctions can be obtained in our model by varying c, x and θ as seen in fig. 3.5. We note that the transition from a $0-$junction to π-junction is related to the change of ground state when increasing the exchange interaction. When the impurity spin is unscreened (screened) in the ground state for all values of ϕ we have a $\pi-$junction ($0-$junction). The $0'-$ and π'-junctions arise for the range of parameters where the bound states $E_{-\sigma}$ cross zero energy as ϕ is varied. If one wishes to experimentally determine which state the system is in, this is often done my determining whether it exhibits $0-$ or $\pi-$junction behaviour. The results in this section reproduces those of [18] and hence also serves as a check that our Green's functions and expressions for the bound state energies are correct.

3.3 Admittance

Having obtained knowledge about the properties of the system in equilibrium, we will now move on to consider the linear response of the system when a harmonic voltage bias is applied. To this end we generalize the calculations of the previous chapter.

We start by considering the current operator, this time working with a spin-dependent one. The spin sum is carried out at a later stage, so that $I = \sum_\sigma I_\sigma$ with $I_\sigma = e\dot{N}_{L\sigma}$ and $N_{L\sigma} = \sum_k c^\dagger_{kL\sigma} c_{kL\sigma}$. We also consider the current operator in terms of electron operators and introduce the Nambu Green's functions later. Hence we need to calculate $\dot{N}_{L\sigma} = i[H, N_{L\sigma}]$ for the Hamiltonian given in eq. 3.3 in the classical spin approximation (using again units where $\hbar = 1$). The relevant commutators are:

$$\sum_{\alpha k\sigma} \sum_{k'} \xi_{k\sigma} [c^\dagger_{\alpha k\sigma} c_{\alpha k\sigma}, c^\dagger_{Lk'\sigma'} c_{Lk'\sigma'}] = 0 \tag{3.35}$$

$$\Delta \sum_{\alpha k} \sum_{k'} [c^\dagger_{\alpha k\uparrow} c^\dagger_{\alpha -k\downarrow}, c^\dagger_{Lk'\sigma'} c_{Lk'\sigma'}] \tag{3.36}$$

$$= \Delta \sum_k (c^\dagger_{L-k\sigma} c^\dagger_{Lk\uparrow} \delta_{\sigma\downarrow} - c^\dagger_{Lk\sigma} c^\dagger_{L-k\downarrow} \delta_{\sigma\uparrow}) \tag{3.37}$$

$$\Delta^* \sum_{\alpha k} \sum_{k'} [c_{\alpha -k\downarrow} c_{\alpha k\uparrow}, c^\dagger_{Lk'\sigma'} c_{Lk'\sigma'}] \tag{3.38}$$

$$= \Delta^* \sum_k (c_{L-k\downarrow} c_{Lk\sigma} \delta_{\sigma\uparrow} - c_{Lk\uparrow} c_{L-k\sigma} \delta_{\sigma\downarrow}) \tag{3.39}$$

$$\sum_{\alpha\alpha' k k'\sigma} \sum_{k'} JS\sigma\Theta_{\alpha\alpha'} [c^\dagger_{\alpha k\sigma} c_{\alpha' k'\sigma}, c^\dagger_{Lk''\sigma'} c_{Lk''\sigma'}] \tag{3.40}$$

$$= JS\sigma' \sum_{kk'} (\Theta_{RL} c^\dagger_{Rk\sigma'} c_{Lk'\sigma'} - \Theta_{LR} c^\dagger_{Lk\sigma'} c_{Rk'\sigma'}). \tag{3.41}$$

The contributions arising from the fact that the BCS-Hamiltonian does not conserve particle number will again be neglected. The potential scattering term in the Hamiltonian contributes with a term similar to the last one in the above equation so that we obtain the current operator

$$I_\sigma = ie \sum_{kk'} ((t_{RL\sigma} c^\dagger_{Rk\sigma} c_{Lk'\sigma} - t_{LR\sigma} c^\dagger_{Lk\sigma} c_{Rk'\sigma})), \tag{3.42}$$

where we defined $t_{RL\sigma} = (JS\sigma + W)\sin(\theta)\cos(\theta) e^{-i\phi/2} = t^*_{LR\sigma}$. As the current operator and the Hamiltonian have forms similar to what we considered for the quantum point contact we again have that the linear response of the system to a harmonic time-dependent voltage bias is associated with the current-current correlation function given in eq. 2.41, the only difference being that it is now a spin-dependent quantitiy. We will again restrict ourselves to considering the part of the response function which contributes to the real part of the admittance:

$$\begin{aligned} \chi_{\sigma\sigma'}(t) = ie\theta(t) \sum_{kp} \sum_{k'p'} \langle [t_{LR\sigma} c^\dagger_{Lk\sigma}(t) c_{Rp\sigma}(t) - t_{RL\sigma} c^\dagger_{Rp\sigma}(t) c_{Lk\sigma}(t), \\ t_{LR\sigma'} c^\dagger_{Lk'\sigma'}(0) c_{Rp'\sigma'}(0) - t_{RL\sigma'} c^\dagger_{Rp'\sigma'}(0) c_{Lk'\sigma'}(0)] \rangle_0. \end{aligned} \tag{3.43}$$

The commutator consists of four individual terms which are each evaluated using Wick's theorem. The first term is given by

$$\begin{aligned}
&\sum_{kp}\sum_{k'p'}\langle[t_{LR\sigma}c^\dagger_{Lk\sigma}(t)c_{Rp\sigma}(t), t_{LR\sigma'}c^\dagger_{Lk'\sigma'}(0)c_{Rp'\sigma'}(0)]\rangle \\
&= t_{LR\sigma}t_{RL\sigma'}\sum_{kp}\sum_{k'p'}(\langle c^\dagger_{Lk\sigma}(t)c_{Rp'\sigma'}(0)\rangle\langle c_{Rp\sigma}(t)c^\dagger_{Lk'\sigma'}(0)\rangle \\
&- \langle c^\dagger_{Lk\sigma}(t)c^\dagger_{Lk'\sigma'}(0)\rangle\langle c_{Rp\sigma}(t)c_{Rp'\sigma'}(0)\rangle \\
&- \langle c^\dagger_{Lk'\sigma'}(0)c_{Rp\sigma}(t)\rangle\langle c_{Rp'\sigma'}(0)c^\dagger_{Lk\sigma}(t)\rangle \\
&+ \langle c^\dagger_{Lk'\sigma'}(0)c^\dagger_{Lk\sigma}(t)\rangle\langle c_{Rp'\sigma'}(0)c_{Rp\sigma}(t)\rangle).
\end{aligned} \tag{3.44}$$

From the three remaining terms in the commutator we get similar contributions. We now wish to write this in terms of the local (momentum summed) greater and lesser Nambu Green's functions for the system. They are given by

$$G^<_{\alpha\beta,\sigma\sigma'}(t) = i\sum_{kk'}\begin{pmatrix}\langle c^\dagger_{\beta k'\sigma'}(0)c_{\alpha k\sigma}(t)\rangle & \langle c_{\beta -k'\bar\sigma'}(0)c_{\alpha k\sigma}(t)\rangle \\ \langle c^\dagger_{\beta k'\sigma'}(0)c^\dagger_{\alpha -k\bar\sigma}(t)\rangle & \langle c_{\beta -k'\bar\sigma'}(0)c^\dagger_{\alpha -k\bar\sigma}(t)\rangle\end{pmatrix} \tag{3.45}$$

$$G^>_{\alpha\beta,\sigma\sigma'}(t) = -i\sum_{kk'}\begin{pmatrix}\langle c_{\alpha k\sigma}(t)c^\dagger_{\beta k'\sigma'}(0)\rangle & \langle c_{\alpha k\sigma}(t)c_{\beta -k'\bar\sigma'}(0)\rangle \\ \langle c^\dagger_{\alpha -k\bar\sigma}(t)c^\dagger_{\beta k'\sigma'}(0)\rangle & \langle c^\dagger_{\alpha -k\bar\sigma}(t)c_{\beta -k'\bar\sigma'}(0)\rangle\end{pmatrix}. \tag{3.46}$$

Using this, we can write eq. 3.44 as

$$\begin{aligned}
t_{LR\sigma}t_{LR\sigma'}\Big(&G^<_{RL,\sigma'\sigma}(-t)_{1,1}G^>_{RL,\sigma\sigma'}(t)_{1,1} - G^<_{LL,\bar\sigma'\sigma}(-t)_{2,1}G^>_{RR,\sigma\bar\sigma'}(t)_{1,2} \\
&+G^<_{RR,\sigma\bar\sigma'}(t)_{1,2}G^>_{LL,\bar\sigma'\sigma}(-t)_{2,1} - G^<_{LR,\bar\sigma\bar\sigma'}(t)_{2,2}G^>_{LR,\bar\sigma'\bar\sigma}(-t)_{2,2}\Big).
\end{aligned} \tag{3.47}$$

When proceeding, we will use that as mentioned above the retarded and advanced Green's functions and hence also the greater and lesser ones are diagonal in spin space so that $G^{\lessgtr}_{\alpha\beta,\sigma\sigma'}(t) = G^{\lessgtr}_{\alpha\beta,\sigma}(t)\delta_{\sigma\sigma'}$. This also makes the response function diagonal in spin. Including all terms in the commutator in 3.43, we find that we can express the correlation function as a trace in Nambu space

$$\begin{aligned}
\chi_\sigma(t) = ie\theta(t)\,\mathrm{Tr}\Big[&\mathbf{t}^*_\sigma G^>_{LL\sigma}(-t)\mathbf{t}_\sigma G^<_{RR\sigma}(t) - \mathbf{t}^*_\sigma G^<_{LL\sigma}(-t)\mathbf{t}_\sigma G^>_{RR\sigma}(t) \\
&+ \mathbf{t}_\sigma G^<_{RL\sigma}(-t)\mathbf{t}_\sigma G^>_{RL\sigma}(t) - \mathbf{t}^*_\sigma G^<_{LR\sigma}(t)\mathbf{t}^*_\sigma G^>_{LR\sigma}(-t)\Big],
\end{aligned} \tag{3.48}$$

where we defined

$$\mathbf{t}_\sigma = \begin{pmatrix}(W+JS\sigma)e^{i\phi/2} & 0 \\ 0 & (W-JS\sigma)e^{-i\phi/2}\end{pmatrix}\sin(\theta)\cos(\theta). \tag{3.49}$$

We will now Fourier transform 3.48. This is done using the results of section 2.3. We repeat here the main result necessary to carry out the Fourier transformation

$$\begin{aligned}\mathcal{F}\left[i\theta(t)G^<(t)G^>(-t)\right] &= \frac{1}{(2\pi)^2}\int_{-\infty}^{\infty}d\omega'\int_{-\infty}^{\infty}d\omega''\, i\pi G^<(\omega')G^>(\omega'')\delta(\omega'-\omega''-\omega)\\ &+\frac{1}{(2\pi)^2}\int_{-\infty}^{\infty}d\omega'\,\text{P.V.}\int_{-\infty}^{\infty}d\omega''\,\frac{1}{\omega'-\omega''-\omega}G^<(\omega')G^>(\omega'')\\ &=\frac{i}{4\pi}\int_{-\infty}^{\infty}d\omega'\,G^<(\omega')G^>(\omega'-\omega)\\ &+\frac{1}{(2\pi)^2}\int_{-\infty}^{\infty}d\omega'\,\text{P.V.}\int_{-\infty}^{\infty}d\omega''\,\frac{1}{\omega'-\omega''-\omega}G^<(\omega')G^>(\omega'').\end{aligned} \tag{3.50}$$

We should now remind ourselves that we are only interested in the real part of the admittance, and that we have the relation $Y(\omega)=\frac{ie}{\omega}\chi(\omega)$ between the reponse function and the admittance. In eq. 3.50 we have two different terms which contribute to the admittance. As was the case for the QPC, the first term in the above expression gives a purely real contribution to the admittance, whereas the second term is an imaginary contribution. From this we also see that the two contributions are related through the Kramers-Kronig relations as expected. Using the expression for the Fourier transform of $\chi(t)$ we find that the real part of the admittance is given by

$$\begin{aligned}\text{Re}\,Y_\sigma(\omega) = \frac{e^2}{4\pi\omega}\int_{-\infty}^{\infty}d\epsilon\ \text{Tr}\Big[&-\mathbf{t}_\sigma^* G^<_{LL\sigma}(\epsilon-\omega)\mathbf{t}_\sigma G^>_{RR\sigma}(\epsilon)+\mathbf{t}_\sigma G^<_{RR\sigma}(\epsilon)\mathbf{t}_\sigma^* G^>_{LL\sigma}(\epsilon-\omega)\\ &+\mathbf{t}_\sigma G^<_{RL\sigma}(\epsilon-\omega)\mathbf{t}_\sigma G^>_{RL\sigma}(\epsilon)-\mathbf{t}_\sigma^* G^<_{LR\sigma}(\epsilon)\mathbf{t}_\sigma^* G^>_{LR\sigma}(\epsilon-\omega)\Big].\end{aligned} \tag{3.51}$$

As we are calculating the linear response of the system, all quantities in the above equation are equilibrium quantities, and we can use the fluctuation-dissipation theorem to find the greater and lesser Green's functions. This yields

$$\begin{aligned}\text{Re}\,Y_\sigma(\omega) = \frac{e^2}{4\pi\omega}\int_{-\infty}^{\infty}d\epsilon\ \text{Tr}\Big[&\mathbf{t}_\sigma^* A_{LL\sigma}(\epsilon-\omega)\mathbf{t}_\sigma A_{RR\sigma}(\epsilon)n_F(\epsilon-\omega)(1-n_F(\epsilon))\\ &-\mathbf{t}_\sigma^* A_{LL\sigma}(\epsilon-\omega)\mathbf{t}_\sigma A_{RR\sigma}(\epsilon)n_F(\epsilon)(1-n_F(\epsilon-\omega))\\ &-\mathbf{t}_\sigma A_{RL\sigma}(\epsilon-\omega)\mathbf{t}_\sigma A_{RL\sigma}(\epsilon)n_F(\epsilon-\omega)(1-n_F(\epsilon))\\ &+\mathbf{t}_\sigma^* A_{LR\sigma}(\epsilon-\omega)\mathbf{t}_\sigma^* A_{LR\sigma}(\epsilon)n_F(\epsilon)(1-n_F(\epsilon-\omega))\Big].\end{aligned} \tag{3.52}$$

When carrying out the integration, we will again consider only the case of $\omega>0$. As we are considering the case of $T=0$, the Fermi functions are step functions $n_F(\omega)=\theta(-\omega)$, and we have that $\theta(\omega-\epsilon)(1-\theta(-\epsilon))=\theta(\omega-\epsilon)-\theta(-\epsilon)$, which means that in the first and third terms in the above equation the lower and upper limit in the integral become 0 and ω respectively. The second and fourth terms are only nonzero for $\omega<0$, so we can discard those.

By also summing over spin, in the end we obtain our final expression for the real part of the admittance in frequency space, which is

$$\mathrm{Re}\, Y(\omega) = \frac{G_0}{4\omega} \sum_\sigma \int_0^\omega d\epsilon \ \mathrm{Tr}\left[\mathbf{t}_\sigma^* A_{LL\sigma}(\epsilon-\omega)\mathbf{t}_\sigma A_{RR\sigma}(\epsilon) - \mathbf{t}_\sigma A_{RL\sigma}(\epsilon-\omega)\mathbf{t}_\sigma A_{RL\sigma}(\epsilon)\right], \tag{3.53}$$

By performing the integration over ϵ numerically, we can obtain a plot of the real part of the admittance as a function of the frequency of the applied harmonic voltage bias. However, in order to enhance our understanding of this result, we will study the analytic properties of the integrand in some detail before doing so.

3.3.1 Analytical study of the admittance

$\mathrm{Re}\, Y$ consists of a sum of convolutions of greater and lesser Green's functions. We find that all terms in the integrand have the general structure

$$\begin{aligned}&\Big(\frac{f_\sigma(\epsilon+i\eta)\sqrt{\Delta^2-(\epsilon+i\eta)^2}+g_\sigma(\epsilon+i\eta)}{D_\sigma(\epsilon+i\eta)} - \frac{f_\sigma(\epsilon-i\eta)\sqrt{\Delta^2-(\epsilon-i\eta)^2}+g_\sigma(\epsilon-i\eta)}{D_\sigma(\epsilon-i\eta)}\Big)\cdot \\ &\Big(\frac{f'_\sigma(\epsilon-\omega+i\eta)\sqrt{\Delta^2-(\epsilon-\omega+i\eta)^2}+g'_\sigma(\epsilon-\omega+i\eta)}{D_\sigma(\epsilon-\omega+i\eta)} - \\ &\frac{f'_\sigma(\epsilon-\omega-i\eta)\sqrt{\Delta^2-(\epsilon-\omega-i\eta)^2}+g'_\sigma(\epsilon-\omega-i\eta)}{D_\sigma(\epsilon-\omega-i\eta)}\Big),\end{aligned} \tag{3.54}$$

where f, g, f' and g' are complex functions. We expand the numerator to leading order in η by remembering that the complex square roots become

$$\sqrt{\Delta^2-(\epsilon\pm i\eta)^2} = \theta(\Delta-|\epsilon|)\sqrt{\Delta^2-\epsilon^2} \mp i\theta(|\epsilon|-\Delta)\mathrm{sgn}(\epsilon)\sqrt{\epsilon^2-\Delta^2}. \tag{3.55}$$

Considering the first factor in eq. 3.54, we find that by substituting this form of the square roots it becomes

$$\begin{aligned}&\Big(f_\sigma(\epsilon)\sqrt{\Delta^2-\epsilon^2}\theta(\Delta-|\epsilon|)+g_\sigma(\epsilon)\Big)\left(\frac{1}{D_\sigma(\epsilon+i\eta)}-\frac{1}{D_\sigma(\epsilon-i\eta)}\right) \\ &-if_\sigma(\epsilon)\sqrt{\epsilon^2-\Delta^2}\theta(|\epsilon|-\Delta)\left(\frac{1}{D_\sigma(\epsilon+i\eta)}+\frac{1}{D_\sigma(\epsilon-i\eta)}\right)\end{aligned} \tag{3.56}$$

We see that two different sign combinations of the denominators are present, so we have to determine the real and imaginary part of the denominator:

$$\frac{1}{D_\sigma(\epsilon+i\eta)}-\frac{1}{D_\sigma(\epsilon-i\eta)} = 2i\,\mathrm{Im}\left(\frac{1}{D_\sigma(\epsilon+i\eta)}\right) \tag{3.57}$$

and

$$\frac{1}{D_\sigma(\epsilon+i\eta)}+\frac{1}{D_\sigma(\epsilon-i\eta)}=2\,\mathrm{Re}\left(\frac{1}{D_\sigma(\epsilon+i\eta)}\right) \tag{3.58}$$

We write the denominator as $D_\sigma(\epsilon+i\eta)=\alpha\Delta^2+\beta(\epsilon+i\eta)^2+\sigma\gamma\epsilon\sqrt{\Delta^2-(\epsilon+i\eta)^2}$ with $\alpha=(1+\chi u)$, $\beta=-(1+u)$ and $\gamma=2g$. We also expand it to leading order in η, which amounts to substituting the expansion of the square roots given above and setting $\eta=0$ in the term proportional to β. The real part is then found to be

$$\begin{aligned}
&\mathrm{Re}\left(\frac{1}{D_\sigma(\epsilon+i\eta)}\right)\\
&=\mathrm{Re}\left(\frac{1}{\alpha\Delta^2+\beta\epsilon^2+\sigma\gamma\epsilon(\theta(\Delta-|\epsilon|)\sqrt{\Delta^2-\epsilon^2}-i\theta(|\epsilon|-\Delta)\mathrm{sgn}(\epsilon)\sqrt{\epsilon^2-\Delta^2}))}\right)\\
&=\frac{\alpha\Delta^2+\beta\epsilon^2}{(\alpha\Delta^2+\beta\epsilon^2)^2+\gamma^2\epsilon^2(\epsilon^2-\Delta^2)}\theta(|\epsilon|-\Delta)+\frac{1}{\alpha\Delta^2+\beta\epsilon^2+\gamma\sigma\epsilon\sqrt{\Delta^2-\epsilon^2}}\theta(\Delta-|\epsilon|).
\end{aligned} \tag{3.59}$$

For the imaginary part, we will have to consider the cases of $|\epsilon|<\Delta$ and $|\epsilon|>\Delta$ separately. When $|\epsilon|<\Delta$ the square root in eq. 3.55 is real, and we can obtain the imaginary part by performing a Taylor expansion of the denominator. As we are mainly interested in absorption processes where quasiparticles are created in the bound states (corresponding to $|\epsilon|<\Delta$,) we will for now restrict ourselves to considering this frequency interval in the terms involving the imaginary part of the denominator. Including also the case of $\epsilon>\Delta$ adds a correction to the admittance which has a form similar to the terms involving the real part of the denominator. To find the imaginary part for $\epsilon<\Delta$ we follow [22] and expand $D_\sigma(\epsilon+i\eta)$ around ϵ to obtain

$$\begin{aligned}
\mathrm{Im}\left(\frac{1}{D_\sigma(\epsilon+i\eta)}\right)&=\mathrm{Im}\left(\frac{1}{D_\sigma(\epsilon)+i\eta D'_\sigma(\epsilon)}\right)=\frac{1}{D'_\sigma(\epsilon)}\,\mathrm{Im}\left(\frac{1}{D_\sigma(\epsilon)D'_\sigma(\epsilon)^{-1}+i\eta}\right)\\
&=-\frac{\pi}{D'_\sigma(\epsilon)}\delta(D_\sigma(\epsilon)D'_\sigma(\epsilon)^{-1})=-\frac{\pi}{D'_\sigma(\epsilon)}\sum_i\frac{\delta(\epsilon-E_{i\sigma})}{|h'_\sigma(E_{i\sigma})|},
\end{aligned} \tag{3.60}$$

where the sum is over roots of $D_\sigma(\epsilon)D'_\sigma(\epsilon)^{-1}$ and we defined $h(\epsilon)=D_\sigma(\epsilon)D'_\sigma(\epsilon)^{-1}$. This expansion is possible because the square root is real for $\epsilon<\Delta$ so that $D_\sigma(\epsilon)$ and $D'_\sigma(\epsilon)$ are real numbers. We find that

$$h'_\sigma(E_{i\sigma})=D'_\sigma(\epsilon)D'_\sigma(\epsilon)^{-1}|_{\epsilon=E_{i\sigma}}-D_\sigma(\epsilon)D'_\sigma(\epsilon)^{-1}\frac{D''_\sigma(\epsilon)}{D'_\sigma(\epsilon)}\bigg|_{\epsilon=E_{i\sigma}}=1, \tag{3.61}$$

where the second term vanishes as E_i are the roots of $D_\sigma(\epsilon)D'_\sigma(\epsilon)^{-1}$. Using also that $D'_\sigma(\epsilon)=2\beta\epsilon+\gamma(\sigma\sqrt{\Delta^2-\epsilon^2}-\sigma\epsilon^2/\sqrt{\Delta^2-\epsilon^2})$, we find that the roots of $h(\epsilon)$ are the bound states because we are considering the region where $\epsilon<\Delta$, and the zeros of $D'_\sigma(\epsilon)^{-1}$ are $\pm\Delta$. Combining everything, we finally find that

$$\mathrm{Im}\left(\frac{1}{D_\sigma(\epsilon+i\eta)}\right)=-\pi D'_\sigma(\epsilon)^{-1}\Big(\delta(\epsilon-E_{+\sigma})+\delta(\epsilon-E_{-\sigma})\Big) \tag{3.62}$$

Expanding eq. 3.54 with eq. 3.56 we obtain four different contributions to the real part of the admittance

$$\begin{aligned}\operatorname{Re} Y_{1\sigma}(\omega) = -\frac{G_0}{\omega}\int_0^{\omega} d\epsilon\, f_\sigma(\epsilon) f'_\sigma(\epsilon-\omega)\sqrt{\epsilon^2-\Delta^2}\sqrt{(\epsilon-\omega)^2-\Delta^2} \\ \operatorname{Re}\left(\frac{1}{D_\sigma(\epsilon+i\eta)}\right)\operatorname{Re}\left(\frac{1}{D_\sigma(\epsilon-\omega+i\eta)}\right)\theta(|\epsilon|-\Delta)\theta(|\epsilon-\omega|-\Delta)\end{aligned} \tag{3.63}$$

$$\begin{aligned}\operatorname{Re} Y_{2A\sigma}(\omega) = \frac{G_0}{\omega}\int_0^{\omega} d\epsilon \left(g_\sigma(\epsilon) + f_\sigma(\epsilon)\sqrt{\Delta^2-\epsilon^2}\theta(\Delta-|\epsilon|)\right) f'_\sigma(\epsilon-\omega) \\ \sqrt{(\epsilon-\omega)^2-\Delta^2}\theta(|\epsilon-\omega|-\Delta)\operatorname{Im}\left(\frac{1}{D_\sigma(\epsilon+i\eta)}\right)\operatorname{Re}\left(\frac{1}{D_\sigma(\epsilon-\omega+i\eta)}\right)\end{aligned} \tag{3.64}$$

$$\begin{aligned}\operatorname{Re} Y_{2B\sigma}(\omega) = \frac{G_0}{\omega}\int_0^{\omega} d\epsilon \left(g'_\sigma(\epsilon-\omega) + f'_\sigma(\epsilon-\omega)\sqrt{\Delta^2-(\epsilon-\omega)^2}\theta(\Delta-|\epsilon-\omega|)\right) \\ f_\sigma(\epsilon)\sqrt{\epsilon^2-\Delta^2}\theta(|\epsilon|-\Delta) \\ \operatorname{Re}\left(\frac{1}{D_\sigma(\epsilon+i\eta)}\right)\operatorname{Im}\left(\frac{1}{D_\sigma(\epsilon-\omega+i\eta)}\right)\end{aligned} \tag{3.65}$$

$$\begin{aligned}\operatorname{Re} Y_{3\sigma}(\omega) = -\frac{G_0}{\omega}\int_0^{\omega} d\epsilon \left(g_\sigma(\epsilon) + f_\sigma(\epsilon)\sqrt{\Delta^2-\epsilon^2}\theta(\Delta-|\epsilon|)\right) \\ \left(g'_\sigma(\epsilon-\omega) + f'_\sigma(\epsilon-\omega)\sqrt{\Delta^2-(\epsilon-\omega)^2}\theta(\Delta-|\epsilon-\omega|)\right) \\ \operatorname{Im}\left(\frac{1}{D_\sigma(\epsilon+i\eta)}\right)\operatorname{Im}\left(\frac{1}{D_\sigma(\epsilon-\omega+i\eta)}\right).\end{aligned} \tag{3.66}$$

Some considerations regarding the Heaviside step functions are now necessary. In $\operatorname{Re} Y_{1\sigma}(\omega)$ the product of step functions is nonzero when $\omega > 2\Delta$, and we have $\theta(|\epsilon| - \Delta)\theta(|\epsilon-\omega|-\Delta) = \theta(\omega-2\Delta)$. In $\operatorname{Re} Y_{3\sigma}(\omega)$ both $\theta(\Delta-|\epsilon|)$ and $\theta(\Delta-|\epsilon-\omega|)$ are always nonzero for $\epsilon = E_{\pm\sigma}$ and $\epsilon-\omega = E_{\pm\sigma}$, which are the contributions we get when using the approximation for the imaginary part described above. Hence we don't have to explicitly write these step-functions. For $\operatorname{Re} Y_{2A\sigma}(\omega)$ and $\operatorname{Re} Y_{2B\sigma}(\omega)$ we similarly find that the step functions which are only present in the terms with two square roots are automatically satisfied due to the delta functions coming from the imaginary part, and we are left with $\theta(\omega-\epsilon-\Delta)$ in $\operatorname{Re} Y_{2A\sigma}(\omega)$ and $\theta(\epsilon-\Delta)$ in $\operatorname{Re} Y_{2B\sigma}(\omega)$. These considerations allow us to write the terms as:

$$\begin{aligned}\operatorname{Re} Y_1(\omega) = -\frac{G_0}{\omega}\sum_\sigma \theta(\omega-2\Delta)\int_0^\omega d\epsilon\, f_\sigma(\epsilon) f'_\sigma(\epsilon-\omega)\sqrt{\epsilon^2-\Delta^2}\sqrt{(\epsilon-\omega)^2-\Delta^2} \\ \operatorname{Re}\left(\frac{1}{D_\sigma(\epsilon+i\eta)}\right)\operatorname{Re}\left(\frac{1}{D_\sigma(\epsilon-\omega+i\eta)}\right)\end{aligned} \tag{3.67}$$

$$\begin{aligned}\operatorname{Re} Y_{2A}(\omega) &= \pi\frac{G_0}{\omega}\sum_\sigma\int_0^\omega d\epsilon\,\theta(\omega-\epsilon-\Delta)\Big(g_\sigma(\epsilon)+f_\sigma(\epsilon)\sqrt{\Delta^2-\epsilon^2}\Big)f'_\sigma(\epsilon-\omega)\sqrt{(\epsilon-\omega)^2-\Delta^2} \\ &\quad \operatorname{Re}\left(\frac{1}{D_\sigma(\epsilon-\omega+i\eta)}\right)D'_\sigma(\epsilon)^{-1}\Big(\delta(\epsilon-E_{\sigma+})+\delta(\epsilon-E_{\sigma-})\Big) \\ &= \pi\frac{G_0}{4\omega}\sum_{\sigma,i=\pm}\theta(\omega-E_{i\sigma}-\Delta)\theta(E_{i\sigma})\Big(g_\sigma(E_{i\sigma})+f_\sigma(E_{i\sigma})\sqrt{\Delta^2-E_{i\sigma}^2}\Big) \\ &\quad f'_\sigma(E_{i\sigma}-\omega)\sqrt{(E_{i\sigma}-\omega)^2-\Delta^2}\operatorname{Re}\left(\frac{1}{D_\sigma(E_{i\sigma}-\omega+i\eta)}\right)D'_\sigma(E_{i\sigma})^{-1}\end{aligned} \tag{3.68}$$

$$\begin{aligned}\operatorname{Re} Y_{2B}(\omega) = \pi\frac{G_0}{\omega}\sum_{\sigma,i=\pm}\theta(\omega+E_{i\sigma}-\Delta)\theta(-E_{i\sigma})\Big(g'_\sigma(E_{i\sigma})+f'_\sigma(E_{i\sigma})\sqrt{\Delta^2-(E_{i\sigma})^2}\Big) \\ f_\sigma(\omega+E_{i\sigma})\sqrt{(\omega+E_{i\sigma})^2-\Delta^2}\operatorname{Re}\left(\frac{1}{D_\sigma(\omega+E_{i\sigma}+i\eta)}\right)D'_\sigma(E_{i\sigma})^{-1}\end{aligned} \tag{3.69}$$

$$\begin{aligned}\operatorname{Re} Y_3(\omega) = -\pi^2 G_0\sum_{\sigma,(i,j)=\pm}\frac{1}{(E_{i\sigma}-E_{j\sigma})}\Big(g_\sigma(E_{i\sigma})+f_\sigma(E_{i\sigma})\sqrt{\Delta^2-E_{i\sigma}^2}\Big) \\ \Big(g'_\sigma(E_{j\sigma})+f'_\sigma(E_{j\sigma})\sqrt{\Delta^2-E_{j\sigma}^2}\Big) \\ D'_\sigma(E_{i\sigma})^{-1}D'_\sigma(E_{j\sigma})^{-1}\theta(E_{i\sigma})\theta(-E_{j\sigma})\delta(\omega-E_{i\sigma}+E_{j\sigma})\end{aligned} \tag{3.70}$$

Based on these expressions we can draw conclusions about the different features we expect to see in the real part of the frequency-dependent admittance, and relate this result to what we found for the QPC. Each term can be ascribed to an excitation process where a quasiparticle pair is created by the absorption of a photon. The first term $\operatorname{Re} Y_1(\omega)$ has a threshold frequency of $\omega = 2\Delta$ and can be associated with the absorption process where two quasiparticles are created in the superconducting continuum at energies larger than the pairing energy 2Δ. This process is always possible in BCS superconductors, even if there are no subgap states as it involves only the continuum. A schematic drawing of excitation spectrum is seen in fig. 3.6, and here $\operatorname{Re} Y_1(\omega)$ arises from two times the process denoted ①.

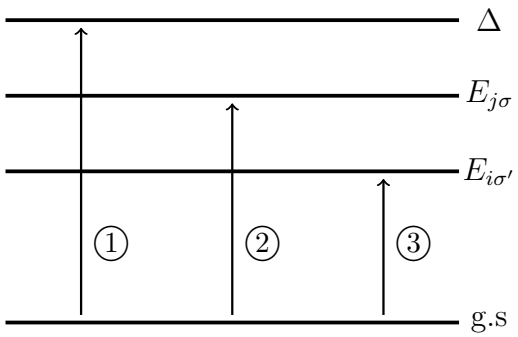

Figure 3.6: Quasiparticle excitation spectrum in the S-QD-S Josephson junction at $T = 0$

$\mathrm{Re}\, Y_{2A}(\omega)$ has a threshold frequency of $\omega = \Delta + E_{\pm\sigma}$ and is associated with the creation of a pair of quasiparticles where one is created in the continuum and one in the bound state with energy $E_{\pm\sigma} > 0$. This is ①+② or ①+③ in fig. 3.6. The contribution from $\mathrm{Re}\, Y_{2B}(\omega)$ is of the same nature which one can infer by remembering that for each negative subgap energy $E_{\pm\sigma}$ there is a positive energy $E_{\pm\bar{\sigma}}$ of equal magnitude. So above the threshold frequency of $\omega = \Delta + |E_{\sigma\pm}|$, one quasiparticle can be created in the continuum and one in the bound state $E_{\pm\bar{\sigma}} > 0$. The absorption processes related to Y_1 and Y_2 are always possible regardsless of whether the excited YSR states above zero energy have same or opposite spins. The term we discarded arising from the imaginary part of the denominator for $\epsilon > \Delta$ add a contribution of the same type as $\mathrm{Re}\, Y_2$.

In contrast, $\mathrm{Re}\, Y_3(\omega)$ is a resonant contribution which is only nonzero for $\omega = E_{i\sigma} - E_{j\sigma}$ with $E_{i\sigma} > 0$ and $E_{j\sigma} < 0$, which we can also write as $\omega = E_{i\sigma} + E_{j\bar{\sigma}}$ with both energies positive. The associated absoprtion process is the one where a quasiparticle is created in each of the bound states (②+③ in fig. 3.6). This process is only possible if two excited states of opposite spin are available. We will see a reason for this restriction later when considering the problem from the point of view of scattering theory.

3.3.2 Numerical integration

The numerical integration of eq. 3.53 is now performed using Mathematica. To do this we have to use a finite value of the positive infinitesimal η. The value $\eta = 10^{-4}$ has been chosen as it is the smallest possible value which still allows the computation to be performed within resonable amounts of time. We note that in a real circuit there will always be interactions with for example the wires which in practice results in η having a finite value (the quasiparticle states have a finite lifetime).

To see how the absorption depends on the position of the bound state energies, we have performed the integration for different values of the phase ϕ with fixed values of the other parameters as shown by the gridlines in fig. 3.7. The results are seen in fig 3.8. We are mainly interested in the processes which involve the subgap states,

but briefly note that we don't see a feature with threshold frequency $\omega = 2\Delta$, which is most likely because the other contributions also present at this frequency are dominant or because it has a slow onset which makes it indistinguishable from the rest of the contributions. By numerically integrating the real part of the admittance for the QPC as a check we found that the same could also be the case there. Otherwise we see that the peaks and threshold frequencies predicted by our analytical calculations above are indeed present at the expected energies.

The peak at $\omega = E_{+\sigma} + E_{-\bar{\sigma}}$ is of most interest to us. This is because it is only present if excited subgap states of both spin species are available, which is the case when the ground state is the screened state and the peak is located at $\omega = E_{+\downarrow} + E_{-\uparrow}$. Going from fig. 3.8 a) to b) we also see how this peak disappears when the ground state is the unscreened state. Hence a measurement of this absorption peak could in principle be used to probe what the ground state of the system is. Or phrased differently, if we vary the static phase bias and this absorption peak suddenly vanishes, we will know that a transition to an unscreened ground state has occured.

In fig. 3.8 we observe that small additional features which we can't explain by our calculations above are appearing close to zero energy. They are due to numerical error caused by the use of a finite value of η, and are located at $\omega = E_{\pm\sigma}$. Their origin is that because we are using a finite value of η, the spectral function can have a nonzero value in $\omega = 0$ when the bound state is deep inside the gap. This then yields a feature in the admittance which looks as what one would expect if a quasiparticle with approximately zero energy was present in the system (which is of course unphysical as no states are available there). By investigating how the height of this peak and the $\delta-$peak change when η is increased, we can verify that this is indeed the origin of the additional peak. This is explained in greater detail in appendix D.

In addition to the results from the numerical integration we present plots for the magnitude of $\mathrm{Re}\, Y_3$ at resonance which are obtained by evaluating eq. 3.70. In fig. 3.10 a), we see how the real part of the admittance vanishes in the doublet-like ground state where the impurity spin is unscreened. Furthermore, $\mathrm{Re}\, Y_3$ is almost zero in the particle-hole symmetric point (for symmetric coupling $\theta = \pi/4$ it is identically zero) and increases in magnitude with the distance from $x = 0$. Fig. 3.10 c) shows (in $x = 0$), that for $\theta \sim 0$ we also have $\mathrm{Re}\, Y_3 \sim 0$ as when only one of the leads is coupled to the dot, the bound state arising from the odd combination of the leads is very close to the gap for all values of ϕ. The magnitude of $\mathrm{Re}\, Y_3$ then increases for increasing θ and reaches its maximum value at approximately $\theta = \pi/8$ and then decreases and reaches zero for symmetric coupling $\theta = \pi/4$. The magnitude of the admittance generally reaches values of the same size as what was found for the QPC, and is on the order of G_0 for most values of the parameters.

3.3.3 Interpretation of absorption features

As we have knowledge about the ground state and excitation spectrum of the system for different values of the parameters, we can now give a description of the relation between

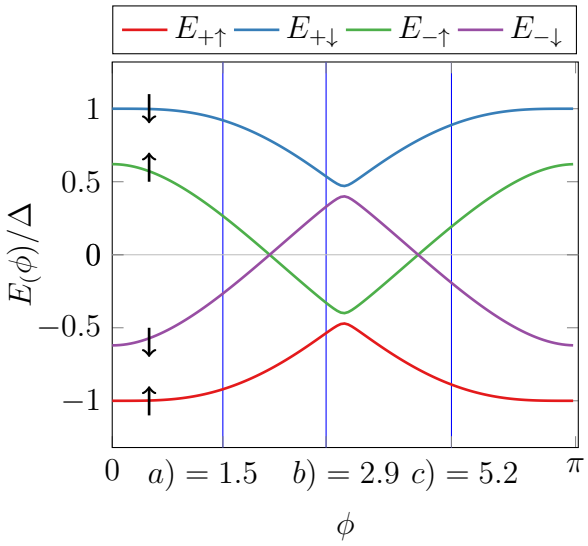

Figure 3.7: Bound state energies for a case of intermediate coupling for parameters $c = 0.5$, $x = 0.1$, $\theta = \pi/4$ and with gridlines where the admittance has been calculated in fig. 3.8.

the quasiparticles created by the absorption of a photon, and the excited state that the system ends up in. We remind ourselves that in the quasiparticle picture, the energies of the excited subgap states with $E > 0$ are quasiparticle creation energies, which is the energy difference between the ground state and the excited states. We now refer to the unscreened state as a doublet state and the screened state as a singlet state, but of course keep in mind that these terms are not strictly correct for a classical impurity spin. However, we use them in anticipation of the fact that in an entirely quantum mechanical treatment of the problem, the eigenstates of the Anderson model are true singlet and doublet states. We will see this in the limit of $\Delta \to \infty$ in chapter 5. This is also what is found by [19] where a quantum mechanical impurity spin is considered and the eigenstates are determined perturbatively in the exchange interaction.

In this terminology, our interpretation of the states involved in the absorption processes is as follows. In the particle-hole symmetric point with only the two YSR bound states, we know from eq. 3.31 that the singlet and doublet states differ by a single quasiparticle. When the ground state is the screened singlet, which we denote by $|S_-\rangle$, the unscreened doublet, which we denote $\left|D_\uparrow\right\rangle$ is the first excited state and vice versa. From this we infer that in the singlet ground state, the creation of a single quasiparticle in the bound state with energy $E_{-\uparrow}$ leads to the excited doublet state. This happens through the absorption process with threshold frequency $\omega = E_{-\uparrow} + \Delta$, as a surplus quasiparticle resulting from the splitting of a Cooper pair is also created in the continuum. The excited state resulting from the creation of a quasiparticle in the other bound state with energy $E_{+\downarrow}$ can be interpreted as another doublet state, denoted $\left|D_\downarrow\right\rangle$, as it has an extra spin-down quasiparticle in addition to the one screening the impurity spin. The related absorption process has threshold frequency $\omega = E_{+\downarrow} + \Delta$. Lastly, by

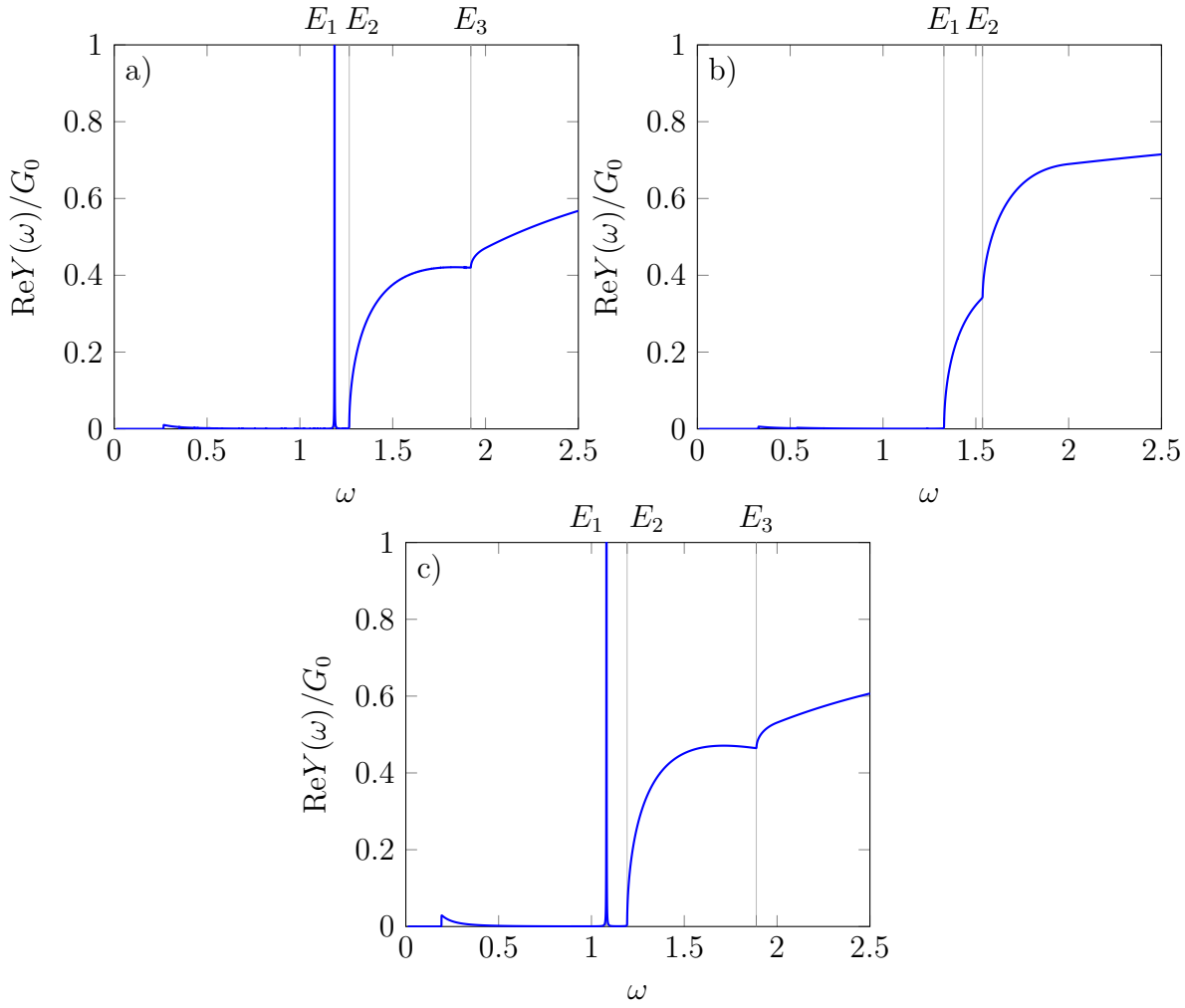

Figure 3.8: Real part of admittance for the different phases shown with gridlines in fig. 3.7. The gridlines are located at $E_1 = E_{-\uparrow} + E_{+\downarrow}$, $E_2 = E_{-\uparrow} + \Delta$ and $E_3 = E_{+\downarrow} + \Delta$ in a) and c), and at $E_1 = \Delta + E_{-\downarrow}$ and $E_2 = \Delta + E_{+\downarrow}$ in b).The peak arising from the creation of two quasiparticles in the bound state is clearly absent in b) where the impurity spin is unscreened in the ground state. Parameters: $x = 0.2$, $c = 0.5$, $\theta = \pi/4$ and $\eta = 10^{-4}$

splitting a Cooper pair it is also possible to create a quasiparticle in each of the bound states as they have opposite spin. This corresponds to removing the quasiparticle in the even state which screens the impurity spin and creating a new screening quasiparticle in the odd state. The resulting state can be interpreted as another singlet (partially screened) state $|S_+\rangle$. This process leads to the discrete absorption peak at frequency $\omega = E_{-\uparrow} + E_{+\downarrow}$ only present for the singlet ground state. A sketch of the states and excitation processes is seen in fig. 3.9 a). For the doublet ground state, the first excited

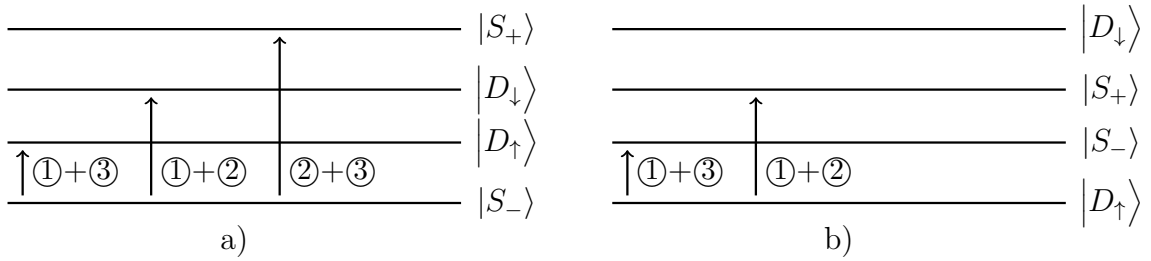

Figure 3.9: Sketch of our interpretation of the ground state and excited states for the two different phases. In a) the ground state is the screened singlet-like state and in b) it is the doublet-like unscreened state. The arrows are labelled by the corresponding quasiparticle creation processes in fig. 3.6 responsible for the transitions between them. We have only included the processes which are possible by splitting a single Cooper pair and are present in the absorption spectrum in the linear response regime.

state is the singlet $|S_-\rangle$ which is reached by creating a single quasiparticle in the bound state $E_{-\downarrow}$ with threshold frequency $\omega = E_{-\downarrow} + \Delta$. Similarly, creating a quasiparticle in the other bound state must result in the other singlet state $|S_+\rangle$ through the absorption process with threshold frequency $\omega = E_{+\downarrow} + \Delta$. The next excited state would be $\left|D_\downarrow\right\rangle$, but it differs from the ground state by two quasiparticles of the same spin and the transition to this state requires the splitting of two Cooper pairs. Hence no absorption feature corresponding to this transition is present in the doublet ground state. This situation is depicted in fig. 3.9 b).

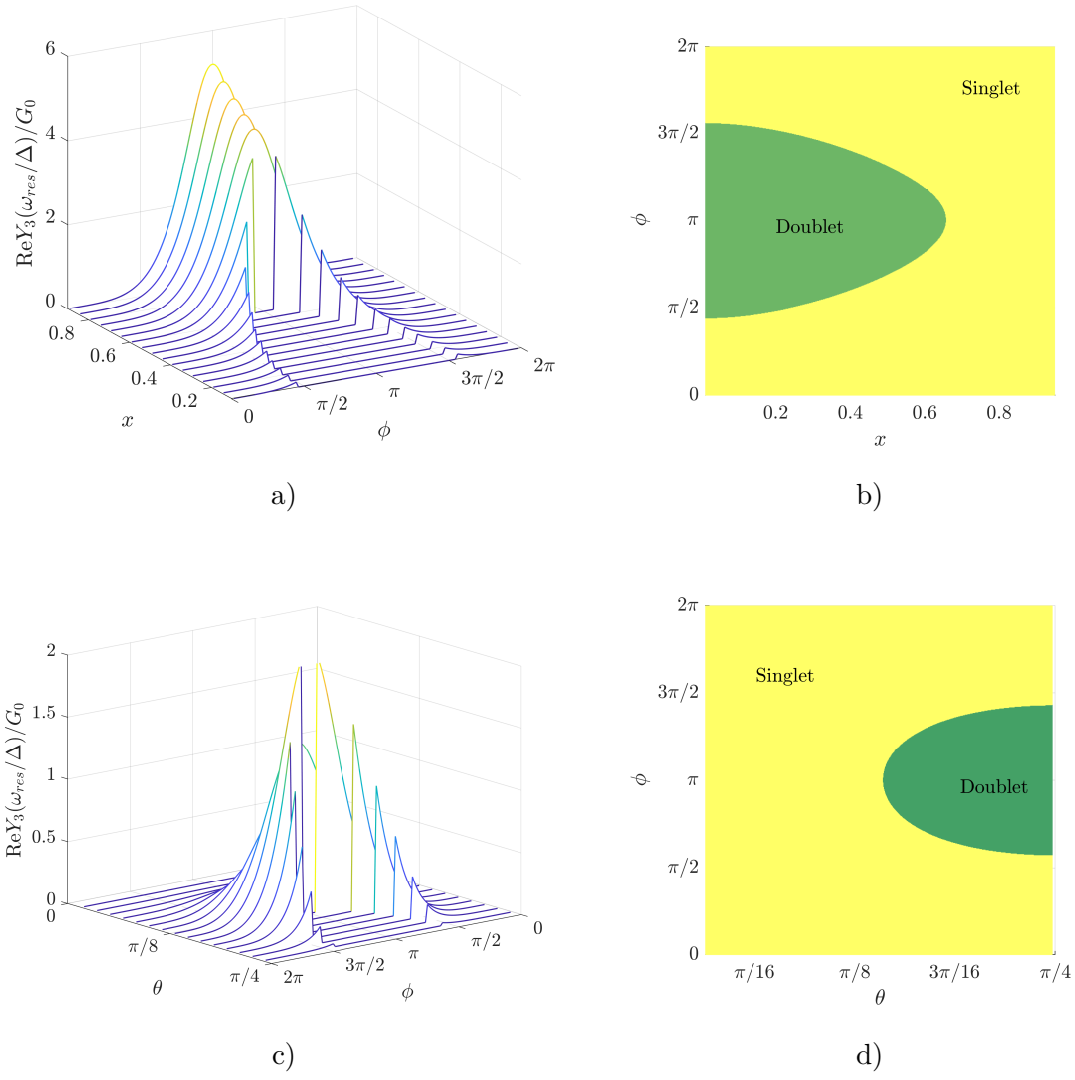

Figure 3.10: **a)** Y_3 as a function of x and ϕ. $c = 0.3$ and $\theta = \pi/3$. **b)** Phase diagram for parameters in a). **c)** Y_3 as a function of θ and ϕ for $x = 0$ and $c = 0.4$. **d)** Phase diagram for parameters in c).

Chapter 4

Transition rates in the scattering problem

As a way checking our results for the admittance obtained with the Green's function method we present in this chapter an alternative calculation of the transition rates for photon absorption processes. The result will reveal information about the limitations on the spin of the quasiparticles created in such an absorption process, and hence the types of states that the perturbation can induce transitions between. The rates are determined using standard first order peturbation theory or more specifically Fermi's golden rule, which states that the transition rate between and initial state $|i\rangle$ and a final state $|f\rangle$ caused by a harmonic perturbation $H(t) = V(e^{i\omega t} + e^{-i\omega t})$ is given by [12]

$$\Gamma_{fi} = \frac{2\pi}{\hbar}\delta(E_f - E_i)|\langle f|\, V\, |i\rangle|^2, \tag{4.1}$$

In the linear-response calculation we found the Hamiltonian describing the perturbation to linear order in the time-dependent phase difference $\phi_1(t)$ to be

$$H'(t) = \frac{\phi_1(t)\hat{I}}{e} = \frac{\phi_1}{e}(e^{i\omega t} + e^{-i\omega t})\hat{I}, \tag{4.2}$$

so that in Fermi's golden rule we should use $V = \phi_1\hat{I}/e$ where ϕ_1 is the time-independent amplitude of the perturbation. We start our calculation by determining the eigenstates of the system constituting a basis in which we can express the current operator to calculate the matrix elements between inital and final states. This will be done using the scattering formalism. We consider first the simple QPC to regain some of the results from section 2.3 and ensure that our formalism is correct, and subsequently generalize the results by including also a magnetic impurity modelled by a spin-dependent scattering potential. All the systems will be modelled as two one-dimensional semi-infinite leads separated by a $\delta-$function barrier at $x = 0$. In the process we will also gain knowledge about the nature of the Andreev reflections. The calcuations in this chapter follow the approach initially used by Blonder, Tinkham and Klapwijk [23] for an

NS-contact and later by others ([24] and [25]), to calculate the lifetime of quasiparticles trapped in a QPC.

4.1 Bogoliubov-de Gennes equations

As a first step towards the calculation of the wave functions for interfaces where one or both leads is superconducting, we consider the eigenstates of the Hamiltonian in the simple case of a single homogeneous superconductor. Those are obtained by diagonalizing the Hamiltonian with a Bogoliubov transformation. The correct transformation is determined by solving the Bogoliubov-de Gennes equations which we will now derive while including an arbitrary spin-dependent potential (our derivation follows ref. [26]). This will shed some light on the redundancy of the BdG-equations and the correspondance between the different solutions. The mean-field BCS-Hamiltonian in real space takes the form

$$H_{BCS} = \int dx \sum_{\sigma} \left(\psi_{\sigma}^{\dagger}(x) \xi_k \psi_{\sigma}(x) + U_{\sigma} \psi_{\sigma}^{\dagger}(x) \psi_{\sigma}(x) \right) \tag{4.3}$$

$$+\Delta^{*}(x) \psi_{\downarrow}(x) \psi_{\uparrow}(x) + \Delta(x) \psi_{\uparrow}^{\dagger}(x) \psi_{\downarrow}^{\dagger}(x), \tag{4.4}$$

with $\xi_k = \frac{-\hbar^2 \nabla^2}{2m} - \mu$ and where $\psi^{\dagger}(x)$ and $\psi(x)$ are the electronic field operators. Using that the momentum k is a good quantum number, we introduce the Bogoliubov-transformation

$$\psi_{\sigma}(x) = \sum_{k} [u_{k\sigma}(x) \gamma_{k\sigma} - \sigma v_{k\sigma}^{*}(x) \gamma_{-k\bar{\sigma}}^{\dagger}], \tag{4.5}$$

where the sum is over states of positive energy only. The coefficients (u, v) are determined by demanding that the transformation diagonalizes the Hamiltonian $H = E_0 + \sum_{k\sigma} E_{k\sigma} \gamma_{k\sigma}^{\dagger} \gamma_{k\sigma}$, with excitation energies $E_{k\sigma}$. We choose the quantum number k as this is a good quantum number for homogeneous systems. This turns out to also be the case when we add a scattering potential. In order to find the coefficients u_{σ} and v_{σ} so that the transformation diagonalizes the Hamiltonian, we calculate first the commutators relevant for the diagonal Hamiltonian:

$$\left[H, \gamma_{k\sigma} \right] = -E_{k\sigma} \gamma_{k\sigma} \quad [H, \gamma_{k\sigma}^{\dagger}] = E_{k\sigma} \gamma_{k\sigma}^{\dagger}. \tag{4.6}$$

And then for the non-diagonal form (suppressing the $x-$dependence)

$$\begin{aligned} [H, \psi_{\uparrow}] &= -\xi_k \psi_{\uparrow} - U_{\uparrow} \psi_{\uparrow} - \Delta \psi_{\downarrow}^{\dagger} \\ [H, \psi_{\downarrow}] &= -\xi_k \psi_{\downarrow} - U_{\downarrow} \psi_{\downarrow} + \Delta \psi_{\uparrow}^{\dagger}. \end{aligned} \tag{4.7}$$

One then inserts the transformation of eq. 4.5 in eq. 4.7 and demand that these commutators are equal to those in eq. 4.6. This procedure yields two matrix equations

$$\begin{pmatrix} \xi_k + U_{\uparrow} & \Delta \\ \Delta^{*} & -(\xi_k + U_{\downarrow}) \end{pmatrix} \begin{pmatrix} u_{k\uparrow} \\ v_{k\downarrow} \end{pmatrix} = E_{k\uparrow} \begin{pmatrix} u_{k\uparrow} \\ v_{k\downarrow} \end{pmatrix} \tag{4.8}$$

$$\begin{pmatrix} \xi_k + U_\downarrow & \Delta \\ \Delta^* & -(\xi_k + U_\uparrow) \end{pmatrix} \begin{pmatrix} u_{k\downarrow} \\ v_{k\uparrow} \end{pmatrix} = E_{-k\downarrow} \begin{pmatrix} u_{k\downarrow} \\ v_{k\uparrow} \end{pmatrix}. \tag{4.9}$$

We can write the two eqs. 4.8 and 4.9 as a single equation by introducing the spin-index σ

$$\begin{pmatrix} \xi_k + U_\sigma & \Delta \\ \Delta^* & -(\xi_k + U_{\bar{\sigma}}) \end{pmatrix} \begin{pmatrix} u_{k\sigma} \\ v_{k\bar{\sigma}} \end{pmatrix} = E_{k\sigma} \begin{pmatrix} u_{k\sigma} \\ v_{k\bar{\sigma}} \end{pmatrix} \tag{4.10}$$

and rewrite it to obtain

$$\begin{aligned} \begin{pmatrix} -(\xi_k + U_\sigma) & -\Delta^* \\ -\Delta & \xi_k + U_{\bar{\sigma}} \end{pmatrix} \begin{pmatrix} u^*_{k\sigma} \\ v^*_{k\bar{\sigma}} \end{pmatrix} &= -E_{k\sigma} \begin{pmatrix} u^*_{k\sigma} \\ v^*_{k\bar{\sigma}} \end{pmatrix} \\ &\Longrightarrow \\ \begin{pmatrix} \xi_k + U_{\bar{\sigma}} & \Delta \\ \Delta^* & -(\xi_k + U_\sigma) \end{pmatrix} \begin{pmatrix} v^*_{k\bar{\sigma}} \\ -u^*_{k\sigma} \end{pmatrix} &= -E_{k\sigma} \begin{pmatrix} v^*_{k\bar{\sigma}} \\ -u^*_{k\sigma} \end{pmatrix}, \end{aligned} \tag{4.11}$$

which is the equation for opposite spin. From this we see that there is a relation between the solutions with a certain spin and positive energy and the ones with opposite spin and negative energy. Consequently, if we have a solution for a certain spin $\psi_{k\sigma}(x) = (u_{k\sigma}(x),\, v_{k\bar{\sigma}}(x))^T$, we also know a solution for the opposite spin

$$\psi_{k\bar{\sigma}}(x) = (u_{k\bar{\sigma}}(x),\, v_{k\sigma}(x))^T = (v^*_{k\bar{\sigma}}(x),\, -u^*_{k\sigma}(x))^T,$$

with negative energy $E_{k\bar{\sigma}} = -E_{k\sigma}$. This property is the well-known particle-hole symmetry of superconductors, which means that removing a spin-up quasiparticle at negative energy is equivalent to creating a spin-down quasiparticle with positive energy. It shows up in the Bogoliubov-de Gennes equations due to the redundancy of the Nambu spinor. Notice that in the Bogoliubov transformation we sum only over the solutions of positve energy for this reason. In spin degenerate cases where $U_\uparrow = U_\downarrow$ such as the QPC it suffices to consider only spin-up solutions as there is only one excitation energy $E_{k\uparrow} = E_k$. Even when the spin degeneracy is broken the above relation is valid and the full set of solutions can be determined either by considering spin-up solutions of both positive and negative energy, or by considering both spin-up and spin-down solutions with positive energy only.

4.1.1 Homogeneous superconductor

We will now study the solutions to the Bogoliubov-de Gennes equation for a homogeneous superconductor with $U_\sigma = 0$ and $\Delta(x) = \Delta e^{i\phi}$ in detail as we need them to construct the wave functions we wish to use as an ansatz when solving the scattering problem. For a homogeneous superconductor we expand the wave function in terms of the plane waves

$$\begin{pmatrix} u_k(x) \\ v_k(x) \end{pmatrix} = e^{ikx} \begin{pmatrix} u_k \\ v_k \end{pmatrix}, \tag{4.12}$$

whereby the BdG-equation (eq. 4.8) for the spin-up quasiparticle wave function takes the following algebraic form (omitting the spin-indices)

$$\begin{pmatrix} \xi_k & \Delta e^{i\phi} \\ \Delta e^{-i\phi} & -\xi_k \end{pmatrix} \begin{pmatrix} u_k \\ v_k \end{pmatrix} = E_k \begin{pmatrix} u_k \\ v_k \end{pmatrix}, \tag{4.13}$$

with $\xi_k = \hbar^2 k^2/2m - \mu$. We are looking for solutions which are excitations above the ground state with $E > \Delta$. The solutions also have to be normalized so that $|u_k|^2 + |v_k|^2 = 1$. Solving this matrix equation we find that there are two solutions $(u_k, v_k)^T$, which both have energy $E_k = \sqrt{\xi_k^2 + \Delta^2}$

$$u_k^{\pm} = e^{i\phi/2} \frac{1}{\sqrt{2}} \sqrt{1 \pm \frac{\sqrt{E_k^2 - \Delta^2}}{E_k}} \tag{4.14}$$

$$v_k^{\pm} = e^{-i\phi/2} \frac{1}{\sqrt{2}} \sqrt{1 \mp \frac{\sqrt{E_k^2 - \Delta^2}}{E_k}}. \tag{4.15}$$

We note that the corresponding solutions with negative energy are $\begin{pmatrix} (v_k^{\pm})^* \\ -(u_k^{\pm})^* \end{pmatrix}$ in accordance with the results of the previous section. To understand the meaning of the two different signs in u and v we have to consider the value of k. For each value of E_k there are two corresponding values of k:

$$E_k = \sqrt{\left(\frac{\hbar^2 k^2}{2m} - \mu\right)^2 + \Delta^2} \implies k_{\pm} = \frac{\sqrt{2m}}{\hbar} \sqrt{\mu \pm \sqrt{E_k^2 - \Delta^2}}. \tag{4.16}$$

In addition $\pm k_{\pm}$ (where the two signs are independent) gives the same quasiparticle energy E_k. As we have $\xi_k = \pm\sqrt{E_k^2 - \Delta^2}$, the sign of ξ_k determines whether we have the solutions with plus or minus for both k and u. We can interpret these different solutions as electron and hole wave functions by the following argument:
k_- (k_+) corresponds to a momentum below (above) the Fermi surface and hence a negative (positive) energy ξ_k. Quasiparticle excitations with $+\xi_k$ can be described as the creation of a quasi-electron above the Fermi level, and similarly excitations with $-\xi_k$ are associated with the creation of a quasihole (removal of a quasielectron) below the Fermi level (see fig. 4.1). This means that the wave function for quasielectrons with positive energy is $\begin{pmatrix} u_k^+ \\ v_k^+ \end{pmatrix}$ and the one for quasiholes is $\begin{pmatrix} u_k^- \\ v_k^- \end{pmatrix}$. We can now define

$$u_k \equiv u_k^+ = \frac{1}{\sqrt{2}} \sqrt{1 + \frac{\sqrt{E_k^2 - \Delta^2}}{E_k}} \tag{4.17}$$

$$v_k \equiv v_k^+ = \frac{1}{\sqrt{2}} \sqrt{1 - \frac{\sqrt{E_k^2 - \Delta^2}}{E_k}}, \tag{4.18}$$

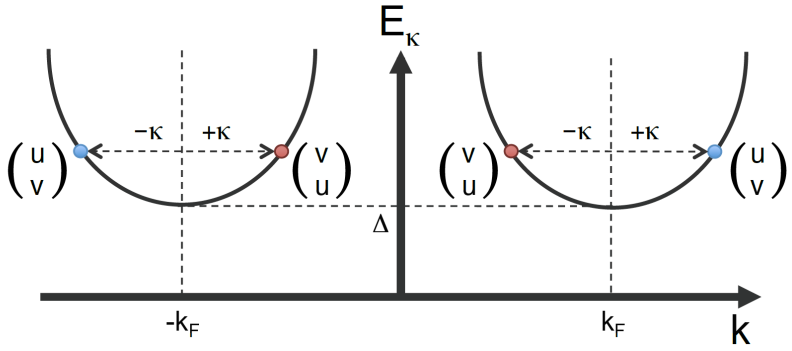

Figure 4.1: Dispersion for Bogoliubov quasiparticles with positive energy. Figure taken from [25].

where we exclude the phase dependence from the definitions as we will write it explicitly in the wave functions for clarity. We have hence determined the wave functions in momentum space for electrons and holes with energy E_k in a homogenous superconductor. When constructing wave functions for incoming, transmitted and reflected waves in the scattering problem we will need to assign a direction of propagation to the wave functions. This is done by considering the sign of the group velocity:

$$v_g(k) = \frac{1}{\hbar}\frac{dE_k}{dk} = \frac{\hbar}{m}\frac{k\xi_k}{\sqrt{\xi_k^2 + \Delta^2}}. \tag{4.19}$$

As a positive (negative) group velocity corresponds to a wavepacket propagating in the positive (negative) x-direction, we see that the sign of $k\xi_k$ determines the direction of motion. That is, for an electron with positive (negative) ξ_k a wave function with positive (negative) k propagates in the positive (negative) $x-$direction and vice versa for quasiholes. With this we have the wave functions for spin-up quasiparticles in a homogeneous superconductor

$$\psi^{\pm}_{e\uparrow}(x) = \begin{pmatrix} u_k e^{i\phi/2} \\ v_k e^{-i\phi/2} \end{pmatrix} e^{\pm ik_+ x} \tag{4.20}$$

$$\psi^{\pm}_{h\uparrow}(x) = \begin{pmatrix} v_k e^{i\phi/2} \\ u_k e^{-i\phi/2} \end{pmatrix} e^{\mp ik_- x}, \tag{4.21}$$

where the sign refers to the direction of propagation. For each positive energy E_k we have four states in total: an electron and a hole state with positive momentum and one with negative momentum. This is seen in fig. 4.1. The wave functions for spin-down with negative energy $E_{k\downarrow} = -E_k$ can as mentioned above be obtained through the substitutions $(u \to v^*, v \to -u^*)$. We can also label the wave functions by their energy $E = E_k$ instead of their momentum, as all relevant quantities can be expressed in terms of the energy instead of momentum and integrals over momentum can be transformed to integrals over energy by employing the density of states. We will use this labelling when proceeding.

4.1.2 Current operator

For use in our calculations later on, we wish to express the current operator for a superconductor in terms of the Bogoliubov quasiparticle operators. In terms of the electron field operators, the current operator is [13]

$$\hat{I}(x) = -\frac{e\hbar}{2mi}\sum_{\sigma}\left(\psi_{\sigma}^{\dagger}(x)\frac{d}{dx}\psi_{\sigma}(x) - \frac{d}{dx}\psi_{\sigma}^{\dagger}(x)\psi_{\sigma}(x)\right). \tag{4.22}$$

We wish to employ the Bogoliubov transformation for a general quantum number i (where $i \to -i$ and $\sigma \to \bar{\sigma}$ is the time-reversed state)

$$\psi_{\sigma}(x) = \sum_{i}(u_{i\sigma}\gamma_{i\sigma} - \sigma v_{i\sigma}^{*}\gamma_{-i\bar{\sigma}}^{\dagger}). \tag{4.23}$$

Plugging this into the current operator we obtain

$$\begin{aligned}\hat{I}(x) = -\frac{e\hbar}{2mi}\sum_{ij\sigma}\Big(&u_{i\sigma}^{*}\frac{du_{j\sigma}}{dx}\gamma_{i\sigma}^{\dagger}\gamma_{j\bar{\sigma}} + v_{-i\sigma}\frac{dV_{-j\sigma}}{dx}\gamma_{i\bar{\sigma}}\gamma_{j\sigma}^{\dagger} - \sigma v_{-i\sigma}\frac{du_{j\sigma}}{dx}\gamma_{i\bar{\sigma}}\gamma_{j\sigma} - \sigma u_{i\sigma}^{*}\frac{dv_{-j\sigma}^{*}}{dx}\gamma_{i\sigma}^{\dagger}\gamma_{j\bar{\sigma}}^{\dagger} \\ &- u_{j\sigma}\frac{du_{i\sigma}^{*}}{dx}\gamma_{i\sigma}^{\dagger}\gamma_{j\sigma} - v_{-j\sigma}^{*}\frac{dv_{-i\sigma}}{dx}\gamma_{i\bar{\sigma}}\gamma_{j\bar{\sigma}}^{\dagger} + \sigma u_{j\sigma}\frac{dv_{-i\sigma}}{dx}\gamma_{i\bar{\sigma}}\gamma_{j\sigma} + \sigma v_{-j\sigma}^{*}\frac{du_{i\sigma}^{*}}{dx}\gamma_{i\sigma}^{\dagger}\gamma_{j\bar{\sigma}}^{\dagger}\Big).\end{aligned} \tag{4.24}$$

This can be written in matrix form as

$$\hat{I}(x) = -\frac{\hbar e}{2mi}\sum_{ij\sigma}\left(\gamma_{i\sigma}^{\dagger}, \gamma_{i\bar{\sigma}}\right)\begin{pmatrix} u_{i\sigma}^{*}\frac{du_{j\sigma}}{dx} - \frac{du_{i\sigma}^{*}}{dx}u_{j\sigma} & -\sigma\left(u_{i\sigma}^{*}\frac{dv_{-j\sigma}^{*}}{dx} - \frac{du_{i\sigma}^{*}}{dx}v_{-j\sigma}^{*}\right) \\ -\sigma\left(v_{-i\sigma}\frac{du_{j\sigma}}{dx} - \frac{dv_{-i\sigma}}{dx}u_{j\sigma}\right) & v_{-i\sigma}\frac{dv_{-j\sigma}^{*}}{dx} - \frac{dv_{-i\sigma}}{dx}v_{-j\sigma}^{*}\end{pmatrix}\begin{pmatrix}\gamma_{j\sigma} \\ \gamma_{j\bar{\sigma}}^{\dagger}\end{pmatrix}. \tag{4.25}$$

4.2 NS-contact

We will now move on to consider systems with a scattering potential modelled by a delta function. We start by the simple case of an NS-contact where the left lead is in the normal state and the right lead is superconducting. The leads are separated by a barrier at $x = 0$ described by the Hamiltonian $V(x) = Z\delta(x)$. We solve the problem using as our ansatz the wave functions of eq. 4.21. We are looking for excitations of the system, so throughout this chapter we will consider wave functions of positive energy $E > 0$. The present scattering problem is also independent of spin, so we consider only the spin-up sector. The relevant electron- and hole-like quasiparticles in the superconductor have the following wave functions labelled by their energy

$$\psi_{e}^{\pm}(x) = \begin{pmatrix}u_E \\ v_E\end{pmatrix}e^{\pm ik_{+}x} \quad \text{and} \quad \psi_{h}^{\pm}(x) = \begin{pmatrix}v_E \\ u_E\end{pmatrix}e^{\mp ik_{-}x}, \tag{4.26}$$

where

$$k_\pm = \frac{\sqrt{2m}}{\hbar}\sqrt{E_F \pm \sqrt{E^2-\Delta^2}}, \quad u = \frac{1}{\sqrt{2}}\sqrt{1+\frac{\sqrt{E^2-\Delta^2}}{E}} \\ \text{and} \quad v = \frac{1}{\sqrt{2}}\sqrt{1-\frac{\sqrt{E^2-\Delta^2}}{E}}. \tag{4.27}$$

We start by considering the case of $E > \Delta$ where the square roots in u and v are real. As only one of the leads are superconducting, we can let the superconducting order parameter be real without loss of generality, as this can always be achieved by a gauge transformation. In the normal lead the states are just either pure electron or hole states, which can be obtained by setting $\Delta = 0$. We will consider the Andreev approximation where $k_+ \approx k_- \approx k_F$. This is a good approximation for energies much smaller than the Fermi energy $E, \Delta \ll E_F$. If we consider an electron approaching the interface from the left in the normal lead, we have the following wave functions for incoming, reflected and transmitted waves

$$\psi_{in}(x<0) = \begin{pmatrix}1\\0\end{pmatrix} e^{ik_F x}, \quad \psi_r(x<0) = r_h \begin{pmatrix}0\\1\end{pmatrix} e^{ik_F x} + r_e \begin{pmatrix}1\\0\end{pmatrix} e^{-ik_F x} \tag{4.28}$$

$$\text{and} \quad \psi_t(x>0) = t_e \begin{pmatrix}u\\v\end{pmatrix} e^{ik_F x} + t_h \begin{pmatrix}v\\u\end{pmatrix} e^{-ik_F x}. \tag{4.29}$$

We seek to determine the reflection and transmission coefficients. This is done using the conditions that the wave function must be continuous at the interface $\psi_{in}(0)+\psi_r(0) = \psi_t(0)$ and that the discontinuity in the derivative is given by [28]

$$\Delta\psi'(x) = \frac{d\psi_-(x)}{dx}|_{x=0^-} - \frac{d\psi_+(x)}{dx}|_{x=0^+} = \frac{2mZ}{\hbar^2}\psi(0). \tag{4.30}$$

This condition is obtained by integrating the Hamiltonian. These two conditions provide us with a linear system of equations

$$\begin{aligned} &t_e u - t_h v - 1 + r_e = -2iz(1+r_e) \\ &t_e v - t_h u - r_h = -2iz r_h \\ &1 + r_e = u t_e + v t_h \\ &r_h = t_e v + t_h u, \end{aligned} \tag{4.31}$$

where we defined the dimensionless quantity $z = \frac{mZ}{\hbar^2 k_F}$ related to the normal state transmission probability by $\tau = 1/(1+z^2)$ [23]. Notice that the simplicity of these expressions relies heavily on the Andreev approximation. The solution is

$$r_h = \frac{uv}{\gamma} \quad r_e = -\frac{(u^2-v^2)(z^2+iz)}{\gamma} \quad t_e = \frac{u(1-iz)}{\gamma} \quad t_h = \frac{ivz}{\gamma}, \tag{4.32}$$

where $\gamma = u^2 + z^2(u^2-v^2)$. We also note that the absolute square of the coefficients are the tunneling and reflection probabilities for electrons and holes which are the elements of the scattering matrix in the electron-hole (i.e. Nambu) basis:

$$|r_h|^2 = R_{e\to h} = \frac{\Delta^2}{(E+(1+2z^2)\sqrt{E^2-\Delta^2})^2} \quad |r_e|^2 = R_{e\to e} = \frac{4z^2(1+z^2)(E^2-\Delta^2)}{(E+(1+2z^2)\sqrt{E^2-\Delta^2})^2} \tag{4.33}$$

$$|t_e|^2 = T_{e\to e} = \frac{(1+z^2)(E+\sqrt{E^2-\Delta^2})}{2E(E+(1+2z^2)\sqrt{E^2-\Delta^2})^2} \quad |t_h|^2 = T_{e\to h} = \frac{z^2(E-\sqrt{E^2-\Delta^2})}{2E(E+(1+2z^2)\sqrt{E^2-\Delta^2})^2}. \tag{4.34}$$

Though the transmission and reflection probabilities depend on the sign of the potential strength, the corresponding probabilities (which are the measureable quantities) don't. In the case of an incoming electron with an energy $E < \Delta$ u and v become complex numbers

$$u = \frac{1}{\sqrt{2}}\sqrt{1+i\frac{\sqrt{\Delta^2-E^2}}{E}} \quad v = u^*. \tag{4.35}$$

Similarly k acquires an imaginary part and becomes $k_\pm \to k_F \pm i\kappa_E$ when expanded to first order in k/k_F. Here $\kappa_E = \sqrt{1-E^2/\Delta^2}/\xi_0$ where $\xi_0 \sim \hbar v_F/\Delta$ is the superconducting coherence length. As there are no available states in the superconductor at energies $E < \Delta$, the incoming electron is prevented from being transmitted to the superconductor as a propagating plane wave. The imaginary part of the wave number ensures that the transmitted wave decays exponentially with a characteristic length given by the coherence length. This means that the transmission probabilities must be zero $c = d = 0$. The reflection probabilities can be obtained in the Andreev approximation using the results of eq. 4.32 with the complex values of u and v:

$$|r_h|^2 = R_{e\to h} = \frac{\Delta^2}{E^2+(\Delta^2-E^2)(1+2z^2)^2} \quad |r_e|^2 = R_{e\to e} = \frac{4(\Delta^2-E^2)(1+z^2)z^2}{E+(\Delta^2-E^2)(1+2z^2)^2} \tag{4.36}$$

$$\tag{4.37}$$

If we consider the particularly simple case of an ideal interface where the normal state transmission probability is $\tau = 1$ corresponding to $z = 0$, we find that $r_{e\to e} = 0$ and $r_{e\to h} = 1$. This means that an incoming electron with energy $E < \Delta$ undergoes an Andreev reflection with probability 1, and is reflected back as a hole. As mentioned previously the Andreev reflection is the underlying mechanism causing the formation of Andreev bound states in Josephson junctions.

4.3 Superconducting quantum point contact

Having established the formalism necessary to calculate the wave functions of interfaces with superconductors, we will now move on to consider the QPC, where we will regain our previous results for the Andreev bound states. We again model the scattering potential by a $\delta-$barrier $V(x) = Z\delta(x)$. When both leads are superconducting, we will need to include the phase difference of the order parameter between them, so that the order parameter is given by $\Delta e^{i\phi}$ in the right lead and Δ in the left lead.

We start by calculating the wave function for the scattering states of an incoming electronlike spin up quasiparticle with energy $E > \Delta$. Hence we can again use the states of eq. 4.26 to construct the wave functions of the reflected and transmitted states as

$$\psi_{in}(x) = \begin{pmatrix} u \\ v \end{pmatrix} e^{ik_+ x} \quad \psi_r(x) = r_e \begin{pmatrix} u \\ v \end{pmatrix} e^{-ik_+ x} + r_h \begin{pmatrix} v \\ u \end{pmatrix} e^{ik_- x} \tag{4.38}$$

$$\psi_t(x) = t_e \begin{pmatrix} ue^{i\phi/2} \\ ve^{-i\phi/2} \end{pmatrix} e^{ik_+ x} + t_h \begin{pmatrix} ve^{i\phi/2} \\ ue^{-i\phi/2} \end{pmatrix} e^{-ik_- x}. \tag{4.39}$$

We will again use the Andreev approximation and let $k_+ = k_- = k_F$. We then have the derivatives

$$\frac{d\psi_-}{dx}|_{x=0} = \frac{d(\psi_{in} + \psi_r)}{dx}|_{x=0} = ik_F \begin{pmatrix} u \\ v \end{pmatrix} - ir_e k_F \begin{pmatrix} u \\ v \end{pmatrix} + ir_h k_F \begin{pmatrix} v \\ u \end{pmatrix} \tag{4.40}$$

$$\frac{d\psi_+}{dx}|_{x=0} = \frac{d\psi_t}{dx}|_{x=0} = it_e k_F \begin{pmatrix} ue^{i\phi/2} \\ ve^{-i\phi/2} \end{pmatrix} - it_h k_F \begin{pmatrix} ve^{i\phi/2} \\ ue^{-i\phi/2} \end{pmatrix}. \tag{4.41}$$

Using this with eq. 4.30 as well as demanding the wave function to be continuous at the interface again yields a linear system of equations

$$\begin{aligned} &u(1 + r_e) + vr_h = (t_e u + t_h v)e^{i\phi/2} \\ &v(1 + r_e) + ur_h = (t_e v + t_h u)e^{-i\phi/2} \\ &(t_e u - t_h v)e^{i\phi/2} - u + r_e u - r_h v = -2iz(r_e u + r_h v)e^{i\phi/2} \\ &(t_e v - t_h u)e^{-i\phi/2} - v + r_e v - r_h u = -2iz(t_e v + t_h u)e^{-i\phi/2}. \end{aligned} \tag{4.42}$$

Solving these equations yields the coefficients

$$\begin{aligned} r_e &= -\frac{(u^2 - v^2)^2 z(i + z)}{u^4 + v^4 + (u^2 - v^2)^2 z^2 - 2u^2 v^2 \cos(\phi)} \\ r_h &= \frac{(1 - e^{-i\phi})uv(v^2 e^{i\phi} - u^2)}{u^4 + v^4 + (u^2 - v^2)^2 z^2 - 2u^2 v^2 \cos(\phi)} \\ t_e &= \frac{e^{-i\phi/2}(u^2 - v^2)(u^2 - v^2 e^{i\phi})(1 - iz)}{u^4 + v^4 + (u^2 - v^2)^2 z^2 - 2u^2 v^2 \cos(\phi)} \\ t_h &= \frac{\sin(\phi/2)uv(u^2 - v^2)z}{u^4 + v^4 + (u^2 - v^2)^2 z^2 - 2u^2 v^2 \cos(\phi)}. \end{aligned} \tag{4.43}$$

When plugging in the expressions for u and v we obtain

$$\begin{aligned}
r_{eE} &= -\frac{z(i+z)(E^2-\Delta^2)}{D} \\
r_{hE} &= -\frac{\Delta\sin(\phi/2)(E\sin(\phi/2)+i\cos(\phi/2)\sqrt{E^2-\Delta^2}/2)}{D} \\
t_{eE} &= -\frac{(i+z)(i(E^2-\Delta^2)\cos(\phi/2)+E\sqrt{E^2-\Delta^2}\sin(\phi/2))}{D} \\
t_{hE} &= \frac{2z\Delta\sqrt{E^2-\Delta^2}\sin(\phi/2)}{D} \\
D &= E^2(1+z^2)-\Delta^2(z^2+\cos^2(\phi/2)).
\end{aligned} \tag{4.44}$$

Having obtained the scattering wave function for a spin-up electron impinging on the contact from the left lead, we can follow [25] and write it on the form

$$\begin{aligned}
\psi^{e+}_{E\uparrow}(x) &= \begin{pmatrix} U^{e+}_{E\uparrow}(x) \\ V^{e+}_{E\uparrow}(x) \end{pmatrix} \\
&= \left(\begin{pmatrix} u_E \\ v_E \end{pmatrix} e^{ik_+x} + r_{eE} \begin{pmatrix} u_E \\ v_E \end{pmatrix} e^{-ik_+x} + r_{hE} \begin{pmatrix} v_E \\ u_E \end{pmatrix} e^{ik_-x} \right) \theta(-x) \\
&+ \left(t_{eE} \begin{pmatrix} u_E e^{i\phi/2} \\ v_E e^{-i\phi/2} \end{pmatrix} e^{ik_+x} + t_{hE} \begin{pmatrix} v_E e^{i\phi/2} \\ u_E e^{-i\phi/2} \end{pmatrix} e^{-ik_-x} \right) \theta(x).
\end{aligned} \tag{4.45}$$

We note that the wave function for the scattering states is not normalizeable, so real single particle states are described by superpositions of wave functions within some energy range, and those are normalizable [28]. This is also in accordance with the fact that a quantum mechanical particle can't have a definite energy. As is done by [25], one can from this result obtain the rest of the solutions for the other possible source wave functions (holes and electrons propagating in different directions), but we will not need the explicit form of those here.

4.3.1 Andreev bound states

Having determined the scattering states the next step is to find the wave function for the Andreev bound states. That is, we are looking for states inside the gap with an energy $E_A < \Delta$. As was the case for the NS-interface, both the wave vector and electron/hole-amplitudes acquire an imaginary part:

$$u = \frac{1}{\sqrt{2}}\sqrt{1+i\frac{\sqrt{\Delta^2-E_A^2}}{E_A}},\ v = \frac{1}{\sqrt{2}}\sqrt{1-i\frac{\sqrt{\Delta^2-E_A^2}}{E_A}} \text{ and } k_\pm = k_F \pm i\kappa_A, \tag{4.46}$$

where we introduced the bound state energy E_A in anticipation of the fact that the bound states only exist for a certain value of the energy $E = E_A$. The bound states

must be normalizable, and hence they should be evanescent waves decaying within a length scale of κ_A^{-1}. This excludes the wave functions with $e^{-\kappa_a x}$ in the left lead, and those with $e^{\kappa_a x}$ in the right lead. The bound states don't require an incoming wave to form, so we have a wave function of the form

$$\psi_A(x) = \begin{pmatrix} U_{E_A} \\ V_{E_A} \end{pmatrix} \tag{4.47}$$

$$= \left(r_{hA} \begin{pmatrix} v_{E_A} \\ u_{E_A} \end{pmatrix} e^{ik_- x} + r_{eA} \begin{pmatrix} u_{E_A} \\ v_{E_A} \end{pmatrix} e^{-ik_+ x} \right) \theta(-x) \tag{4.48}$$

$$+ \left(t_{eA} \begin{pmatrix} u_{E_A} e^{i\phi/2} \\ v_{E_A} e^{-i\phi/2} \end{pmatrix} e^{ik_+ x} + t_{hA} \begin{pmatrix} v_{E_A} e^{i\phi/2} \\ u_{E_A} e^{-i\phi/2} \end{pmatrix} e^{-ik_- x} \right) \theta(x). \tag{4.49}$$

We start by considering the normalization condition in the Andreev approximation. For the wave function to be normalized, we must have

$$1 = \int_{-\infty}^{\infty} dx \, |\psi_A(x)|^2 = \int_{-\infty}^{0} dx \, |\psi_A(x<0)|^2 + \int_{0}^{\infty} dx \, |\psi_A(x>0)|^2. \tag{4.50}$$

So we start by calculating

$$|\psi_A(x<0)|^2 = (r_{hA} u_{E_A} e^{-ik_+ x} + r_{eA} v_{E_A} e^{ik_- x})(r_{hA}^* u_{E_A}^* e^{ik_- x} + r_{eA}^* v_{E_A}^* e^{-ik_+ x}) \tag{4.51}$$

$$+ (r_{hA} v_{E_A} e^{-ik_+ x} + r_{eA} u_{E_A} e^{ik_- x})(r_{hA}^* v_{E_A}^* e^{ik_- x} + r_{eA}^* u_{E_A}^* e^{-ik_+ x}) \tag{4.52}$$

$$= |r_{hA}|^2 (|v_{E_A}|^2 + |u_{E_A}|^2) e^{2\kappa_A x} + |r_{eA}|^2 (|v_{E_A}|^2 + |u_{E_A}|^2) e^{2\kappa_A x} \tag{4.53}$$

$$+ (r_{hA} r_{eA}^* u_{E_A} v_{E_A}^* + r_{hA} r_{eA}^* v_{E_A} u_{E_A}^*) e^{-2(ik_F - \kappa_A)x} \tag{4.54}$$

$$+ (r_{hA}^* r_{eA} (u_{E_A}^* v_{E_A} + v_{E_A}^* u_{E_A}) e^{2(ik_F + \kappa_A)x}. \tag{4.55}$$

All the $x-$dependence is in the exponents, so the relevant integrals are

$$\int_{-\infty}^{0} dx \, e^{\pm 2(ik_F \pm \kappa_A)x} = \frac{1}{\pm 2(ik_F \pm \kappa_A)} \tag{4.56}$$

and

$$\int_{-\infty}^{0} dx \, e^{2\kappa_A x} = \frac{1}{2\kappa_A}. \tag{4.57}$$

In the Andreev approximation $k_F \gg \kappa_A$ which means that $\frac{1}{2\kappa_A} \gg \frac{1}{\pm 2(ik_F \pm \kappa_A)}$, and we can neglect the contribution from the terms with $1/k_F$. Usually it is the case for the Bogoliubov wave functions that $|u|^2 + |v|^2 = 1$. However, this is not the case for $E < \Delta$ Here we instead have $|u|^2 = |v|^2 = \frac{\Delta}{2E_A}$. This means that we obtain

$$\int_{-\infty}^{0} dx \, |\psi_A(x<0)|^2 = \frac{|r_{hA}|^2 + |r_{eA}|^2}{2\kappa_A} \frac{\Delta}{E_A}. \tag{4.58}$$

The contribution to the norm of the wave function from $x > 0$ is similar, and we find that the normalization condition gives the constraint

$$|r_{hA}|^2 + |r_{eA}|^2 + |t_{eA}|^2 + |t_{hA}|^2 = \frac{2\kappa_A E_A}{\Delta}. \tag{4.59}$$

Once again we impose the previously mentioned conditions for continuity of the wave function and the discontinuity of the derivative. This results in a homogenous matrix equation

$$\begin{pmatrix} v & u & -ue^{i\phi/2} & -ve^{i\phi/2} \\ u & v & -ve^{-i\phi/2} & -ue^{-i\phi/2} \\ -v(1-2iz) & u(1+2iz) & ue^{i\phi/2} & -ve^{i\phi/2} \\ -u(1+2iz) & v(1+2iz) & ve^{-i\phi/2} & -ue^{-i\phi/2} \end{pmatrix} \begin{pmatrix} r_{hA} \\ r_{eA} \\ t_{eA} \\ t_{hA} \end{pmatrix} = \mathbf{mv} = \mathbf{0} \tag{4.60}$$

Such an equation has a nontrivial solution if the determinant of $\mathbf{m}$ is zero. By plugging in the expressions for u and v and solving the equation $\det(\mathbf{m}) = 0$ we regain the Andreev bound state energy

$$E_A = \pm\Delta\sqrt{1 - \tau\sin^2(\phi/2)} \tag{4.61}$$

Using this value of the energy in the coefficients u and v we obtain a solution for the reflection and transmission coefficients which we then have to normalize by determining the normalization constant N

$$r_{hA} = -N\sigma\sqrt{1+z^2}\left(\sqrt{\cos^2(\phi/2)+z^2} - \sigma\cos(\phi/2)\right) \tag{4.62}$$

$$r_{eA} = Ni\sigma(1-iz)z \tag{4.63}$$

$$t_{eA} = N(1-iz)\left(\sqrt{\cos^2(\phi/2)+z^2} - \sigma\cos(\phi/2)\right) \tag{4.64}$$

$$t_{hA} = iNz\sqrt{1+z^2}, \tag{4.65}$$

where $\sigma = \mathrm{sign}(\phi)$ and we defined the phase difference across the contact to be $-\pi < \phi < \pi$ so that $|\sin(\phi/2)| = \sigma\sin(\phi/2)$. To simplify the calculation of N we define the quantities $x = \sqrt{\cos^2(\phi/2)+z^2}$ and $y = \cos(\phi/2)$ so that $\sin(\phi/2) = \sqrt{1-y^2}$ and $z^2 = x^2 - y^2$. Furthermore

$$\kappa_A = \sqrt{1 - E_A^2/\Delta^2}/\xi_0 = \frac{\sigma\sqrt{\tau}}{\xi_0}\sin(\phi/2) = \frac{\sigma\sqrt{\tau}\sqrt{1-y^2}}{\xi_0}. \tag{4.66}$$

The normalization constant is then

$$\begin{aligned} &|r_{hA}|^2 + |r_{eA}|^2 + |t_{hA}|^2 + |t_eA|^2 = 2(|r_{hA}|^2 + |r_{eA}|^2) = 2N^2(1+z^2)(z^2 + (x-\sigma y)^2) \\ &= 2N^2(1+z^2)(2x(x-\sigma y)) \overset{!}{=} \frac{2\kappa_A E_A}{\Delta} = \frac{2\Delta\sigma\tau x\sqrt{1-y^2}}{\hbar v_F} \\ &\implies N^2 = \frac{\Delta\sigma}{\hbar v_F}\tau^2\frac{x\sqrt{1-y^2}}{2x(x-\sigma y)} = \frac{\Delta\sigma\sin(\phi/2)}{2\hbar v_F(1+z^2)\left(\sqrt{z^2+\cos^2(\phi/2)} - \sigma\cos(\phi/2)\right)}. \end{aligned} \tag{4.67}$$

With this we have fully determined the wave function for the Andreev bound state and confirmed the results of [24]. What we have obtained is equivalent to the result of solving the BdG-equations explicitly with a scattering potential. We can hence expand the electron field operators in terms of the quasiparticle operators γ_E by employing the Bogoliubov transformation of equation 4.5. However, we wish to label the states by their energy, direction of propagation ($\pm$) and electron/hole nature (η) and not by their momentum, $\gamma_{k\sigma} \to \gamma_{E\eta\pm\sigma}$. For the time-reversed states we note that as an electron with momentum $-k$ has the same energy as one with momentum k but propagates in the opposite direction, $\gamma_{-k\bar{\sigma}} \to \gamma_{E\eta\mp\bar{\sigma}}$ annihilates a quasiparticle in the time-reversed state of $\gamma_{k\sigma}$. For the bound states which are not propagating we have $\gamma_{-k_A\bar{\sigma}} \to \gamma_{E_A\bar{\sigma}}$. The Bogoliubov transformation then has a discrete (in energy) contribution from the bound state and a sum over contributions from the scattering states

$$\begin{aligned}\psi_\sigma(x) &= U_{E_A}(x)\gamma_{E_A\sigma} - \sigma V_{E_A}(x)^*\gamma^\dagger_{E_A\bar{\sigma}} + \sum_{E,\eta,\pm}(U_E^{\eta\pm}(x)\gamma_{E\eta\pm\sigma} - \sigma(V_E^{\eta\pm}(x))^*\gamma^\dagger_{E\eta\mp\bar{\sigma}}) \\ &= \sum_i (U_i(x)\gamma_{i\sigma} - \sigma(V_i(x))^*\gamma^\dagger_{-i\bar{\sigma}}).\end{aligned} \tag{4.68}$$

Here the electron and hole amplitudes U, V have no spin-index as the problem is spin-degenerate. We remind ourselves that the Bogoliubov transformation contains only energies $E > 0$ as it is a description in terms of excitations above the ground state.

4.3.2 Absorption rates

We have now solved the scattering problem for a QPC and determined both the scattering and bound states of the system. This means that we can express the current operator in the basis formed by these states using eq. 4.25. We will now see that we can use this to regain some of our previous results for the QPC. With our expression for the current operator and U_i and V_i, the equilibrium current carried by the groundstate at $T = 0$ is easily calculated. We also know that the equilibrium current is carried solely by the bound state in the short junction limit, so we don't have to include the continuum states in this calculation. The current is the same everywhere in the system, so we can calculate it at $x = 0^+$. We denote the ground state without quasiparticles by $|\Phi_0\rangle$ and calculate the expectation value of the current operator

$$\begin{aligned}\langle\Phi_0|\,\hat{I}(x)\,|\Phi_0\rangle &= \sum_\sigma \langle\Phi_0|\,\gamma_{E_A\sigma}\gamma^\dagger_{E_A\sigma}\,|\Phi_0\rangle \\ &= -2\frac{\hbar e}{2mi}\left(V_{E_A}\frac{dV^*_{E_A}}{dx} - \frac{dV_{E_A}}{dx}V^*_{E_A}\right)\end{aligned} \tag{4.69}$$

$$
\begin{aligned}
&= \frac{\hbar e}{mi} ik_F \left((t_{eA} v_A + t_{hA} u_A)(t_{eA}^* v_A^* - t_{hA}^* u_A^*) + (t_{eA} v_A - t_{hA} u_A)(t_{eA}^* v_A^* + t_{hA}^* u_A^*) \right) \\
&= \frac{2\hbar e k_F}{m} (|t_{eA}|^2 |v_A|^2 - |t_{hA}|^2 |u_A|^2) \\
&= \frac{2\hbar e k_F}{m} (|t_{eA}|^2 - |t_{hA}|^2) u_A v_A.
\end{aligned} \tag{4.70}
$$

Plugging in the values for u_A, v_A, t_{eA} and t_{hA} and using that the normal-state conductance is $G = 2e^2/h(1+z^2)$ we find

$$
\langle I \rangle_0 = -\frac{\pi G \Delta^2 \sin(\phi)}{2e E_A(\phi)}, \tag{4.71}
$$

in accordance with the expression we previously obtained using the Green's function method.

We have also calculated the admittance for a QPC and know that its real part has a discrete peak at the frequency where the absorption of a photon causes the creation of a pair of quasiparticles in the bound state. The same result can now be obtained using Fermi's golden rule. In eq. 2.70 we gave an expression for the absorption rate of an inductor with admittance Y. The contribution from the term $\operatorname{Re} Y_3$ related to the creation of a pair of quasiparticles in the Andreev bound state is particularly simple as it involves no continuum states and hence no energy-integrals. For this reason we can easily obtain an expression for the related absorption rate Γ_3 using Fermi's golden rule. The absorption rate found from the linear response calculation using the result for $\operatorname{Re} Y_3$ (eq. 2.68) in eq. 2.70 is

$$
\Gamma_3 = \phi_1^2 \frac{\pi^2 G}{2e^2} \frac{\Delta^4 \tau(1-\tau) \sin^4(\phi/2)}{E_A^2} \delta(\omega - 2E_A). \tag{4.72}
$$

From Fermi's golden rule with initial state $|\Phi_0\rangle$ and final state $\gamma_{E_A\uparrow}^\dagger \gamma_{E_A\downarrow}^\dagger |\Phi_0\rangle$ and the perturbation in eq. 4.2 we find

$$
\Gamma_3 = \frac{2\pi}{e^2\hbar} \phi_1^2 |\langle \Phi_0 | \gamma_{E_A\downarrow} \gamma_{E_A\uparrow} \hat{I} | \Phi_0 \rangle|^2 \delta(2E_A - \omega). \tag{4.73}
$$

The matrix element is given by

$$
\begin{aligned}
\langle \Phi_0 | \gamma_{E_A\downarrow} \gamma_{E_A\uparrow} \hat{I} | \Phi_0 \rangle &= \frac{\hbar e k_F}{m} t_{eA}^* t_{hA}^* (v_A^2 - u_A^2) \\
&= -\frac{e\hbar k_F \Delta\sigma}{2m\hbar v_F} \frac{(1+iz) z \sqrt{1+z^2}}{(1+z^2)^2} \frac{\sqrt{\Delta^2 - E_A^2} \sin(\phi/2)}{E_A}.
\end{aligned} \tag{4.74}
$$

The absolute square of this is

$$
|\langle \Phi_0 | \gamma_{E_A\downarrow} \gamma_{E_A\uparrow} \hat{I} | \Phi_0 \rangle|^2 = \frac{\pi G}{4\hbar} \frac{\Delta^4 \sin^4(\phi/2) \tau(1-\tau)}{E_A^2}. \tag{4.75}
$$

Using this in eq. 4.73 we find

$$\Gamma_3 = \phi_1^2 \frac{\pi^2 G}{2\hbar^2 e^2} \frac{\Delta^4 \tau(1-\tau)\sin^4(\phi/2)}{E_A^2} \delta(2E_A - \omega). \tag{4.76}$$

We have thus shown that the transition rate obtained using Fermi's golden rule is the same as the one we got from the linear response calculation. Though it is not feasible to obtain analytical results for the absorption rates corresponding to Y_1 and Y_2 using this method we can explain why these three terms and no additional ones are present. Naively one might anticipate that absorption peaks arising from the creation of a single quasiparticle in an excited state could be seen, but this is not the case (when $|i\rangle$ is the ground state). This is due to the fact that the perturbation (phase fluctuations) couples to the current operator, which only has terms of the form $\psi_\sigma^\dagger \psi_\sigma$ and is hence also bilinear in the Bogoliubov quasiparticle operators. Consequently only the matrix elements of the current operator between an initial state with zero quasiparticles and a final state with two quasiparticles are nonzero. Furthermore we observe that there are also restrictions on the spin of the created quasiparticles, as the relevant matrix element for this process is $\hat{I}_{ij} \propto \gamma_{i\sigma}^\dagger \gamma_{j\bar{\sigma}}^\dagger$, from which we can infer that the created quasiparticles must have opposite spin. This is as expected when remebering that they must arise from the splitting of a Cooper pair consisting of time-reversed electrons. All of this is in accordance with the fact that excitation processes due to photon absorption must conserve parity.

4.4 Magnetic impurity

We will now investigate how the solutions to the scattering problem change when a spin-dependent term is added to the potential. Such a term can for example describe a local magnetic field or a magnetic impurity. As we will see, this model yields the same result as the Anderson model in the cotunneling limit with a classical spin. However, we will not include coupling asymmetry between the leads here, as this would require two barriers and make the calculations even more complicated. As the problem is now spin-dependent, we know that the energy levels will not be spin-degenerate, and it is no longer sufficient to consider spin up-electrons only. Hence we now use in our ansatz the four-Nambu spinor containing states of both spins

$$\psi(x) = \begin{pmatrix} u_\uparrow(x) \\ u_\downarrow(x) \\ v_\uparrow(x) \\ v_\downarrow(x), \end{pmatrix} \tag{4.77}$$

and consider states of positive energy. We know all quantities here from eqs. 4.8 and 4.9 and remind ourselves that in a homogeneous superconductor

$$\psi_{e\uparrow}(x) = \begin{pmatrix} u_\uparrow(x) \\ 0 \\ 0 \\ v_\downarrow(x) \end{pmatrix} = \begin{pmatrix} u_E(x) \\ 0 \\ 0 \\ v_E(x) \end{pmatrix} \tag{4.78}$$

with the definitions for u_E and v_E used previously. The corresponding solution for a hole with spin-down is

$$\psi_{h\downarrow}(x) = \begin{pmatrix} v_\uparrow(x) \\ 0 \\ 0 \\ u_\downarrow(x) \end{pmatrix} = \begin{pmatrix} v_E(x) \\ 0 \\ 0 \\ u_E(x). \end{pmatrix} \tag{4.79}$$

This is the solution of positive energy to eq. 4.8 which gives the spin-up space of solutions. Now we wish to include also the spin-down space in our ansatz, and to this end we note that in a homogeneous superconductor without a potential U_σ the equations 4.8 and 4.9 are identical. Hence the spin-down states of positive energy in four-Nambu basis are just:

$$\psi_{e\downarrow}(x) = \begin{pmatrix} 0 \\ u_\downarrow(x) \\ v_\uparrow(x) \\ 0 \end{pmatrix} = \begin{pmatrix} 0 \\ u_E(x) \\ v_E(x) \\ 0 \end{pmatrix} \quad \text{and} \quad \psi_{h\uparrow}(x) = \begin{pmatrix} 0 \\ v_\downarrow(x) \\ u_\uparrow(x) \\ 0 \end{pmatrix} = \begin{pmatrix} 0 \\ v_E(x) \\ u_E(x) \\ 0 \end{pmatrix}. \tag{4.80}$$

We are now ready to find the solutions to the full problem described by the Hamiltonian $H = H_{BCS} + \delta(x)(Z + B\sigma)$, where σ is the electron spin. The ansatz is again constructed using the wave functions given above. We start by considering the bound states, which means that the wave function has to be outgoing and decay exponentially in the superconducting leads within the coherence length, and that we need no incoming wave. We remain in the Andreev approximation and assume E_F to be the dominating energy scale of the problem. The full form of the ansatz is

$$\Psi(x) = \left[r_{e\uparrow} \begin{pmatrix} u \\ 0 \\ 0 \\ v \end{pmatrix} e^{-ik_+ x} + r_{h\downarrow} \begin{pmatrix} v \\ 0 \\ 0 \\ u \end{pmatrix} e^{ik_- x} + r_{e\downarrow} \begin{pmatrix} 0 \\ u \\ v \\ 0 \end{pmatrix} e^{-ik_+ x} + r_{h\uparrow} \begin{pmatrix} 0 \\ v \\ u \\ 0 \end{pmatrix} e^{ik_- x} \right] \theta(-x) +$$
$$\left[t_{e\uparrow} \begin{pmatrix} ue^{i\phi/2} \\ 0 \\ 0 \\ ve^{-i\phi/2} \end{pmatrix} e^{ik_+ x} + t_{h\downarrow} \begin{pmatrix} ve^{i\phi/2} \\ 0 \\ 0 \\ ue^{-i\phi/2} \end{pmatrix} e^{-ik_- x} + t_{e\downarrow} \begin{pmatrix} 0 \\ ue^{i\phi/2} \\ ve^{-i\phi/2} \\ 0 \end{pmatrix} e^{ik_+ x} + t_{h\uparrow} \begin{pmatrix} 0 \\ ve^{i\phi/2} \\ ue^{-i\phi/2} \\ 0 \end{pmatrix} e^{-ik_- x} \right] \theta(x). \tag{4.81}$$

The reflection and transmission coefficients are now determined using the boundary conditions for continuity of the wave function and the discontinuity of the derivative. This second condition requires some extra care in our four-Nambu basis. It is obtained by integrating the Hamiltonian - in this case the BdG-Hamiltonian - over an infinitesimal interval around $x = 0$ [28]. From eq. 4.8 we have the two equations

$$-\frac{\hbar^2}{2m}\frac{\partial^2 u_\uparrow}{\partial x^2} + U_\uparrow u_\uparrow + \Delta v_\downarrow = E_\uparrow u_\uparrow \tag{4.82}$$

$$\frac{\hbar^2}{2m}\frac{\partial^2 v_\downarrow}{\partial x^2} - U_\downarrow v_\downarrow + \Delta^* u_\uparrow = E_\uparrow v_\downarrow \tag{4.83}$$

with $U_\sigma(x) = (Z + B\sigma)\delta(x)$. Integration of the first equation yields

$$\begin{aligned} &-\frac{\hbar^2}{2m}\int_{-\epsilon}^{\epsilon} dx\, \left(\frac{\partial^2 u_\uparrow}{\partial x^2} + (Z+B)\delta(x)u_\uparrow + \Delta v_\downarrow\right) = \int_{-\epsilon}^{\epsilon} dx\, E_\uparrow u_\uparrow \\ &\implies \frac{\hbar^2}{2m}\left(\left.\frac{\partial u_\uparrow}{\partial x}\right|_{x=0^+} - \left.\frac{\partial u_\uparrow}{\partial x}\right|_{x=0^-}\right) = (Z+B)u_\uparrow. \end{aligned} \tag{4.84}$$

Similarly from the second equation we obtain the condition

$$\frac{\hbar^2}{2m}\left(\left.\frac{\partial v_\downarrow}{\partial x}\right|_{x=0^+} - \left.\frac{\partial v_\downarrow}{\partial x}\right|_{x=0^-}\right) = (Z-B)v_\downarrow. \tag{4.85}$$

In the same way we can obtain conditions for the derivatives of $u_\downarrow$ and $v_\uparrow$, so that we can write the condition for the derivative of the wave function as

$$\Delta\frac{\partial\psi(x)}{\partial x} = \frac{2m}{\hbar^2}\begin{pmatrix}(Z+B)u_\uparrow\\(Z-B)u_\downarrow\\(Z+B)v_\uparrow\\(Z-B)v_\downarrow\end{pmatrix}. \tag{4.86}$$

Imposing the two boundary conditions we obtain a homogenous system of eight equations. However, this system of equations consists of two individual subsystems corresponding to spin up and spin down, and we have for the spin up subsystem:

$$\begin{pmatrix} u & v & -ue^{i\phi/2} & -ve^{i\phi/2}\\ v & u & -ve^{-i\phi/2} & -ue^{-i\phi/2}\\ u(1+2i(z+b)) & -v(1-2i(z+b)) & ue^{i\phi/2} & -ve^{i\phi/2}\\ v(1+2i(z-b)) & -u(1-2i(z-b)) & ve^{-i\phi/2} & -ue^{-i\phi/2}\end{pmatrix}\begin{pmatrix}r_{e\uparrow}\\r_{h\downarrow}\\t_{e\uparrow}\\t_{h\downarrow}\end{pmatrix} = \mathbf{0}, \tag{4.87}$$

where we defined the dimensionless potential strengths $z = mZ/\hbar^2 k_F$ and $b = mB/\hbar^2 k_F$. The equation for the spin-down sector is identical, apart from the substitution $b \to -b$. Hence it suffices to consider only a single equation if we let $b \to \sigma b$:

$$\begin{pmatrix} u & v & -ue^{i\phi/2} & -ve^{i\phi/2} \\ v & u & -ve^{-i\phi/2} & -ue^{-i\phi/2} \\ u(1+2i(z+\sigma b)) & -v(1-2i(z+\sigma b)) & ue^{i\phi/2} & -ve^{i\phi/2} \\ v(1+2i(z-\sigma b)) & -u(1-2i(z-\sigma b)) & ve^{-i\phi/2} & -ue^{-i\phi/2} \end{pmatrix} \begin{pmatrix} r_{e\sigma} \\ r_{h\bar{\sigma}} \\ t_{e\sigma} \\ t_{h\bar{\sigma}} \end{pmatrix} = \mathbf{0}. \tag{4.88}$$

Plugging in the expression for u and v and demanding the system of equations to have nontrivial solutions yields an equation which allows us to determine the bound state energies

$$\begin{aligned} &\det(m_\sigma) = 0 \\ &\implies (z^2 - b^2 + \cos^2(\phi/2))\Delta^2 - (1 - b^2 + z^2)E^2 + 2g\sigma E\sqrt{\Delta^2 - E^2} = 0 \\ &\implies \alpha - \beta x^2 = -\sigma\gamma x\sqrt{1-x^2} \quad \text{with} \\ &\alpha = (z^2 - b^2 + \cos^2(\phi/2)),\ \beta = (1 - b^2 + z^2),\ \gamma = 2b \quad \text{and} \quad x = \frac{E}{\Delta}. \end{aligned} \tag{4.89}$$

This equation can be solved by squaring both sides, which yields the solutions

$$x = \pm\sqrt{\frac{2\alpha\beta \pm \gamma\sqrt{\alpha(\beta-\alpha)+\gamma^2}}{\beta^2 - \gamma^2}}. \tag{4.90}$$

Defining $a = \frac{2\alpha\beta\Delta^2+\gamma^2\Delta^2}{2\beta^2+2\gamma^2}$ and $b = \frac{\gamma\Delta\sqrt{\alpha\beta-\alpha^2+\gamma^2}}{\beta^2+\gamma^2}$ we can write the solution as $x = s\sqrt{a+tb}$. Here $(s,t) = \pm 1$ and s is the sign we must determine to ensure that we pick the right solution which also satisfies $\alpha - \beta x^2 = -\sigma\gamma x\sqrt{1-x^2}$. Rewriting the condition we find

$$\beta(a+tb) - \alpha = \gamma\sigma s\sqrt{a+tb}\sqrt{1-a-tb} \implies s(\sigma) = \text{sign}\left(\frac{\beta(a+tb)-\alpha}{\sigma\gamma}\right). \tag{4.91}$$

With this we find that the bound state energies $E_{\pm\sigma} = s(\sigma)\sqrt{a \pm b}$ obtained here are consistent with those obtained with the Green's function method. But here we don't have the same parametrization of the parameters in terms of the displacement from the particle-hole symmetric point so z and b can be varied freely. To reach the same regime as we studied in the cotunneling model we should use $b < 0$, $b \to 1/g$ and $z \to 1/w$. That is, for the parametrization used for the magnetic impurity where $w < g$, we here have $z > b$. This means that the model with two superconducting leads and a classical magnetic impurity corresponds to scattering on a $\delta-$barrier where the strength of the (repulsive) potential depends on the spin of the electrons and $0 < U_\uparrow < U_\downarrow$. The bound states are plotted for $g = -0.5$ and $z = 0.3$ in fig. 4.2. For $g > 0$, we instead reach the regime of spin-split Andreev bound states as in figs. 3.2 and 5.4.

The general solution for the coefficients which is nontrivial when $E = E_{i\sigma}$ in u and v where $E_{i\sigma}$ is one of the positive bound state energies has a complicated form which is not particularly enlightening, but we state it here for completeness:

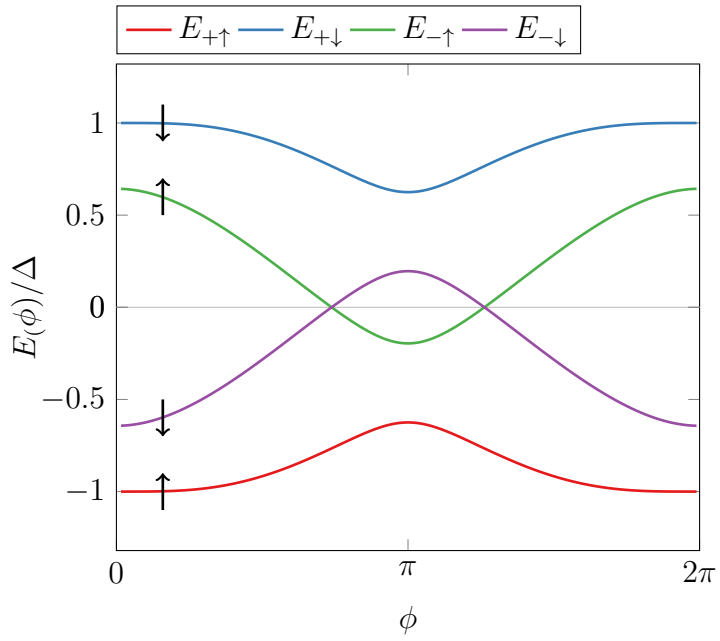

Figure 4.2: Bound state energies for $g = -0.5$ and $z = 0.3$, which reproduces the result for the YSR-states in the classical spin approximation for intermediate exchange coupling.

$$
\begin{aligned}
Nr_{e\uparrow} &= \frac{e^{i\phi/2}}{u+v}\Big(uv((u+v)\sin(\phi) + i(v-u)\cos(\phi)) \\
&\quad - (u-v)\left(u^2(-g\sigma + z + i) + v^2(g\sigma + z + i) + uv(2z+i)\right)\Big) \\
Nr_{h\uparrow} &= \frac{e^{i\phi/2}}{u+v}\Big(uv(-(u+v)\sin(\phi) + i(v-u)\cos(\phi)) \\
&\quad + (u-v)\left(u^2(g\sigma + z - i) + v^2(-g\sigma + z - i) + uv(2z-i)\right)\Big) \\
Nt_{e\uparrow} &= ve^{i\phi}(-u(g\sigma + z) + v(g\sigma + z + i)) + u(v(z - g\sigma) - u(z - g\sigma + i)) \\
Nt_{h\uparrow} &= ue^{i\phi}(-v(g\sigma + z) + u(g\sigma + z - i)) + v(u(z - g\sigma) - v(z - g\sigma - i)),
\end{aligned}
\tag{4.92}
$$

where N is a normalization constant which should be determined in the same way as for the Andreev bound states. We will not do that here, as the full expression when inserting the energy dependent expressions for u and v is too complicated for an analytical calcuation. The absolute square of the electron wave functions for the bound states in fig. 4.2 with $\phi = 1.5$ are plotted in fig. 4.3. By remembering our comment about the two-channel nature of the problem in section 3.1 we can understand the different forms of the two wave-functions. $|\psi_{E_{-\uparrow}}|^2$ has its maximum value at $x = 0$, which is consistent with the fact that it arises from the even combination of the leads. On the other hand $|\psi_{E_{+\downarrow}}|^2$ belongs to the odd sector and has a minimum in $x = 0$. The reason why it has a finite value here is that for $\phi \neq 0$ the even and odd sectors

are coupled, so that this state is no longer purely odd. $|\psi_{E_{+\downarrow}}(x=0)|^2$ decreases for decreasing ϕ until it reaches zero at $\phi = 0$. This is seen in fig. 4.4 where $|\psi_{E\sigma}(x=0)|^2$ is plotted for different values of the phase. At $\phi = 0$ this state is in principle purely odd, but then it is also no longer a bound state as it delocalizes and merges with the continuum of scattering states.

4.4.1 Scattering states

The scattering states for a magnetic potential are obtained in a way completely analogous to what was done above for the QPC. Only the two equations for the discontinuity of the derivative are modified due to the spin-dependent potential. We start by considering the scattering states for an incoming electron with spin-up using the ansatz from eq. 4.81 and adding a source term for a spin-up electron. With such a source term we get only scattering states which are spin-up electrons and spin-down holes. But if we had used a source-term for a spin-down electron we would as in the last section have obtained a similar result with the substitution $b \to \sigma b$. This allows us to write the system of equations for a general spin as

$$\begin{aligned}
(1+r_{e\sigma})u + r_{h\bar{\sigma}}v &= (t_{e\sigma}u + t_{h\bar{\sigma}}v)e^{i\phi/2} \\
(1+r_{e\sigma})v + r_{h\bar{\sigma}}u &= (t_{e\sigma}v + t_{h\bar{\sigma}}u)e^{-i\phi/2} \\
(t_{e\sigma}u - t_{h\bar{\sigma}}v)e^{i\phi/2} - (1-r_{e\sigma})u - r_{h\bar{\sigma}}v &= -2i(z+\sigma g)\left[u(1+r_{e\sigma}) + r_{h\bar{\sigma}}v\right] \\
(t_{e\sigma}v - t_{h\bar{\sigma}}u)e^{-i\phi/2} - (1-r_{e\sigma})v - r_{h\bar{\sigma}}u &= -2i(z-\sigma g)\left[v(1+r_{e\sigma}) + r_{h\bar{\sigma}}u\right].
\end{aligned} \tag{4.93}$$

These equations have the solution

$$\begin{aligned}
r_{e\sigma} &= \frac{(u^2-v^2)(g^2(v^2-u^2) + ig\sigma(u^2+v^2) + (u^2-v^2)z(i+z))}{D} \\
r_{h\bar{\sigma}} &= \frac{(1-e^{-i\phi}+2ig\sigma)u^3v + (1-e^{i\phi}-2ig)uv^3)}{D} \\
t_{e\sigma} &= -\frac{i(u^2-v^2)(e^{i\phi/2}v^2(i+g\sigma+z) - u^2e^{-i\phi/2}(i+z-g\sigma))}{D} \\
t_{h\bar{\sigma}} &= \frac{2iuv(u^2-v^2)(g\sigma\cos(\phi/2) + iz\sin(\phi/2))}{D}
\end{aligned} \tag{4.94}$$

with $D = u^4((-i+g\sigma)^2 - w^2) + v^4((i+g\sigma)^2 - w^2) + 2u^2v^2(w^2-g^2) + 2u^2v^2\cos(\phi)$. We can then plug in the explicit forms of (u, v) to obtain an expression for the coefficients which includes the dependence on energy:

$$\begin{aligned}
r_{e\sigma}D &= (E^2-\Delta^2)(z(i+z)-g^2) + ig\sigma E\sqrt{E^2-\Delta^2} \\
r_{h\bar{\sigma}}D &= \frac{\Delta}{2}\left[E(1-\cos(\phi)) + i\sqrt{E^2-\Delta^2}(2ig\sigma + \sin(\phi))\right] \\
t_{e\sigma}D &= -i\cos(\phi/2)\left[g\sigma E\sqrt{E^2-\Delta^2} - (i+z)(E^2-\Delta^2)\right] \\
&\quad + \sin(\phi/2)\left[E(i+z)\sqrt{E^2-\Delta^2} - g\sigma(E^2-\Delta^2)\right] \\
t_{h\bar{\sigma}}D &= i\Delta\sqrt{E^2-\Delta^2}\left[g\sigma\cos(\phi/2) + iz\sin(\phi/2)\right].
\end{aligned} \tag{4.95}$$

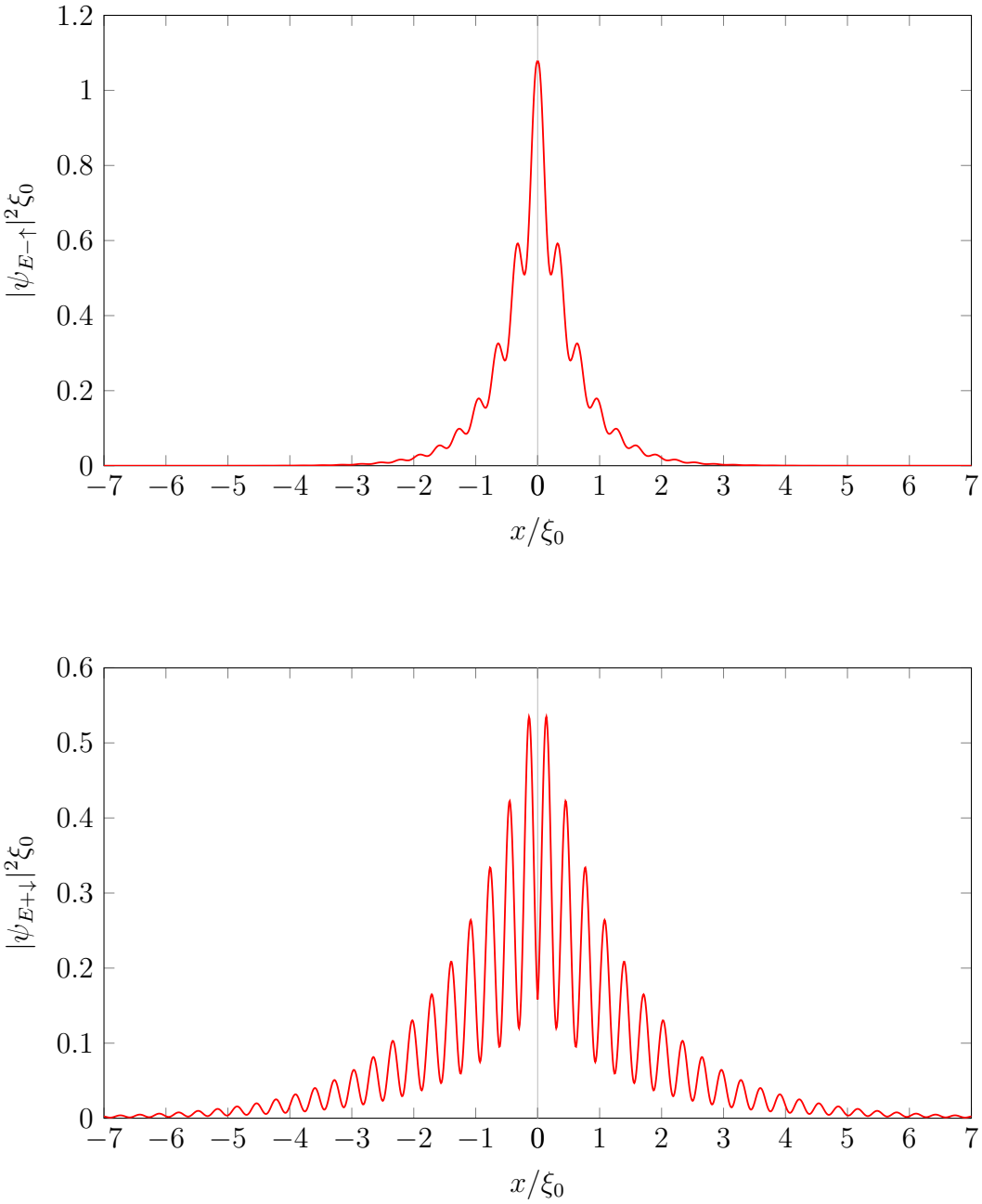

Figure 4.3: Absolute square of the normalized wave functions for the two bound states of opposite spin with $g = -0.5$, $z = 0.3$ and $\phi = 1.5$. The wave functions have a maximum (top plot) and minimum (bottom plot) in $x = 0$ as they arise from the even and odd combinations of the leads (see section 3.1). They decay on a length scale given by the coherence length. A value of $k_F\xi_0 = 10$ has been chosen for plotting purposes to make the oscillations visible. In reality their period is much shorter, eg. for Al we have $k_F\xi_0 = 28 \cdot 10^3$.

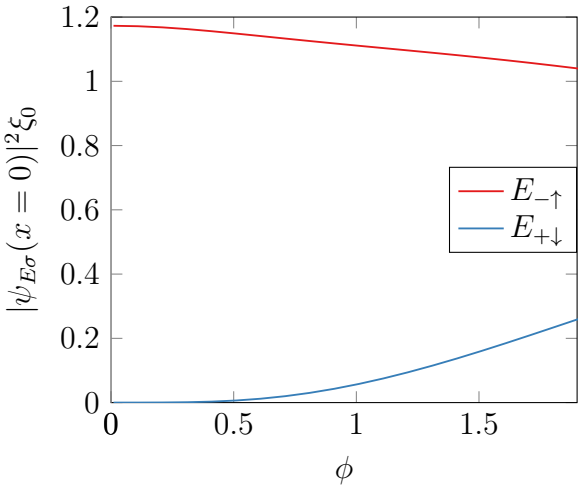

Figure 4.4: Absolute square of the two normalized bound state wave functions in fig. 4.3 evaluated in $x = 0$ for different values of ϕ. For the wave function arising from the odd combination of the leads we see that it goes to zero for $\phi = 0$ as it is decoupled from the even sector.

Here the denominator is $D = E^2(g^2-z^2-1)-\Delta^2(g^2-w^2-\cos^2(\phi/2))+2ig\sigma E\sqrt{E^2-\Delta^2}$.

4.4.2 Transition matrix elements

We have seen that for a Josephson junction consisting of two superconducting leads separated by a tunnel barrier also in the presence of a magnetic scattering term the wave functions in the energy basis can be determined using the solution for a homogeneous superconductor as an ansatz. The Bogoliubov-transformation again takes the form

$$\begin{aligned}\hat{\psi}_\sigma(x) &= \sum_{i=\pm} U_{E_i\sigma}(x)\gamma_{E_i\sigma} - \sigma V_{E_i\sigma}(x)^*\gamma^\dagger_{E_i\bar{\sigma}} + \sum_{E,\eta,\pm}(U^{\eta\pm}_{E\sigma}(x)\gamma_{E\eta\pm\sigma} - \sigma(V^{\eta\pm}_{E\sigma}(x))^*\gamma^\dagger_{E\eta\mp\bar{\sigma}}) \\ &= \sum_i (U_{i\sigma}(x)\gamma_{i\sigma} - \sigma(V_{i\sigma}(x))^*\gamma^\dagger_{-i\bar{\sigma}}),\end{aligned} \tag{4.96}$$

with discrete contributions from the bound states within the gap ($0 < E_i < \Delta$) and a continuum of scattering states above the gap ($E > \Delta$). We can relate this to our previous study of the YSR-states and change of ground state for a system with a magnetic impurity. First of all, we have learned that also in this more complicated case, we can describe the excitations of the system in terms of spin-dependent Bogoliubov quasiparticles labelled by their energy.

We have expressed the current operator in terms of the quasiparticle operators in eq. 4.25 and found from Fermi's golden rule that whenever the matrix element $\langle f|\,\hat{I}\,|i\rangle$ is nonzero a photon can be absorbed whereby the system ends up in an excited state. In contrast, if the matrix elements are zero the system can't absorb any photons and the admittance will also be zero. In particular, we can use this knowledge to explain why

the $\delta-$peak in the real part of the admittance vanished for the doublet-like ground state where the impurity spin is unscreened. We denote the ground state by $|\Phi_0\rangle$. When $|\Phi_0\rangle$ is the singlet-like screened state, the excited states with two quasiparticles of opposite spin are

$$\begin{aligned} |f_1\rangle &= \gamma^\dagger_{E\eta\pm\uparrow}\gamma^\dagger_{E_+\downarrow}|\Phi_0\rangle\,, \\ |f_2\rangle &= \gamma^\dagger_{E\eta\pm\downarrow}\gamma^\dagger_{E_-\uparrow}|\Phi_0\rangle \text{ and} \\ |f_3\rangle &= \gamma^\dagger_{E_-\uparrow}\gamma^\dagger_{E_+\downarrow}|\Phi_0\rangle \end{aligned} \tag{4.97}$$

(with $\eta \in e, h$). These states are all connected with the ground state by the current operator, $\langle f_i|\,\hat{I}\,|\Phi_0\rangle \neq 0$. In contrast, the other phase where the impurity spin is unscreened only has two possible final states which can be reached by means of the current operator:

$$\begin{aligned} &\gamma^\dagger_{E\eta\pm\uparrow}\gamma^\dagger_{E_+\downarrow}|\Phi_0\rangle \text{ and} \\ &\gamma^\dagger_{E\eta\pm\uparrow}\gamma^\dagger_{E_-\downarrow}|\Phi_0\rangle\,, \end{aligned} \tag{4.98}$$

because $\langle\Phi_0|\,\gamma_{E_-\downarrow}\gamma_{E_+\downarrow}\hat{I}\,|\Phi_0\rangle = 0$. This explains why the discrete absorption peak arising from the creation of two quasiparticles in the bound states is absent for this ground state and aids our understanding of the results of section 3.3. The underlying physical reason is as described in section 4.3.2 that the perturbation couples to the current which in superconductors is carried by Cooper pairs, so that the absorption of a photon causes the splitting of a Cooper pair whereby two quasiparticles of opposite spin are created and there must be available states for these quasiparticles to occupy, for which reason they can't both be created in the bound states for the doublet-like ground state. Such a transition would require the splitting of two Cooper pairs and is not possible in a first-order process where a single photon is absorbed.

Our results are related to the concept of quasiparticle poisoning which is a problem in the proposed transmon qubits constructed from a QPC. The operation of such qubits relies on coherent manipulation of the states in the even-parity subsystem formed by the states with zero or two quasiparticles in the ABS. But in a real circuit non-equilibrium effects can result in the apperance of a single quasiparticle in the Andreev bound state so that the qubit is unintentionally in an odd parity state [25]. This impedes the manipulation of the qubit, as the supercurrent is then blocked. Furthermore the quasiparticle can be long-lived as due to the superconducting gap it can only be removed by either being excited to the continuum by absorption of a photon of energy $\omega = E - E_A$ with $E > \Delta$ or by forming a Cooper pair with a quasiparticle from the continuum whereby a photon of energy $\omega = E + E_A$ is emitted. These processes have been shown both theoretically and experimentally to have small transition rates, especially when the ABS are deep inside the gap [29].

Chapter 5

Noninteracting quantum dot

To aid our understanding of the results of chapter 3 and the effect of the approximations we made there, we will now study the Anderson model outside of the cotunneling regime and classical spin approximation. Starting again from the Hamiltonian for the Anderson model in eq. 3.1, we now consider the opposite limit of the strength of the Coulomb interaction $U \ll \Delta$ and let $U = 0$. In the noninteracting limit the Anderson model describes resonant tunneling through a single energy level between the superconducting leads. This model exhibits the so-called proximity effect where the quantum dot (resonant level) becomes superconducting due to Cooper pairs hybridizing with the dot level. Bound states are also in this model forming inside the superconducting gap, and they are similar to the Andreev bound states of the QPC and hence have a more straightforward interpretation than the YSR-states. We will follow the approach used in ref. [22] and apply a magnetic field to the resonant level, which causes a Zeeman splitting of the dot levels as $\xi_{d\sigma} = \xi_d + \sigma\frac{B}{2}$. Applying a local magnetic field is in effect equivalent to performing a mean-field approximation of the Coulomb interaction in the weakly interacting limit for a local field $B = U(n_\downarrow - n_\uparrow)/2$ [30].

5.1 Green's functions

The Hamiltonian describing the system is similar to the one we have used previously. We write it in terms of the spin-indexed Nambu spinors for the dot $\psi_{d\sigma} = (d_\sigma,\, d^\dagger_{\bar{\sigma}})^T$ and for the leads $\psi_{\alpha k\sigma} = (c_{\alpha k\sigma},\, c^\dagger_{\alpha -k\bar{\sigma}})$. Again we move the phase of the order parameter to the tunneling terms by a gauge transformation and obtain:

$$H = \frac{1}{2}\sum_{\alpha k\sigma} \psi^\dagger_{\alpha k\sigma}\mathbf{m}^{SC}_k\psi_{\alpha k\sigma} + \frac{1}{2}\psi^\dagger_{d\sigma}\mathbf{m}^d\psi_d + \frac{1}{2}\sum_{\alpha k\sigma}(\psi^\dagger_{\alpha k\sigma}\mathbf{m}^t_\alpha\psi_{d\sigma} + h.c.) \tag{5.1}$$

where we have assumed symmetric coupling to the leads $t_L = t_R = t$ and where

$$\begin{aligned} \mathbf{m}_k^{SC} &= \begin{pmatrix} \xi_k & -\sigma\Delta \\ -\sigma\Delta & -\xi_k \end{pmatrix} \quad \mathbf{m}^d = \begin{pmatrix} \xi_d + \sigma\frac{B}{2} & 0 \\ 0 & -(\xi_d - \sigma\frac{B}{2}) \end{pmatrix} \\ \mathbf{m}_R^t &= \begin{pmatrix} t & 0 \\ 0 & -t \end{pmatrix} \quad \mathbf{m}_L^t = \begin{pmatrix} te^{i\phi/2} & 0 \\ 0 & -te^{-i\phi/2} \end{pmatrix}. \end{aligned} \tag{5.2}$$

Again the current operator has the characteristic form which we have encountered several times

$$\hat{I}_L = e\dot{N}_L = ie\Big[H, \hat{N}_L\Big] = -iet\sum_{k\sigma}(e^{i\phi/2}c_{Lk\sigma}^\dagger d_\sigma - e^{-i\phi/2}d_\sigma^\dagger c_{Lk\sigma}) \tag{5.3}$$

in terms of the electron and dot operators.

We will now calculate the local Matsubara Green's functions for the system. The procedure is very similar to what was done in the previous chapters, but this time there are three different types of Nambu Green's functions: One for the individual leads $\mathcal{G}_{\alpha\alpha;\sigma\sigma'}(\tau,\tau') = -\sum_{kk'}\langle T_\tau \psi_{\alpha k\sigma}(\tau)\psi_{\alpha k'\sigma'}^\dagger(\tau')\rangle$, one for the dot $\mathcal{G}_{dd;\sigma\sigma'}(\tau,\tau') = -\langle T_\tau \psi_{d\sigma}(\tau)\psi_{d\sigma'}^\dagger(\tau')\rangle$ and one describing the hybridization of the dot level and the leads $G_{\alpha d;\sigma\sigma'}(\tau,\tau') = -\sum_k\langle T_\tau \psi_{\alpha k\sigma}(\tau)\psi_{d\sigma'}^\dagger(\tau')\rangle$. The bare Green's functions for the leads and dot in Fourier space are given by $\mathcal{G}_{LL\sigma}^0(i\omega_l) = (i\omega_l\sigma_0 - \mathbf{m}_k^{SC})^{-1}$ and $\mathcal{G}_{dd\sigma}^0(i\omega_l) = (i\omega_l\sigma_0 - \mathbf{m}^d)^{-1}$. We note that for our purposes it suffices to consider the dot and the left lead as our aim is again to calculate the current-current correlation function and obtain the real part of the admittance. As conservation of current requires that $I_L = -I_R$, we can express the current operator with reference to the left lead and dot only, and we only need the Green's functions involving those.

Writing up the equation of motion for the Green's functions involving the left lead gives a closed set of equations determining all three Green's functions. As was the case in the last chapter, the Green's functions are diagonal in spin because the Hamiltonian has no spin-flip terms, and we find that the set of equations is

$$\mathcal{G}_{LL\sigma}(i\omega_l) = \mathcal{G}_{LL\sigma}^0(i\omega_l) + \mathcal{G}_{LL\sigma}^0(i\omega_l)\mathbf{m}_L^t\mathcal{G}_{dd\sigma}(i\omega_l)(\mathbf{m}_L^t)^\dagger\mathcal{G}_{LL\sigma}^0(i\omega_l) \tag{5.4}$$

$$\mathcal{G}_{dd\sigma}(i\omega_l) = \mathcal{G}_{dd\sigma}^0(i\omega_l) + \mathcal{G}_{dd\sigma}^0(i\omega_l)\Sigma_{d\sigma}(i\omega_l)\mathcal{G}_{dd\sigma}(i\omega_l) \tag{5.5}$$

$$\mathcal{G}_{Ld\sigma}(i\omega_l) = \mathcal{G}_{LL\sigma}^0(i\omega_l)\mathbf{m}_L^t\mathcal{G}_{dd\sigma}(i\omega_l) \tag{5.6}$$

$$\mathcal{G}_{dL\sigma}(i\omega_l) = \mathcal{G}_{dd\sigma}(i\omega_l)(\mathbf{m}_L^t)^\dagger\mathcal{G}_{LL\sigma}^0(i\omega_l). \tag{5.7}$$

Here we introduced the self-energy for the dot $\Sigma_{d\sigma}(i\omega_l) = \sum_{i=L,R}(\mathbf{m}_i^t)^\dagger\mathcal{G}_{ii\sigma}^0(i\omega_l)\mathbf{m}_i^t$. We solve the above equations using Mathematica and obtain all the relevant Green's functions. From the Green's functions for the dot we can obtain the spectral functions. Some of the normal components are plotted in fig. 5.1 and here we see that indeed a gap opens in the density of states, and that there are discrete bound states within the gap. This shows that the dot has become superconducting due to the proximity effect.

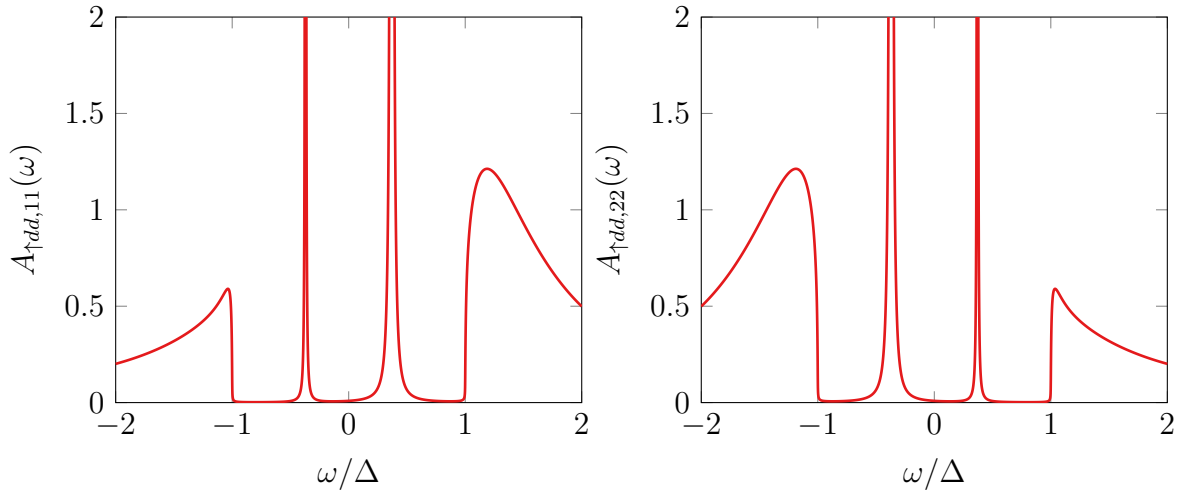

Figure 5.1: Normal components of the spectral function for the dot with $\xi_d = 0.5\Delta$, $B = 0$, $\phi = 2, \Gamma = 0.6\Delta$ and $\eta = 10^{-3}$. Without a magnetic field $A_\uparrow = A_\downarrow$. We see that the spectral function is asymmetric as we are away from the particle-hole symmetric point $\xi_d = 0$, and that an energy gap with two discrete bound states appears due to the hybridization with the superconducting leads.

All the retarded Green's functions have the same denominator, and from the zeros of this we can find the bound state energies of the system. We will start by considering the case of $B = 0$ as we here get a simple expression which shows a connection with the Andreev bound states in the QPC. For $\eta \to 0$ the denominator is

$$D(\omega) = \frac{1}{\Delta^2 - \omega^2}\left[\Delta^2(\xi_d^2 + \frac{\Gamma^2}{2} - \omega^2) - \omega^2(\xi_d^2 + \Gamma^2 + 2\Gamma\sqrt{\Delta^2 - \omega^2} - \omega^2) + \frac{\Gamma^2}{2}\Delta^2\cos(\phi)\right] \tag{5.8}$$

$$= \frac{\Delta^2\Gamma^2\cos^2(\phi/2)}{\Delta^2 - \omega^2} - (\omega - \xi_d - \frac{\Gamma\omega}{\sqrt{\Delta^2 - \omega^2}})(\omega + \xi_d - \frac{\Gamma\omega}{\sqrt{\Delta^2 - \omega^2}}) \tag{5.9}$$

where $\Gamma_L = \Gamma_R = 2\pi\nu_F t^2 \equiv \Gamma$ is the transition rate for tunneling between the leads and the resonant level. By solving the equation $D(\omega) = 0$ we find an equation for the bound state energies:

$$\begin{aligned} 0 &= \Delta^2\Gamma^2(1 - \sin^2(\phi/2)) - (\Delta^2 - E_B^2)(E_B - \xi_d - \frac{\Gamma E_B}{\sqrt{\Delta^2 - E_B^2}})(E_B + \xi_d - \frac{\Gamma E_B}{\sqrt{\Delta^2 - E_B^2}}) \\ &= \Delta^2(\xi_d^2 + \Gamma^2(1 - \sin^2(\phi/2))) - E_B^2(\xi_d^2 + (\Gamma + \sqrt{\Delta^2 - E_B^2})^2) \end{aligned} \tag{5.10}$$

$$\Rightarrow E_B^2 = \frac{\Delta^2(\xi_d^2 + \Gamma^2(1-\sin^2(\phi/2)))}{\xi_d^2 + (\Gamma + \sqrt{\Delta^2 - E_B^2})^2}$$
$$\Rightarrow E_B^2 = \Delta^2 \frac{\xi_d^2 + \Gamma^2}{\xi_d^2 + (\Gamma + \sqrt{\Delta^2 - E_B^2})^2} \left(1 - \frac{\Gamma^2}{\xi_d^2 + \Gamma^2} \sin^2(\phi/2)\right). \tag{5.11}$$

This is a self-consistency equation which for a given set of parameters can be solved numerically as seen in fig. 5.2 where the bound state energies are plotted for $\phi = 0$ as a function of the level position ξ_d. In the QPC the bound states reached the gap at $\pm\Delta$ at $\phi = 0$, but this is not the case here, which can be interpreted as the existence of an effective gap which depends on ξ_d and Γ. The overall dependence on the phase difference is however similar to what was found for the QPC. Introducing the Breit-Wigner transmission probability at the Fermi level which is given by [31]

$$T_{BW} = \frac{\Gamma_L \Gamma_R}{(\xi_d^2 + \frac{1}{4}\Gamma_{tot}^2)} = \frac{\Gamma^2}{\xi_d + \Gamma^2},$$

where $\Gamma_{tot} = \Gamma_L + \Gamma_R = 2\Gamma$ is the total transmission rate we can write

$$E_B^2 = \Delta^2 \frac{\xi_d^2 + \Gamma^2}{\xi_d^2 + (\Gamma + \sqrt{\Delta^2 - E_B^2})^2} \left(1 - T_{BW} \sin^2(\phi/2)\right). \tag{5.12}$$

In the limit $\Gamma \gg \sqrt{\Delta^2 - E_B^2}$ where the bound state energies are close to the gap eq. 5.12 reduces to the familiar form

$$E_B^2 = \Delta^2 \left(1 - T_{BW} \sin^2(\phi/2)\right), \tag{5.13}$$

which is the Andreev bound state energy. From this we see that the bound states are similar to the Andreev bound states for the QPC. Their physical origin is also the same as a Cooper pair can tunnel to the dot from the right lead and either proceed to the right lead or tunnel back to the left lead. This can happen repeatedly and is reminiscent of the Andreev reflections.

5.1.1 Magnetic field

When applying a magnetic field to the resonant level, the bound states described in the previous section become spin-split, as the energies for spin-down (up) are pushed down (up) in energy. This is seen in fig. 5.4 a). For sufficiently large magnetic fields ($B \sim \Delta$), the lowest Andreev bound states can cross zero energy implying the transition to a new ground state as was also the case for YSR-states in the previous chapter. However, in this case it is easier to give a physical description of the different states involved. To enhance our understanding of the system, we start by considering the energy levels of the dot in the absence of coupling to the leads. The dot can be occupied by zero

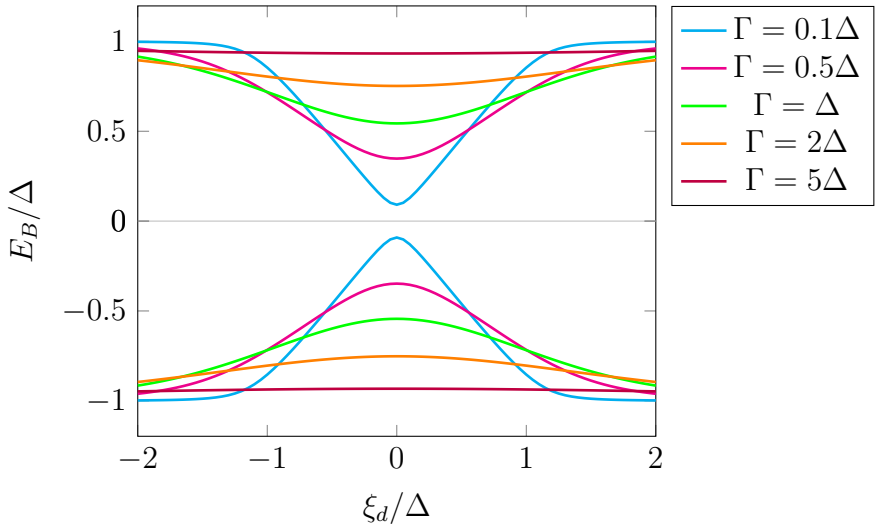

Figure 5.2: Bound state energies for different values of the coupling strength Γ with $B = 0$ and $\phi = 0$. At weak coupling the bound state energy (and hence effective energy gap) is approximately equal to $\pm\xi_d$, whereas for strong coupling it becomes more independent of the level position and moves towards the gap.

electrons $|0\rangle$, one electron of spin up $|\uparrow\rangle$ or spin down $|\downarrow\rangle$ or two electrons of opposite spin $|\uparrow\downarrow\rangle$. These states have energies

$$E_0 = 0 \quad E_\uparrow = \xi_d + \frac{B}{2} \quad E_\downarrow = \xi_d - \frac{B}{2} \quad E_2 = 2\xi_d \tag{5.14}$$

At zero magnetic field the state with an empty level has the lowest energy and is the ground state. But when the strength of the magnetic field is increased sufficiently the state $|\downarrow\rangle$ crosses zero and becomes the favored state of the dot as seen in fig. 5.3.

Of course these states are no longer eigenstates when the coupling to the leads is turned on, $\Gamma \neq 0$. But we will see later that the dot states are modified by the interaction in such a way that a similar interpretation is still possible with the singlet states $|0\rangle$ and $|\uparrow\downarrow\rangle$ being substituted by singlet BCS-states. Based on this simple argument we have obtained an intuition for the reason why the system exhibits two different ground states, and in what follows we will refer to them as $|-\rangle$ and $|\sigma\rangle$ due to their singlet and doublet nature. We should however keep in mind that our use of a magnetic field has spin-polarised the states $|\sigma\rangle$, so that they are not true spin-degenerate doublet states.

Importantly, we now see that this simpler model exhibits the same characteristic features as in the classical spin approximation with a similar bound state spectrum as seen in fig. 5.4 and two possible ground states of different parity. Fig. 5.4 b) depicts the crossing of the bound states signifying a change of ground state for an intermediate strength of the magnetic field where both ground states can be attained by variying the phase difference. For small values of ϕ, the excited bound states have opposite spin

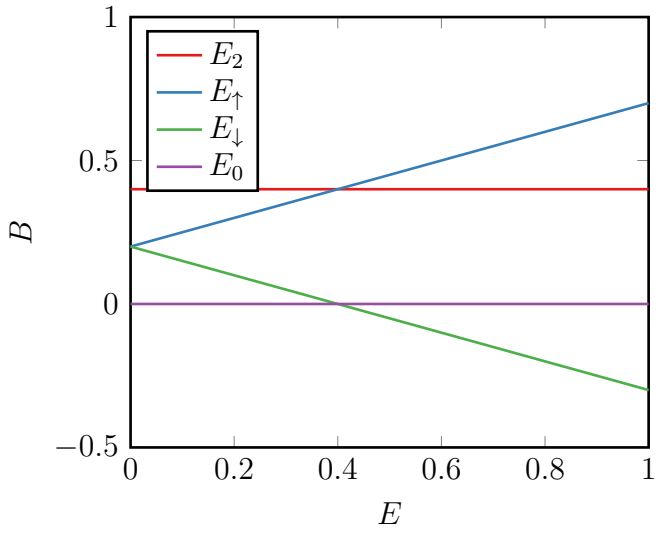

Figure 5.3: Energy levels of the uncoupled quantum dot with a magnetic field but without Coulomb repulsion.

and are a spin-split pair of Andreev bound states. Here the ground state is a BCS-like singlet state. The excited states are then the two states where the dot is occupied by a single quasiparticle of either spin and the excited BCS-like state $|+\rangle$. At $\phi \sim \pi/2$ the two bound states with the smallest energies cross zero energy and the crossing signifies that the ground state changes. Now the ground state is the doublet state where a quasiparticle of spin down is occupying the dot (with the spin determined by the direction of the magnetic field). The excited states are then the two singlet states and the doublet state of opposite spin $|\uparrow\rangle$.

For sufficiently strong fields both bound states with spin-up are above zero energy for all values of ϕ as seen in fig. 5.4 c), and the ground state is always the doublet state. To obtain the same spins of the bound states as in the classical spin approximation, we have to use a magnetic field in the $-\hat{z}-$direction here. In this model it is very easy to understand that the spin-dependence of the bound state energies is due to the states with spin anti-parallel to the magnetic spin being energetically favored, and that the singlet and doublet nature of the states has to do with the occupation of the dot level.

5.1.2 Linear response

Using our results from the previous chapter it is very easy to obtain a result for the admittance in the presently studied model. Eq. 5.3 is almost identical to eq. 3.42, except for the electron operators for the left lead being replaced by the ones for the dot. This means that through the substitution $R \to d$ in the spectral functions, we can directly use the expression for $\mathrm{Re}\, Y(\omega)$ in eq. 3.53 with the Green's functions determined by eq. 5.7. We then have

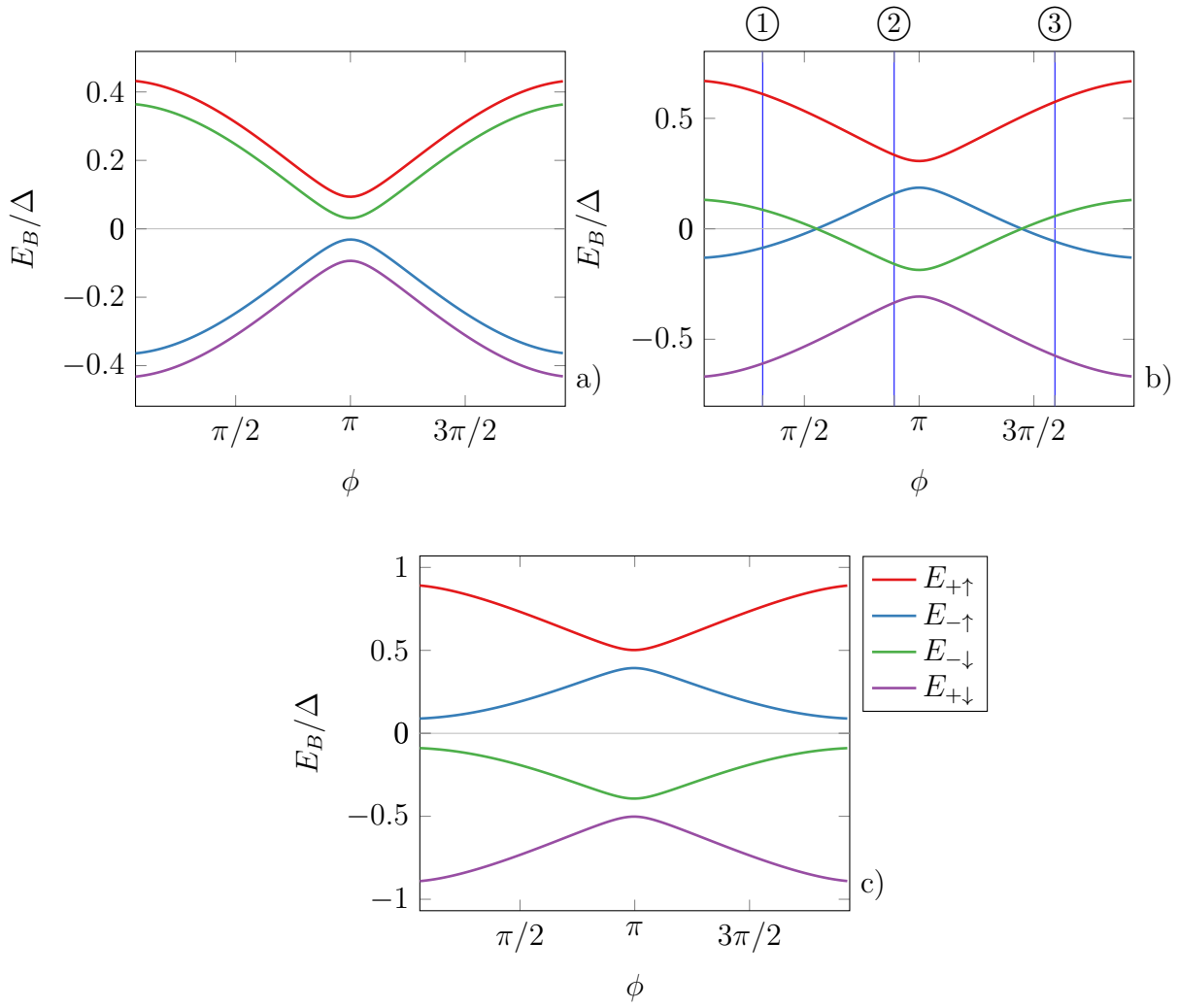

Figure 5.4: When a local magnetic field is applied to the energy level ξ_d this causes a Zeeman shift which splits the spin-degenerate Andreev bound states. As the magnetic field is increased, the ground states changes and the doublet state is energetically favored. The parameters used are $\xi_d = 0.1\Delta$ and $\Gamma = 0.6\Delta$ and $B = 0.1\Delta$ in **a)**, $B = 0.8\Delta$ in **b)** and $B = 1.5\Delta$ in **c)**.

$$\mathrm{Re}\, Y(\omega) = -\frac{G_0}{4\omega}\sum_\sigma \mathrm{Re}\int_0^\omega d\epsilon\ \mathrm{Tr}\left[\mathbf{t}^* A_{LL\sigma}(\epsilon-\omega)\mathbf{t}A_{dd\sigma}(\epsilon) - \mathbf{t}A_{dL\sigma}(\epsilon-\omega)\mathbf{t}A_{dL\sigma}(\epsilon)\right], \tag{5.15}$$

with

$$\mathbf{t} = \begin{pmatrix} te^{i\phi/2} & 0 \\ 0 & te^{-i\phi/2}. \end{pmatrix}$$

Even without performing the numerical integration, we anticipate that the results will be very similar to what we obtained for the YSR states. This is because the bound states acquire a similar form here for a nonzero magnetic field, and we know from eqs. 3.67-3.70 that the different features in $\mathrm{Re}\, Y(\omega)$ mathematically depend mainly on the spin and energy of the bound states. The only difference is that here the ground- and excited states of the system have a slightly different and more straightforward interpretation. We perform the integration in eq. 5.15 numerically for the parameters used in fig. 5.4 b) at the values of ϕ indicated by gridlines ①- ③ there. The result is seen in fig. 5.5.

It is obvious that the results are similar to the ones obtained in the classical spin approximation, and we are able to give a physical explanation for the different absorption peaks as well as explain why the $\delta-$peak disappears when the ground state changes from being the singlet state to the doublet state. We start by considering the case of a singlet-like BCS ground state, which yields the admittance seen in figs. 5.5 a) and c). Here we see three features in the admittance. Two contributions with threshold frequencies $E_{-\downarrow}+\Delta$ and $E_{+\uparrow}+\Delta$ and a discrete peak at frequency $E_{-\downarrow}+E_{+\uparrow}$. For the singlet ground state the first excited state is the doublet state $|\downarrow\rangle$ (in terms of level occupation) and the second excited state is the other doublet state $|\uparrow\rangle$. Each of these states are reached by creating a quasiparticle on the dot with energy $E_{-\downarrow}$ and $E_{+\uparrow}$ respectively. This is done by splitting a Cooper pair whereby a surplus quasiparticle with energy Δ is created in the continuum. This gives the threshold frequencies stated above. It is also possible to reach the third excited state by creating a quasiparticle in each of the bound states whereby the dot ends up being in the doubly occupied singlet state $|+\rangle$. This process is responsible for the absorption peak at $\omega = E_{-\downarrow}+E_{+\uparrow}$. All the processes mentioned here conserve parity as they should.

In contrast, when the ground state changes to the doublet state where the dot is occupied by a spin-down electron $|\downarrow\rangle$ the admittance exhibits no discrete peak but only the two features at threshold frequencies $E_{+\uparrow}+\Delta$ and $E_{-\uparrow}+\Delta$. These threshold frequencies arise from the following excitation processes: The first excited state is the unoccupied dot which is reached by removing the spin-down quasiparticle on the dot (or correspondingly, creating a spin-up quasiparticle). The second excited state is the two-quasiparticle singlet state $|+\rangle$, achieved by creating a spin-up quasiparticle. In both cases the splitting of a Cooper pair again results in the creation of an additional quasiparticle in the continuum.

We can interpret the absence of the discrete peak as being due to the fact that it

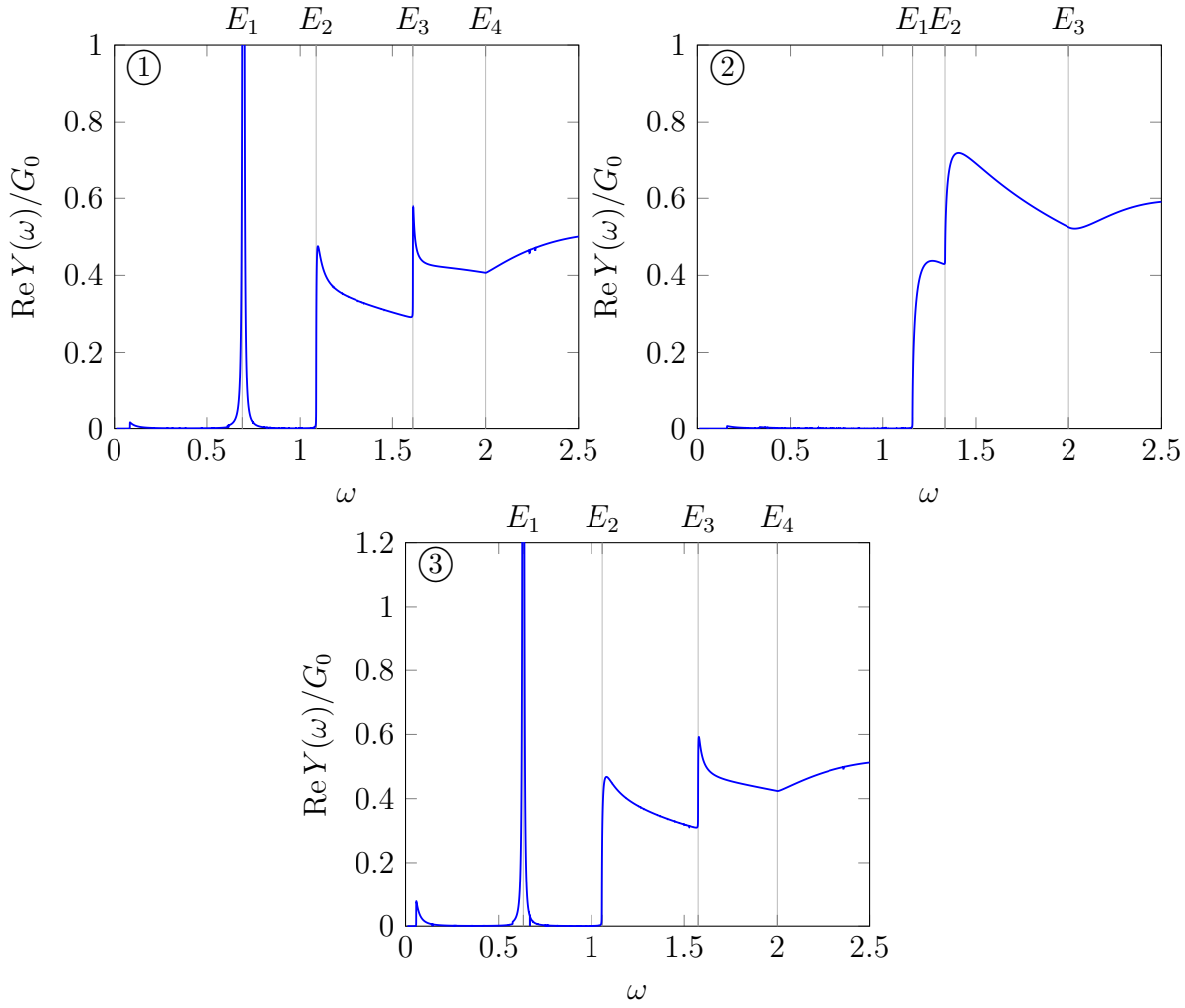

Figure 5.5: $\mathrm{Re}\,Y(\omega)$ for a noninteracting S-QD-S junction with the parameters of fig. 5.4 and $\phi = 1$ i ①, $\phi = 2.8$ in ② and $\phi = 5$ in ③. The different features are similar to what was obtained for a classical magnetic impurity in the strongly interacting limit. The gridlines are at energies $E_1 = E_{+\uparrow} + E_{-\downarrow}$, $E_2 = \Delta + E_{-\downarrow}$, $E_3 = \Delta + E_{+\uparrow}$ and $E_4 = 2\Delta$ in ① and ③ and $E_1 = \Delta + E_{-\uparrow}$, $E_2 = \Delta + E_{+\uparrow}$ and $E_3 = 2\Delta$ in ②.

is impossible to create a quasiparticle in each of the bound states by splitting a single Cooper pair. This is in accordance with the fact that to get from the ground state $|\downarrow\rangle$ to the excited doublet state $|\uparrow\rangle$ the spin-down quasiparticle must first be removed (corresponding to the creation of a spin-up quasiparticle), and subsequently a spin-up quasiparticle must be created on the dot. This would require the splitting of two Cooper pairs and would result in two additional quasiparticles being created above the gap. Hence that excitation can't be caused by the absorption of a single photon, and furthermore has an excitation energy larger than 2Δ, so that we can describe the excited doublet state as being above the gap. In the next section we show that the description of the different states given here is correct, which is done by analytically determining the eigenstates and possible excitation processeses following the approach used by Meng et al. [32].

5.2 Limit of infinite gap

As mentioned several times, a central challenge when dealing with systems described by the Anderson model is finding ways to approximate the interaction term and make the problem solvable. We have previously studied the limits of $U \gg \Delta$ and $U = 0$, and now we will present an approach which allows for calculations which are exact in the Coulomb interaction. We will study the limit of infite gap $\Delta \gg \omega_l$, which makes it possible to determine exactly the eigenstates of the Hamiltonian. That is, we assume that the characteristic energies of the problem are much smaller than the superconducting gap. In this limit the bare Matsubara (Nambu) Green's function for the leads becomes

$$\mathcal{G}_0(i\omega_l) = \frac{\pi\nu_F}{\sqrt{|\Delta|^2 - (i\omega_l)^2}} \begin{pmatrix} -i\omega_l & \Delta e^{-i\phi} \\ \Delta^* e^{i\phi} & -i\omega_l \end{pmatrix} \approx \pi\nu_F \begin{pmatrix} 0 & e^{-i\phi} \\ e^{i\phi} & 0 \end{pmatrix}. \tag{5.16}$$

We start by using the equation of motion for $\mathcal{G}_{dd}(i\omega_l)$ with $U = 0$, which is given by (eq. 5.7)

$$\begin{aligned} \mathcal{G}_{dd}(i\omega_l)^{-1} &= \mathcal{G}^0_{dd}(i\omega_l)^{-1} - \Sigma_d(i\omega_l) \\ &= i\omega_l\sigma_0 - \xi_d\sigma_z - t^2 \sum_{i=L,R} \sigma_z \mathcal{G}^0_{ii}(i\omega l)\sigma_z. \end{aligned} \tag{5.17}$$

Here we only consider $\sigma = \uparrow$. We are not including a magnetic field, so we no longer need to use spin-indexed Nambu spinors. Furthermore we now keep the $\phi-$dependence on the order parameter, which means that $\mathbf{m}^t_R = \mathbf{m}^t_L = t\sigma_z$. The above equation is easily inverted to yield an expression for the dot Green's function

$$\mathcal{G}_{dd} = \frac{1}{(i\omega_l)^2 - \xi_d^2 - (\Gamma\cos(\phi/2))^2} \begin{pmatrix} i\omega_l + \xi_d & -\Gamma e^{-i\phi/2}\cos(\phi/2) \\ -\Gamma e^{i\phi/2}\cos(\phi/2) & i\omega_l - \xi_d \end{pmatrix}. \tag{5.18}$$

Which is identical to the Green's function for a homogeneous superconductor in eq. 1.16 with an effective gap $\Gamma_\phi = \Gamma\cos\left(\frac{\phi}{2}\right)$. We can thus readily define an effective Hamiltonian which produces this Green's function:

$$H_{eff} = \sum_\sigma \xi_d d_\sigma^\dagger d_\sigma - (\Gamma_\phi e^{-i\phi/2} d_\uparrow^\dagger d_\downarrow^\dagger + \Gamma_\phi e^{i\phi/2} d_\downarrow d_\uparrow), \tag{5.19}$$

which includes no reference to the leads but only depends on the total phase difference across the junction. The phases $e^{\pm i\phi/2}$ can be removed by a gauge transformation, and we then follow ref. [32] and reintroduce the interaction term

$$H_{eff} = \sum_\sigma \tilde{\xi}_d d_\sigma^\dagger d_\sigma - \Gamma_\phi(d_\uparrow^\dagger d_\downarrow^\dagger + d_\downarrow d_\uparrow) + \frac{U}{2}\Big(\sum_\sigma d_\sigma^\dagger d_\sigma - 1\Big)^2. \tag{5.20}$$

where now $\tilde{\xi}_d = \xi_d + U/2$, which yields the correct interaction energy for the different possible dot states. Here we explicitly see how the dot level hybridizing with the leads causes an energy gap to form, which is again the proximity effect. The leads act as reservoirs of Cooper pairs. To diagonalize the Hamiltonian in eq. 5.20, we start by diagonalizing eq. 5.19 and to this end we write it in the ordered basis of dot states $\{|0\rangle, |\uparrow\rangle, |\downarrow\rangle, |\uparrow\downarrow\rangle\}$, where it is a 4×4-matrix

$$H_{eff} = \begin{pmatrix} 0 & 0 & 0 & \Gamma_\phi \\ 0 & \xi_d & 0 & 0 \\ 0 & 0 & \xi_d & 0 \\ \Gamma_\phi & 0 & 0 & 2\xi_d \end{pmatrix}. \tag{5.21}$$

Diagonalization of this matrix yields the eigenstates

$$|\uparrow\rangle, \quad |\downarrow\rangle, \quad |-\rangle = u|0\rangle - v|\uparrow\downarrow\rangle \quad \text{and} \quad |+\rangle = v|0\rangle + u|\uparrow\downarrow\rangle \tag{5.22}$$

with

$$u = \frac{1}{\sqrt{2}}\sqrt{1 + \frac{\xi_d}{\sqrt{\xi_d^2 + \Gamma_\phi^2}}} \quad v = \frac{1}{\sqrt{2}}\sqrt{1 - \frac{\xi_d}{\sqrt{\xi_d^2 + \Gamma_\phi^2}}} \tag{5.23}$$

and the eigenenergies are $E_\uparrow = E_\downarrow = E_0 = \xi_d$ and $E_\pm = \xi_d \pm \sqrt{\xi_d^2 + \Gamma_\phi^2}$. Hence the noninteracting Hamiltonian is diagonal in the Bogoliubov quasiparticle operators

$$\gamma_\sigma = u d_\sigma - v\sigma d_{\bar{\sigma}}^\dagger, \tag{5.24}$$

By acting with the full Hamiltonian in eq. 5.20 on these states and redefining $\xi_d \to \tilde{\xi}_d$, we find that they are eigenstates also when the interaction term is included and the effect of the interaction is just to shift the energies of the singlet states to become $E_\pm = \frac{U}{2} + \tilde{\xi}_d \pm \sqrt{\tilde{\xi}_d^2 + \Gamma_\phi^2}$. The quasiparticle operators act as expected on the eigenstates:

$$\begin{aligned} \gamma_\sigma|\sigma\rangle &= (u d_\sigma - v\sigma d_{\bar{\sigma}}^\dagger)|\sigma\rangle = (u|0\rangle - v\sigma^2|\uparrow\downarrow\rangle) = |-\rangle \\ \gamma_\sigma|+\rangle &= (u d_\sigma - v\sigma d_{\bar{\sigma}}^\dagger)(v|0\rangle + u|\uparrow\downarrow\rangle) = -\sigma|\bar{\sigma}\rangle \\ \gamma_\sigma|-\rangle &= uv|\bar{\sigma}\rangle - uv|\bar{\sigma}\rangle = 0, \end{aligned} \tag{5.25}$$

with similar relations for the quasiparticle creation operators. Even though the interacting Hamiltonian is *not* diagonal in the quasiparticle operators, it will we useful to express it in terms of these operators. By inspection we find that the Hamiltonian

$$H = \sum_{\sigma} E\gamma_{\sigma}^{\dagger}\gamma_{\sigma} + \tilde{\xi}_d - E + U\gamma_{\uparrow}\gamma_{\uparrow}^{\dagger}\gamma_{\downarrow}\gamma_{\downarrow}^{\dagger} \tag{5.26}$$

with $E = \frac{U}{2} + \sqrt{\Gamma_\phi^2 + \tilde{\xi}_d^2}$ yields the correct eigenenergies.

By considering the eigenenergies of the Hamiltonian which are plotted in fig. 5.6 as a function of interaction strength and phase, we can infer that this model exhibits a phase transition from a (singlet) BCS ground state $|-\rangle$ to a degenerate doublet state $|\sigma\rangle$ where it is energetically favorable for the dot to be occupied by a single quasiparticle of either spin. The phase transition happens at a critical value of the interaction strength determined by

$$E_- \stackrel{!}{=} E_0 \quad \rightarrow \quad \frac{U_c}{2} - \sqrt{\tilde{\xi}_d^2 + \Gamma_\phi^2} = 0 \quad \rightarrow \quad U_c = 2\sqrt{\tilde{\xi}_d^2 + \Gamma_\phi^2}. \tag{5.27}$$

We have hence found that this simple model which is exact in U exhibits the singlet-doublet phase transition which we also found in the other limits of the Anderson model previously studied. Here the phase transition requires no external field but is solely due to the Coulomb interaction. In addition we are here also able to find the eigenstates and see that they are true quantum mechanical singlet and doublet states in contrast with what we had for the classical spin approximation. We will now proceed by calculating the admittance in the infinte gap limit to see if this confirms our previous results that the absorption peak corresponding to the creation of two quasiparticles in the subgap states vanishes for a doublet ground state.

5.2.1 Admittance

From the original form of the Hamiltonian in eq. 5.1 where the phase-dependence enters in the same way as for the QPC, we can infer that the relevant response function for investigating photon absorption processes is still the current-current correlation function,

$$\chi_{II}(t) = -\theta(t)\frac{i}{e}\langle[I(t), I(0)]\rangle_0. \tag{5.28}$$

The easiest way to express the current operator in terms of the quasiparticle operators in the limit of infinite gap is by taking the phase-derivative of the Hamiltonian [12]

$$\hat{I} = -2e\frac{\partial H}{\partial \phi} = -e\Gamma \sin\left(\frac{\phi}{2}\right)\left(d_{\uparrow}^{\dagger}d_{\downarrow}^{\dagger} + d_{\downarrow}d_{\uparrow}\right). \tag{5.29}$$

That the current is obtained as the phase derivative of the Hamiltonian can be intuitively understood by remembering our result from section 1.3 that charge and phase are conjugate variables. From classical mechanics we then have a relation for the time

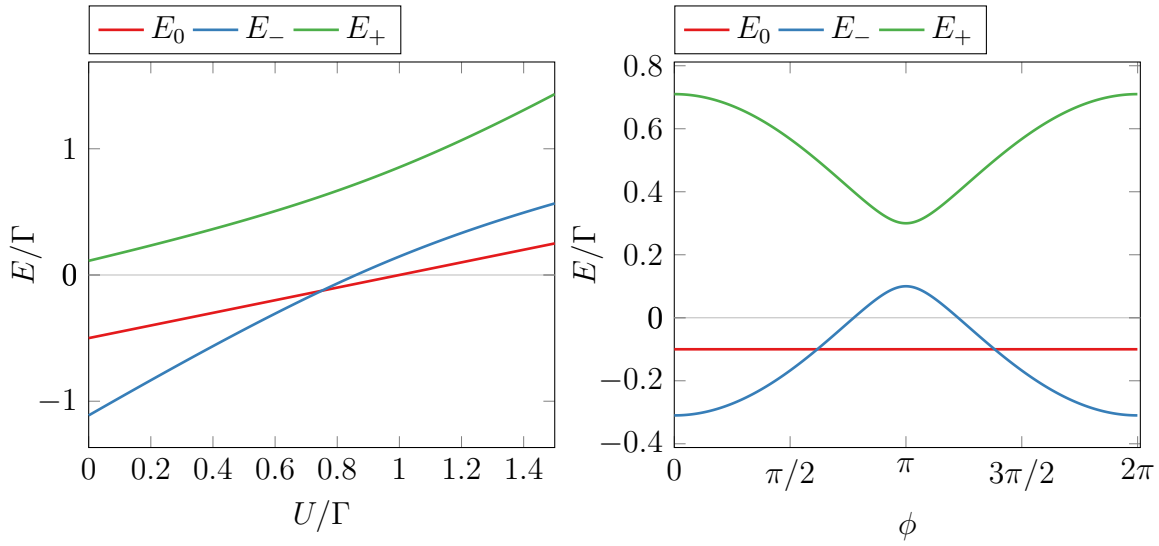

Figure 5.6: Eigenenergies for the interacting quantum dot in the limit of $\Delta \to \infty$. **Left:** As a function of dimensionless interaction strength U/Γ for $\xi_d/\Gamma = -0.5$ and $\phi = \pi/2$. **Right:** As a function of phase bias across the junction for the parameters $\xi_d/\Gamma = -0.4$ and $U/\Gamma = 0.6$. The crossing of E_0 and E_- signifies a phase transition from a singlet to a doublet ground state.

derivative of the charge, which is $\dot{q} = \partial_\phi H$. By inserting the Bogoliubov transformation we find the current operator

$$\hat{I} = -e\Gamma \sin\left(\frac{\phi}{2}\right)\Big((u^2 - v^2)(\gamma_\uparrow^\dagger\gamma_\downarrow^\dagger + \gamma_\downarrow\gamma_\uparrow) + 2uv(\gamma_\downarrow\gamma_\downarrow^\dagger - \gamma_\uparrow^\dagger\gamma_\uparrow)\Big). \tag{5.30}$$

We note that the expectation value is

$$\begin{aligned}\langle\hat{I}\rangle &= -2euv\Gamma \sin\left(\frac{\phi}{2}\right)\langle\gamma_\downarrow\gamma_\downarrow^\dagger - \gamma_\uparrow^\dagger\gamma_\uparrow\rangle \\ &= -2euv\Gamma \sin\left(\frac{\phi}{2}\right)(1 - n_\gamma),\end{aligned} \tag{5.31}$$

where the occupation factor $1 - n_\gamma = 1 - \langle\gamma_\uparrow^\dagger\gamma_\uparrow + \gamma_\downarrow^\dagger\gamma_\downarrow\rangle$ is zero in the doublet ground state and one in the singlet ground state. The doublet ground state doesn't carry any supercurrent when there is no contribution from the superconducting continuum, whereas the current in the singlet ground state has a sinusoidal dependence on the phase as expected for a Josephson junction. This is equivalent to a QPC where the current is carried only by the bound states and is blocked if the system is in an odd-partiy state (with a single quasiparticle occupying the Andreev bound state). In order to calculate the retarded two-particle Green's functions in $\chi_{II}(\omega)$, we note that the two-quasiparticle operators have a simple time evolution. This is seen by considering

their equation of motion. For the anomalous operators we find:

$$\begin{aligned} i\partial_t(\gamma_\uparrow^\dagger(t)\gamma_\downarrow^\dagger(t)) = -[H,\gamma_\uparrow^\dagger\gamma_\downarrow^\dagger](t) = -(2E-U)(\gamma_\uparrow^\dagger(t)\gamma_\downarrow^\dagger(t)) \\ \rightarrow \gamma_\uparrow^\dagger(t)\gamma_\downarrow^\dagger(t) = e^{i(2E-U)t}\gamma_\uparrow^\dagger\gamma_\downarrow^\dagger \end{aligned} \tag{5.32}$$

and

$$\begin{aligned} i\partial_t(\gamma_\downarrow(t)\gamma_\uparrow(t)) = -[H,\gamma_\downarrow\gamma_\uparrow](t) = (2E-U)(\gamma_\downarrow(t)\gamma_\uparrow(t)) \\ \rightarrow \gamma_\downarrow(t)\gamma_\uparrow(t) = e^{-i(2E-U)t}\gamma_\downarrow\gamma_\uparrow. \end{aligned} \tag{5.33}$$

And the normal operators are constant in time as they commute with the Hamiltonian

$$\begin{aligned} \gamma_\downarrow(t)\gamma_\downarrow^\dagger(t) = \gamma_\downarrow\gamma_\downarrow^\dagger \\ \gamma_\uparrow^\dagger(t)\gamma_\uparrow(t) = \gamma_\uparrow^\dagger\gamma_\uparrow. \end{aligned} \tag{5.34}$$

We can now easily obtain all two-particle Green's functions in the current-current correlation function just by calculating commutators. For ease of notation, we define the anomalous pair-operator $\hat{\Delta}_\gamma = \gamma_\uparrow^\dagger\gamma_\downarrow^\dagger$. The Green's functions with only anomalous operators are

$$\begin{aligned} G^R_{\Delta\Delta^\dagger}(t) &= -i\theta(t)\langle[\hat{\Delta}_\gamma(t),\hat{\Delta}_\gamma^\dagger(0)]\rangle_0 \\ &= -i\theta(t)e^{i(2E-U)t}\langle[\hat{\Delta}_\gamma,\hat{\Delta}_\gamma^\dagger]\rangle_0 \\ &= i\theta(t)e^{i(2E-U)t}(1-n_\gamma), \end{aligned} \tag{5.35}$$

with n_γ defined above and

$$\begin{aligned} G^R_{\Delta^\dagger\Delta}(t) &= -i\theta(t)\langle[\hat{\Delta}_\gamma^\dagger(t),\hat{\Delta}_\gamma(0)]\rangle_0 \\ &= -i\theta(t)e^{-i(2E-U)t}(1-n_\gamma). \end{aligned} \tag{5.36}$$

The Green's functions with normal two-particle operators vanish:

$$G^R_{n_\uparrow n_\downarrow^\dagger}(t) = -i\theta(t)\langle[\gamma_\uparrow^\dagger\gamma_\uparrow,\gamma_\downarrow\gamma_\downarrow^\dagger]\rangle_0 = 0, \tag{5.37}$$

and the mixed Green's functions similarly evaluate to

$$G^R_{n_\uparrow\Delta}(t) = -i\theta(t)\langle[\hat{n}_\uparrow,\hat{\Delta}_\gamma]\rangle_0 = -i\theta(t)\langle\hat{\Delta}_\gamma\rangle_0 = 0, \tag{5.38}$$

with the same result for all other combinations. Here we used that the expectation value of the anomalous operators is zero. Collecting everything, we find that the response function is

$$\begin{aligned} \chi_{II}(t) &= e\Gamma^2\sin^2\left(\frac{\phi}{2}\right)(u^2-v^2)^2\Big(G_{\Delta^\dagger\Delta}(t)+G_{\Delta\Delta^\dagger}(t)\Big) \\ &= -i\theta(t)e\Gamma^2\sin^2\left(\frac{\phi}{2}\right)(u^2-v^2)^2\Big(e^{i(2E-U)t}(1-n_\gamma)-e^{-i(2E-U)t}(1-n_\gamma)\Big). \end{aligned} \tag{5.39}$$

Fourier transformation yields

$$\chi_{II}(\omega) = e\Gamma^2 \sin^2\left(\frac{\phi}{2}\right)\left(\frac{1}{\omega + i\eta + (2E-U)} - \frac{1}{\omega + i\eta - (2E-U)}\right)(1-n_\gamma). \quad (5.40)$$

Remembering that the relation between response function and admittance is $Y(\omega) = \frac{ie}{\omega}\chi_{II}(\omega)$, we obtain the real part of the admittance, which is the main result of this section

$$\begin{aligned} \mathrm{Re}\, Y(\omega) &= -\frac{e}{\omega}\,\mathrm{Im}\,\chi_{II}(\omega) \\ &= -\frac{e^2\Gamma^2}{\omega}\sin^2\left(\frac{\phi}{2}\right)\left(\delta(\omega + (2E-U)) - \delta(\omega - (2E-U))\right)(1-n_\gamma) \end{aligned} \quad (5.41)$$

$\mathrm{Re}\, Y(\omega)$ is an even function as expected and always positive. The occupation factor $(1-n_\gamma)$ is zero when the ground state is a doublet. Hence the system is unable to absorb radiation in the doublet ground state. This is as expected, as no parity-conserving transitions are possible from the state $|\sigma\rangle$ to the states $|-\rangle$ and $|+\rangle$ in the absence of the superconducting continuum. Such a transition would have to involve an exchange of electrons with the leads, and this is not possible in the limit $\Delta \to \infty$.

In the singlet ground state, the system can absorb a photon with energy $\omega = 2E - U = 2\sqrt{\tilde{\xi}_d^2 + \Gamma_\phi^2} = E_+ - E_-$. From this energy, we can infer that the absorbed photon causes the system to be excited from the ground state $|-\rangle$ to the excited singlet state $|+\rangle$. This process conserves parity as it should. And as the state $|-\rangle$ has zero quasiparticles and $|+\rangle$ has two, this is a process where the system absorbs a photon and two quasiparticles are created in the bound states. In conclusion, our results from studying S-QD-S-junctions in the limits $U \gg \Delta$ and $U \ll \Delta$ that no absorption process related to the creation of two quasiparticles with energy $E < \Delta$ is possible when the system is in a doublet ground state has been confirmed for this approach which is exact in U, and where we included only the bound states in our calculation. As the eigenstates of the system were known, it was here very easy to understand the possible transition. Importantly, this approach captured the quantum mechanical nature of the singlet and doublet states in an exact manner.

In conclusion, the results of this chapter indicate that both the noninteracting quantum dot with a magnetic field and the classical spin approximation correctly capture the singlet and doublet nature of the states of an S-QD-S Josephson junction described by the Anderson model. The main effect of both approximations is to spin-polarise the problem and break the degeneracy of the doublet state. But this doesn't affect the results for the admittance and generally the photon absorption properties in the linear response regime, as when the ground state is a doublet the energy of the excited doublet state is pushed above the gap in the sense that it takes two photons to induce a transition between these states. Hence we expect that our results for the real part of the admittance in figs. 3.8 and 5.5 are valid also outside of these approximations, eg. for a quantum mechanical impurity spin in the cotunneling model.

Chapter 6

Summary and conclusion

Having studied different types of Josephson junctions subject to a small, harmonic phase bias from many different angles, we are now in a position to provide some general results for the ability of such a junction to absorb photons. The quantum point contact is a particularly simple system, which exhibits the well-known Andreev bound states. By calculating the linear response of the current to a time-dependent voltage bias we obtained a result for the real part of the admittance, which is related to the absorbed power. The absorption spectrum had three different contributions, which could all easily be associated with the creation of quasiparticles in the bound state or in the superconducting continuum.

This calculation was then repeated for an S-QD-S junction studied in the regime of strong Coulomb interaction, with the dot being occupied by a classical impurity spin. In contrast with the simple QPC, this system has four bound states below the gap which are not spin-degenerate, and which can cross zero energy, signifying a change of ground state. The results for the admittance showed to be dependent on whether the ground state of the system was the singlet-like screened state or the doublet-like unscreened state. In particular, the δ-peak in $\mathrm{Re}\, Y(\omega)$ arising from the creation of two quasiparticles in the subgap states was not present for the doublet ground state. As it was not immediately clear how these results were affected by the classical spin approximation it proved necessary to approach the problem from another point of view.

This motivated the study of an S-QD-S-junction in the opposite noninteracting limit of $U = 0$, but with a magnetic field which in effect is equivalent to a mean-field treatment of the Coulomb interaction and results in a spin-splitting of the Andreev-like bound states. It was clear that by tuning the magnetic field, it was possible to obtain bound states with the same properties as the YSR-states, again showing that the system exhibited a phase transition between a singlet and a doublet ground state. As expected, the discrete absorption peak disappeared for the doublet ground state. However also in this model the eigenstates of the system weren't known, so to see how the dot states where modified by the coupling to the leads and establish whether they were actually singlet and doublet states also in a fully quantum mechanical treatment of the problem we studied the limit of $\Delta \to \infty$.

Here it was possible to write up an effective Hamiltonian involving only the dot. In this reduced Hilbert space, the eigenstates were found to be true quantum mechanical singlet and doublet states. Calculating the real part of the admittance confirmed our previous results. When excluding the superconducting continuum, only the peak related to the creation of two quasiparticles in the subgap states was present, and this peak vanished for the doublet ground state. This enhanced our belief that the calculations for a classical magnetic impurity and weakly interacting dot captured correctly the singlet and doublet nature of the eigenstates, at least to the extend necessary for the calculations in the regime of linear response to be correct.

We found that the physical reason behind the absorption peak being absent in the doublet ground state had a simple explanation which is most easily accessible in perturbation theory. By determining the eigenstates of a scattering problem with a magnetic potential, we found that the current operator can only induce transitions between initial and final states which differ by two quasiparticles of opposite spin. This is related to the fact that the perturbation couples to the current operator so that the quasiparticles are created by splitting a Cooper pair. Transitions between doublet and singlet states requires electron exchange with the superconducting leads and hence result in the creation of a quasiparticle in the continuum.

6.1 Outlook

A natural extension of our work would be to seek further evidence that the results for an S-QD-S-junction with a magnetic impurity are also valid outside the regime studied here with $U \gg \Delta$ and assuming a classical magnetic impurity. The assumption that the impurity spin is classical somewhat limits our ability to predict whether the results extend to the more physically correct description in terms of a quantum impurity spin in the cotunneling regime where spin-flips play an important role. It is possible to include the possibility for spin-flips in the scattering formalism of chapter 4 as done in ref. [33] where the DC Josephson effect is investigated for a SFS-junction where spin-flips can occur at the interface between superconductor and ferromagnet. Multiple approximation methods applicable to the Anderson model with a magnetic impurity also exist. One such approach is the Numerical Renormalization Group (NRG) method which can be used to deal with a quantum mechanical impurity coupled to a noninteracting bath eg. of Cooper pairs with a continuous spectrum [34]. Here a logarithmic discretization of the energy spectrum is performed, which yields a high resolution of the low-energy excitations. Subsequently the system can be mapped onto an effective tight-binding model where the number of sites depends exponentially on the size of the discrete energy intervals. An iterative diagonalization is performed adding one site at a time, a process which has to be truncated at a suitable point. This method has been used by Jellinggaard et al. [35] to describe the YSR-states in good agreement with experiments and by [36] to capture the quantum phase transition between the singlet and doublet ground states. Another approach used by ref. [20] is taking the

zero bandwidth-limit where the Anderson model can be diagonalized exactly. It is valid in the limit where Δ is much larger than the other energy scales of the problem. Here the leads are approximated by a single level, which drastically reduces the size of the Hilbert space and allows for exact diagonalization. This model again captures the phase transition and the nature of the bound states but has no information about the superconducting gap.

Lastly, it would of course be of great interest of us to know if our results can be verified experimentally. This should be done using reflectometry as described in section 1.3. Related experiments designed to perform spectroscopy of Andreev bound states have already been carried out eg. by Bretheau et al. [37] in a QPC. Here the Josephson junction which is subject to the measurement is connected in parallel with a superconducting tunnel junction to form a SQUID. This makes it possible to apply a phase bias to the junction by means of a magnetic flux in the loop of the SQUID. The SQUID is capacitively coupled to the spectrometer which is a voltage-biased tunnel junction and also acts as a source of microwave radiation. When the spectrometer is subject to a voltage bias V_J it emits photons with energy $\nu_J = 2eV_J/h$ which can be absorbed by the Josephson junction causing a Cooper pair to tunnel across the spectrometer. This can then be measured as a current. With today's experimental techniques it should be possible to carry out experiments such as these also for the type of system studied in this thesis.

Bibliography

[1] C. Janvier et al. "Coherent manipulation of Andreev states in superconducting atomic contacts". In: *Science* 349.6253 (Sept. 11, 2015), pp. 1199–1202. DOI: 10.1126/science.aab2179.

[2] Yu Luh. "BOUND STATE IN SUPERCONDUCTORS WITH PARAMAGNETIC IMPURITIES". In: *wlxb* 21.1 (1965), p. 75. DOI: 10.7498/aps.21.75.

[3] Hiroyuki Shiba. "Classical Spins in Superconductors". In: *Prog. Theor. Phys.* 40.3 (Sept. 1968), pp. 435–451. DOI: 10.1143/PTP.40.435.

[4] A. I. Rusinov. "Superconductivity near a Paramagnetic Impurity". In: *Soviet Journal of Experimental and Theoretical Physics Letters* 9 (Jan. 1969), p. 85.

[5] F. Kos, S. E. Nigg, and L. I. Glazman. "Frequency-dependent admittance of a short superconducting weak link". In: *Phys. Rev. B* 87.17 (May 28, 2013), p. 174521. DOI: 10.1103/PhysRevB.87.174521.

[6] B.D. Josephson. "Possible new effects in superconductive tunnelling". In: *Physics Letters* 1.7 (July 1962), pp. 251–253. DOI: 10.1016/0031-9163(62)91369-0.

[7] Michael Tinkham. *INTRODUCTION TO SUPERCONDUCTIVITY*. OCLC: 1019647961. Dehli: Scientific International, 2017.

[8] P. Krantz et al. "A quantum engineer's guide to superconducting qubits". In: *Applied Physics Reviews* 6.2 (June 2019), p. 021318. DOI: 10.1063/1.5089550.

[9] Anders Kringhøj. "Exploring the Semiconducting Josephson Junction of Nanowire-based Superconducting Qubits". PhD thesis. Center for Quantum Devices, Niels Bohr Institute: University of Copenhagen, Jan. 2020. 162 pp.

[10] S. M. Girvin. "Circuit QED: superconducting qubits coupled to microwave photons". In: *Quantum Machines: Measurement and Control of Engineered Quantum Systems*. Ed. by Michel Devoret et al. Oxford University Press, June 12, 2014, pp. 113–256. DOI: 10.1093/acprof:oso/9780199681181.003.0003.

[11] Thomas Ihn. *Semiconductor nanostructures: quantum states and electronic transport*. OCLC: ocn430496978. Oxford ; New York: Oxford University Press, 2010. 552 pp.

[12] Henrik Bruus and Karsten Flensberg. *Many-body quantum theory in condensed matter physics: an introduction*. Oxford graduate texts. OCLC: ocm56694794. Oxford ; New York: Oxford University Press, 2004. 435 pp.

[13] Landry Bretheau. "Localized Excitations in Superconducting Atomic Contacts: Probing the Andreev Doublet". PhD thesis. Paris Institute of Technology, 2013.

[14] Alex Kamenev and Alex Levchenko. "Keldysh technique and non-linear -model: basic principles and applications". In: *Advances in Physics* 58.3 (May 2009), pp. 197–319. DOI: 10.1080/00018730902850504.

[15] Supriyo Datta, Philip Bagwell, and M.P Anantram. *Scattering Theory of Transport for Mesoscopic Superconductors*. Technical Report. School of Electrical and Computer Engineering: Purdue University, Jan. 1, 1996, p. 94.

[16] C. W. J. Beenakker and H. van Houten. "Josephson current through a superconducting quantum point contact shorter than the coherence length". In: *Phys. Rev. Lett.* 66.23 (June 10, 1991), pp. 3056–3059. DOI: 10.1103/PhysRevLett.66.3056.

[17] A. Martín-Rodero, A. Levy Yeyati, and F. J. García-Vidal. "Thermal noise in superconducting quantum point contacts". In: *Phys. Rev. B* 53.14 (Apr. 1, 1996), R8891–R8894. DOI: 10.1103/PhysRevB.53.R8891.

[18] Gediminas Kiršanskas et al. "Yu-Shiba-Rusinov states in phase-biased superconductor–quantum dot–superconductor junctions". In: *Phys. Rev. B* 92.23 (Dec. 14, 2015), p. 235422. DOI: 10.1103/PhysRevB.92.235422.

[19] Gediminas Kiršanskas. "Electron Transport in Quantum Dots and Heat Transport in Molecules". PhD thesis. University of Copenhagen, 2014.

[20] Gorm O. Steffensen. "Yu-Shiba-Rusinov bound states in quantum dots". Master Thesis. University of Copenhagen, July 25, 2017.

[21] A. V. Balatsky, I. Vekhter, and Jian-Xin Zhu. "Impurity-induced states in conventional and unconventional superconductors". In: *Rev. Mod. Phys.* 78.2 (May 9, 2006), pp. 373–433. DOI: 10.1103/RevModPhys.78.373.

[22] Anika Haller. "Sub-gap transport in superconductor-dot junctions". Master Thesis. Niels Bohr Institute: University of Copenhagen, Apr. 2014. 63 pp.

[23] G. E. Blonder, M. Tinkham, and T. M. Klapwijk. "Transition from metallic to tunneling regimes in superconducting microconstrictions: Excess current, charge imbalance, and supercurrent conversion". In: *Phys. Rev. B* 25.7 (Apr. 1, 1982), pp. 4515–4532. DOI: 10.1103/PhysRevB.25.4515.

[24] Akira Furusaki. "Josephson current carried by Andreev levels in superconducting quantum point contacts". In: *Superlattices and Microstructures* 25.5 (May 1999), pp. 809–818. DOI: 10.1006/spmi.1999.0730.

[25] D. G. Olivares et al. “Dynamics of quasiparticle trapping in Andreev levels”. In: *Phys. Rev. B* 89.10 (Mar. 4, 2014), p. 104504. DOI: 10.1103/PhysRevB.89.104504.

[26] Cecilie Hermansen. “Vortices in s-Wave Superconductors -A Numerical Study of the Bogoliubov-de Gennes Equations”. Bachelor thesis. Niels Bohr Institute: University of Copenhagen, June 13, 2018. 37 pp.

[27] Jian-Xin Zhu. *Bogoliubov-de Gennes Method and Its Applications*. 1st ed. 2016. Lecture Notes in Physics 924. Cham: Springer International Publishing : Imprint: Springer, 2016. 1 p. DOI: 10.1007/978-3-319-31314-6.

[28] David J. Griffiths. *Introduction to quantum mechanics*. Second edition [2017 edition]. Cambridge: Cambridge University Press, 2017. 468 pp.

[29] M. Zgirski et al. “Evidence for Long-Lived Quasiparticles Trapped in Superconducting Point Contacts”. In: *Phys. Rev. Lett.* 106.25 (June 22, 2011), p. 257003. DOI: 10.1103/PhysRevLett.106.257003.

[30] E. Vecino, A. Martín-Rodero, and A. Levy Yeyati. “Josephson current through a correlated quantum level: Andreev states and junction behavior”. In: *Phys. Rev. B* 68.3 (July 10, 2003), p. 035105. DOI: 10.1103/PhysRevB.68.035105.

[31] C. W. J. Beenakker and H. van Houten. “Resonant Josephson Current Through a Quantum Dot”. In: *Single-Electron Tunneling and Mesoscopic Devices*. Ed. by Hans Koch and Heinz Lübbig. Red. by Klaus von Klitzing et al. Vol. 31. Series Title: Springer Series in Electronics and Photonics. Berlin, Heidelberg: Springer Berlin Heidelberg, 1992, pp. 175–179. DOI: 10.1007/978-3-642-77274-0_20.

[32] Tobias Meng, Serge Florens, and Pascal Simon. “Self-consistent description of Andreev bound states in Josephson quantum dot devices”. In: *Phys. Rev. B* 79.22 (June 19, 2009), p. 224521. DOI: 10.1103/PhysRevB.79.224521.

[33] Henrik Enoksen, Jacob Linder, and Asle Sudbø. “Spin-flip scattering and critical currents in ballistic half-metallic d -wave Josephson junctions”. In: *Phys. Rev. B* 85.1 (Jan. 18, 2012), p. 014512. DOI: 10.1103/PhysRevB.85.014512.

[34] A. Martín-Rodero and A. Levy Yeyati. “Josephson and Andreev transport through quantum dots”. In: *Advances in Physics* 60.6 (Dec. 2011), pp. 899–958. DOI: 10.1080/00018732.2011.624266.

[35] Anders Jellinggaard et al. “Tuning Yu-Shiba-Rusinov states in a quantum dot”. In: *Phys. Rev. B* 94.6 (Aug. 29, 2016), p. 064520. DOI: 10.1103/PhysRevB.94.064520.

[36] Yoshihide Tanaka, Akira Oguri, and A C Hewson. “Kondo effect in asymmetric Josephson couplings through a quantum dot”. In: *New J. Phys.* 9.5 (May 9, 2007), pp. 115–115. DOI: 10.1088/1367-2630/9/5/115.

[37] L. Bretheau et al. “Exciting Andreev pairs in a superconducting atomic contact”. In: *Nature* 499.7458 (July 18, 2013), pp. 312–315. DOI: 10.1038/nature12315.

[38] Dmitry Ryndyk. *Theory of Quantum Transport at Nanoscale*. Vol. 184. Springer Series in Solid-State Sciences. Cham: Springer International Publishing, 2016. DOI: 10.1007/978-3-319-24088-6.

[39] Hartmut Haug and Antti-Pekka Jauho. *Quantum kinetics in transport and optics of semiconductors*. 2nd, substantially rev. ed. Springer series in solid-state sciences 123. OCLC: ocn176628667. Berlin ; New York: Springer, 2008. 360 pp.

[40] C Caroli et al. "Direct calculation of the tunneling current". In: *J. Phys. C: Solid State Phys.* 4.8 (June 14, 1971), pp. 916–929. DOI: 10.1088/0022-3719/4/8/018.

Appendices

Appendix A

Conductance

We wish to determine the conductance for a system described by the tunneling Hamiltonian denoted H_T in eq. 2.1. The well-known Landauer-Büttiker formula states that the conductance G for such a system consisting of two leads separated by a tunneling barrier with just a single transmission mode is given in terms of the transmission coefficient τ as [38]

$$G = \frac{e^2}{\pi}\tau = G_0\tau, \tag{A.1}$$

where G_0 is the conductance quantum (here in units where $\hbar = 1$). Such problems are often treated using scattering theory, but here we will present another approach using non-equilibrium Green's functions in the Keldysh formalism. This allows us to calculate the current exactly, and we will then see that to linear order in the applied potential V our result reduces to the Landauer-Büttiker formula. We will start by considering the case of a time-independent voltage, $V(t) = V$. This creates a difference in the chemical potentials of the two leads given by $\mu_L - \mu_R = eV$. In a normal metal we don't need Nambu spinors, and the current operator in Fourier space from eq. 2.27 is simply

$$\langle \hat{I}(0)\rangle_0 = -\frac{ew}{\pi}\int_{-\infty}^{\infty} d\omega (G^<_{RL}(\omega) - G^<_{LR}(\omega)). \tag{A.2}$$

The lesser Green's function is now found using the Keldysh (matrix) equation [39]

$$G^< = (1 + G^R\Sigma^R)G_0^<(1 + \Sigma^A G^A) + G^R\Sigma^< G^A, \tag{A.3}$$

where the retarded and advanced Green's functions for the coupled system are found using the Dyson equation:

$$G^{R,A} = G_0^{R,A} + G_0^{R,A}\Sigma^{R,A}G^{R,A}, \tag{A.4}$$

with a self-energy which in the LR-basis is given by $\Sigma^{R,A} = \begin{pmatrix} w & w \\ w & w \end{pmatrix}$. As argued in ref. [40] the self-energy in the Keldysh basis doesn't connect the two branches of the contour, which means that $\Sigma^< = 0$ so that the second term in the equation above

vanishes. The remaining term in eq. A.3 is usually assumed to vanish by an argument where one assumes that the system was in a noninteracting state in the infinite past or due to thermalization which removes all dependence on the initial state. Here no relaxation mechanism has been included in the description of the leads and in our case this term is nonzero. We proceed by calculating the retarded Green's function

$$G^R = \begin{pmatrix} G_{LL} & G_{LR} \\ G_{RL} & G_{RR} \end{pmatrix}$$

using eq. A.4 where G_0^R is the Green's function without interactions, so that $G_{LR}^{0,R} = G_{RL}^{0,R} = 0$ and where $G_{LL}^{0,R} = G_{RR}^{0,R} \equiv G_0 = \sum_k \frac{1}{\omega - \xi_k + i\eta} \approx -i\pi\nu_F$ in the wide-band approximation. We thus obtain

$$\mathbf{G}^R = \begin{pmatrix} (G_{LL}^{0,R})^{-1} - w & -w \\ -w & (G_{RR}^{0,R})^{-1} - w \end{pmatrix}^{-1}, \tag{A.5}$$

from which it is seen that

$$G_{LR}^R(\omega) = G_{RL}^R(\omega) = \frac{wG_0^2}{1 - 2wG_0}, \quad G_{LL}^R = G_{RR}^R = \frac{G_0(1 - wG_0)}{1 - 2wG_0}. \tag{A.6}$$

From this we can then find the advanced Green's function as $G^A = (G^R)^\dagger$

Once the advanced and retarded Green's functions are known the lesser Green's functions $G_{LR}^<$ and $G_{RL}^<$ are easily obtained using eq. A.3. Evaluating the matrix products yields

$$\begin{aligned} G_{LR}^<(\omega) = w(G_{LR}^R + G_{LL}^R)(1 + wG_{RR}^A + wG_{LR}^A)G_{RR}^{0,<} + \\ (1 + wG_{LR}^R + wG_{LL}^R)w(G_{RR}^A + G_{LR}^A)G_{LL}^{0,<}, \end{aligned} \tag{A.7}$$

where the dependence on ω of the Green's functions has been suppressed. A similar expression is found for $G_{RL}^<$. Furthermore we have:

$$\begin{aligned} G_{LL}^{0,<} &= i\sum_k A(k,\omega) n_F(\omega + eV/2) = i\sum_k 2\pi\delta(\omega - \xi_k) n_F(\omega + eV/2) \\ &= i\nu_F \pi n_F(\omega + eV/2) \approx i\pi\nu_F \left(n_F(\omega) + e\frac{V}{2}\frac{\partial n_F}{\partial \omega} \right), \end{aligned} \tag{A.8}$$

and similarly $G_{RR}^{0,<} \approx i\pi\nu_F \left(n_F(\omega) - \frac{V}{2}\frac{\partial n_F}{\partial \omega} \right)$. Here the Fermi function was expanded to linear order in V as we will eventually take this limit to obtain the conductance which is given by the linear response of the current to the voltage bias. Plugging the

expressions for the Green's functions into eq. A.2 the current is found to be

$$\langle \hat{I} \rangle = -\frac{ew^2}{\pi} \int_{-\infty}^{\infty} d\omega \left((G^R_{LR} + G^R_{LL} - (G^A_{RL} + G^A_{LL}) \right) (G^{0,<}_{RR} - G^{0,<}_{LL}) \tag{A.9}$$

$$= -\frac{ew^2}{\pi} \int_{-\infty}^{\infty} d\omega 2i \, \mathrm{Im}(G^R_{LR} + G^R_{LL})(G^{0,<}_{RR} - G^{0,<}_{LL}) \tag{A.10}$$

$$\approx -\frac{2ie^2w^2}{\pi} i\pi\nu_F \, \mathrm{Im} \left[\frac{-2i\pi\nu_F}{1 + 2i\pi\nu_F w} \right] V \int_{-\infty}^{\infty} d\omega \frac{\partial n_F}{\partial \omega} \tag{A.11}$$

$$= -\frac{e^2}{\pi} \frac{(2\pi\nu_F w)^2}{1 + (2\pi\nu_F w)^2} V. \tag{A.12}$$

From this the conductance is immediatly read off to be $G = \frac{e^2}{\pi} \frac{(2\pi\nu_F w)^2}{1+(2\pi\nu_F w)^2} = G_0\tau$. Hence the Landauer formula is regained at zero temperature by taking the linear response limit in the expression for the current obtained using the Keldysh formalism. In addition to finding the conductance, we have also obtained an exact result for the current at any bias

$$\langle \hat{I} \rangle = G_0 \frac{(2\pi\nu_F w)^2}{1 + (2\pi\nu_F w)^2} \int_{\infty}^{\infty} (n_F(\omega + eV/2) - n_F(\omega - eV/2)). \tag{A.13}$$

The value given above for the tunneling coefficient τ is determined from the transfer matrix using the optical theorem. The transfer matrix is defined according to:

$$T^R = \Sigma^R + \Sigma^R G^R_0 T^R \implies T^R = (\mathbb{1} - \Sigma^R G^R_0)^{-1} \Sigma^R. \tag{A.14}$$

To find the scattering matrix the optical theorem is then invoked

$$S = \mathbb{1} - 2\pi i \nu_F T = \begin{pmatrix} r & t \\ t & r \end{pmatrix} \tag{A.15}$$

where r and t are the reflection and transmission coefficients. Plugging in the self-energy with $G_0 = -i\pi\nu_F$ in the wide-band limit, the transmission probability is determined from the scattering matrix as

$$\tau = |t|^2 = \frac{(2\pi\nu_F w)^2}{1 + (2\pi\nu_F w)^2}. \tag{A.16}$$

Appendix B

Time-dependent unitary transformation

Here we show how a time-dependent unitary transformation can transfer the phase $\phi_1(t)$ from Δ to the tunneling part of the Hamiltonian. As $\Delta_R = \Delta$ and $\Delta_L = e^{2i\phi_1(t)}\Delta$ with Δ real, the unitary transformation acts only on the left lead. To see how this works, we write the Hamiltonian in terms of a four-Nambu spinor for both the left and the right lead as

$$\begin{aligned} H =& \sum_{kk'} \Psi_k^\dagger \begin{pmatrix} \xi_k\delta_{kk'} + w & -\Delta_L\delta_{kk'} & w & 0 \\ -\Delta_L^*\delta_{kk'} & -(\xi_k\delta_{kk'} + w) & 0 & -w \\ w & 0 & \xi_k\delta_{kk'} + w & -\Delta_R\delta_{kk'} \\ 0 & -w & -\Delta_R^*\delta_{kk'} & -(\xi_k\delta_{kk'} + w) \end{pmatrix} \Psi_{k'} \\ =& \sum_{kk'} \Psi_k^\dagger \mathbf{M}_{kk'} \Psi_{k'} \end{aligned} \tag{B.1}$$

with $\Psi_k^\dagger = (c_{Lk\uparrow}^\dagger,\, c_{L-k\downarrow},\, c_{Rk\uparrow}^\dagger,\, c_{R-k\downarrow})$. The unitary transformation which transfers the phase to the tunneling part is then

$$U(t) = \begin{pmatrix} e^{-i\phi_1(t)} & 0 & 0 & 0 \\ 0 & e^{i\phi_1(t)} & 0 & 0 \\ 0 & 0 & 1 & 0 \\ 0 & 0 & 0 & 1 \end{pmatrix}. \tag{B.2}$$

We will now study how the time-dependent unitary transformation affects the equation of motion for the Nambu spinors which transform as $\tilde{\Psi} = U(t)\Psi$ (omitting the

$k-$subscript of Ψ for notational ease)

$$\begin{aligned}
\dot{\tilde{\Psi}}_\alpha &= \dot{U}_{\alpha\beta}\Psi_\beta + U_{\alpha\beta}\dot{\Psi}_\beta \\
&= \dot{U}_{\alpha\beta}\Psi_\beta + iU_{\alpha\beta}\sum_{\eta\mu}\Big[\Psi^\dagger_\eta M_{\eta\mu}\Psi_\mu, \Psi_\beta\Big] \\
&= \dot{U}_{\alpha\beta}U^\dagger_{\beta\gamma}\tilde{\Psi}_\gamma + iU_{\alpha\beta}\sum_{\eta\mu} M_{\eta\mu}(-\delta_{\eta\beta}\Psi_\mu) \\
&= \dot{U}_{\alpha\beta}U^\dagger_{\beta\gamma}\tilde{\Psi}_\gamma - iU_{\alpha\beta}M_{\beta\mu}\Psi_\mu \\
&= \dot{U}_{\alpha\beta}U^\dagger_{\beta\gamma}\tilde{\Psi}_\gamma - iU_{\alpha\beta}M_{\beta\mu}U^\dagger_{\mu\nu}U_{\nu\mu}\Psi_\nu \\
&= \dot{U}_{\alpha\beta}U^\dagger_{\beta\gamma}\tilde{\Psi}_\gamma - i\tilde{M}_{\alpha\nu}\tilde{\Psi}_\nu,
\end{aligned} \tag{B.3}$$

where we used that we can always multiply by $UU^\dagger = 1$ and defined $\tilde{M} = UMU^\dagger$. Collecting everything, we can write the equation of motion on matrix form as

$$\dot{\tilde{\Psi}} = -i\Big(i\dot{U}U^\dagger + \tilde{M}\Big)\tilde{\Psi}. \tag{B.4}$$

This is the same as what we would have obtained for a Hamiltonian

$$H = \sum_{kk'}\tilde{\Psi}^\dagger_k\Big(i\dot{U}U^\dagger\delta_{kk'} + UM_{kk'}U^\dagger\Big)\tilde{\Psi}_{k'}, \tag{B.5}$$

where the term

$$\sum_{kk'}\tilde{\Psi}^\dagger_k\Big(i\dot{U}U^\dagger\Big)\tilde{\Psi}_{k'} = \phi_1(t)\sum_{k\sigma}\tilde{c}^\dagger_{Lk\sigma}\tilde{c}_{Lk\sigma} = \phi_1(t)\sum_{k\sigma}c^\dagger_{Lk\sigma}c_{Lk\sigma} = eV(t)\hat{N}_L \tag{B.6}$$

cancels exactly the term which was added to the Hamiltonian due to the shift of the chemical potential of the left lead in eq. 2.33. This means that after the transformation, the total Hamiltonian for a nonzero time-dependent voltage bias is

$$\begin{aligned}
H(t) &= H_0 + H_T(t) \\
H_{LR} &= \sum_{\alpha k\sigma}\xi_{k\alpha}c^\dagger_{k\alpha\sigma}c_{k\alpha\sigma} - \Delta\Big(\sum_{\alpha k}c^\dagger_{k\alpha\uparrow}c^\dagger_{-k\alpha\downarrow} + \sum_{\alpha k}c_{k\alpha\downarrow}c_{-k\alpha\uparrow}\Big) + w\sum_{\alpha\sigma kk'}c^\dagger_{k\alpha\sigma}c_{k'\alpha\sigma} \\
H_T(t) &= w\sum_{kp\sigma}(e^{-i\phi_1(t)}c^\dagger_{kL\sigma}c_{pR\sigma} + e^{i\phi_1(t)}c^\dagger_{pR\sigma}c_{kL\sigma}),
\end{aligned} \tag{B.7}$$

where we redefined $c_{\alpha k\sigma} \equiv \tilde{c}_{\alpha k\sigma}$.

Appendix C

Two-channel problem

Here we follow Kiršanskas [18] in explaining why the quantum dot with a classical magnetic impurity studied in chapter 3 is a two-channel problem, This can be used to understand the origin of the two different kinds of bound state energies. For the simple Anderson model with normal leads one can perform a rotation of the operators for the left and right lead. This separates the Hamiltonian into an even and an odd sector which are not mixed, and the tunneling part of the Hamiltonian then involves only the even sector [12]. We will see that here something similar happens, but the two channels are coupled for finite phase difference ϕ between the leads. We write the cotunneling part of the Hamiltonian in eq. 3.3 as

$$\begin{aligned} H_T &= H_J + H_W \\ &= \sum_{kk'\sigma} (W + JS\sigma) \begin{pmatrix} c^\dagger_{Lk\sigma} & c^\dagger_{Rk\sigma} \end{pmatrix} \begin{pmatrix} \cos^2(\theta) & \sin(\theta)\cos(\theta)e^{i\phi/2} \\ \sin(\theta)\cos(\theta)e^{-i\phi/2} & \sin^2(\theta) \end{pmatrix} \begin{pmatrix} c_{Lk'\sigma} \\ c_{Rk'\sigma} \end{pmatrix} \\ &= \sum_{kk'\sigma} (W + JS\sigma) \mathbf{c}^\dagger \mathbf{\Theta} \mathbf{c}. \end{aligned} \tag{C.1}$$

This part of the Hamiltonian can be diagonalized by means of a unitary transformation which is constructed from the eigenvectors of $\mathbf{\Theta}$

$$\begin{aligned} \mathbf{v}_0 &= \begin{pmatrix} e^{i\phi/2}\sin(\theta) \\ -\cos(\theta) \end{pmatrix} \quad \text{with eigenvalue} \quad \lambda_0 = 0 \quad \text{and} \\ \mathbf{v}_1 &= \begin{pmatrix} \cos(\theta) \\ e^{-i\phi/2}\sin(\theta) \end{pmatrix} \quad \text{with eigenvalue} \quad \lambda_1 = 1 \end{aligned} \tag{C.2}$$

Defining

$$\mathbf{U} = \begin{pmatrix} \cos(\theta) & e^{i\phi/2}\sin(\theta) \\ e^{-i\phi/2}\sin(\theta) & -\cos(\theta), \end{pmatrix} \tag{C.3}$$

the Hamiltonian transforms according to

$$\mathbf{U}^\dagger \mathbf{\Theta} \mathbf{U} = \begin{pmatrix} 1 & 0 \\ 0 & 0 \end{pmatrix} \tag{C.4}$$

and

$$\tilde{\mathbf{c}} = \mathbf{U}\mathbf{c} = \begin{pmatrix} \cos(\theta)c_{Lk\sigma} + e^{i\phi/2}\sin(\theta)c_{Rk\sigma} \\ \sin(\theta)e^{-i\phi/2}c_{Lk\sigma} - \cos(\theta)c_{Rk\sigma} \end{pmatrix} \equiv \begin{pmatrix} c_{ek\sigma} \\ c_{ok\sigma} \end{pmatrix}. \tag{C.5}$$

Here the names $c_{ek\sigma}$ and $c_{ok\sigma}$ refer to the even and odd sectors, which the transformed basis reduced to for zero phase bias [12]. The transformed Hamiltonian is then

$$H_T = \sum_{kk'\sigma}(W + JS\sigma)\begin{pmatrix} c^\dagger_{ek\sigma} & c^\dagger_{ok\sigma} \end{pmatrix}\begin{pmatrix} 1 & 0 \\ 0 & 0 \end{pmatrix}\begin{pmatrix} c_{ek'\sigma} \\ c_{ok'\sigma} \end{pmatrix} = \sum_{kk'\sigma}(W + JS\sigma)c^\dagger_{ek\sigma}c_{ek'\sigma}, \tag{C.6}$$

so that as expected only the even combination of the lead operators appear in the cotunneling term. To see that the even and odd channels are coupled by the superconducting (lead) part of the Hamiltonian, we write it in terms of the four-spinors $\Psi_{k\sigma} = (c_{Lk\sigma},\, c_{Rk\sigma},\, c^\dagger_{L-k\bar{\sigma}},\, c^\dagger_{R-k\bar{\sigma}})$:

$$H_{LR} = \frac{1}{2}\sum_{k\sigma}\Psi^\dagger_{k\sigma}\begin{pmatrix} \xi_k\sigma_0 & -\sigma\Delta\sigma_0 \\ -\sigma\Delta\sigma_0 & -\xi_k\sigma_0 \end{pmatrix}\Psi_{k\sigma}. \tag{C.7}$$

The four-spinors transform as

$$\tilde{\Psi}_{k\sigma} = \begin{pmatrix} U & 0 \\ 0 & U^* \end{pmatrix}\Psi_{k\sigma} \quad \Longrightarrow \quad \tilde{\Psi}^\dagger_{k\sigma} = \begin{pmatrix} U^\dagger & 0 \\ 0 & U^T \end{pmatrix}\Psi^\dagger_{k\sigma}, \tag{C.8}$$

and after the transformation the lead Hamiltonian becomes

$$H_{LR} = \frac{1}{2}\sum_{k\sigma}\tilde{\Psi}^\dagger_{k\sigma}\begin{pmatrix} \xi_k\sigma_0 & -\sigma\Delta\mathbf{V} \\ -\sigma\Delta\mathbf{V}^\dagger_0 & -\xi_k\sigma_0 \end{pmatrix}\tilde{\Psi}_{k\sigma} \tag{C.9}$$

with

$$\mathbf{V} = \begin{pmatrix} \cos^2(\theta) + e^{i\phi}\sin^2(\theta) & -i\sin(\phi/2)\sin(2\theta) \\ -i\sin(\phi/2)\sin(2\theta) & \cos^2(\theta) + e^{-i\phi}\sin^2(\theta) \end{pmatrix}. \tag{C.10}$$

For $\phi = 0$ where $\mathbf{V}$ is just the identity matrix, the even and odd channels are uncoupled, but for $\phi \neq 0$ this is not the case, and they are mixed in a nontrivial manner. From this calculation we have learned that the problem at hand is a two-channel problem, which explains the two different energy bands. The bound state energies $E_{+\sigma}$ originate from one channel and $E_{-\sigma}$ originate from the other. For $\phi = 0$ only one channel is involved in the formation of bound states - namely the even one, which appears in the cotunneling term. For $\phi = 0$ the YSR state is still present, as it requires only a single lead to form and doesn't rely on the tunneling between the leads. We can hence interpret the bound states $E_{-\sigma}$ as the YSR-states which originate from the even sector, and the $E_{+\sigma}$ as an Andreev-like bound state arising from the odd sector, which only appears when the two sectors are coupled for $\phi = 0$, in accordance with the fact that the Andreev bound states are related to tunneling between two superconducting leads with a phase bias.

Appendix D

Error in numerical integration

In section 3.3.2 we saw that extra features which could not be explained by our analytical calculation were present in the result for the admittance found from numerical integration. Here we investigate the correspondence between the value of η and the size of the unexpected peak in order to verify that it arises due to the finite width of the spectral function for $\eta \neq 0$. We determine the height of the peak for different values of η (for a specific set of parameters where the peak was found to be prominent) and compare this with the change in height for the sharp delta peak at $\omega = E_{-\uparrow} + E_{+\downarrow}$. To check whether our suspicion that the unexpected peak specifically arises from the normal components of the spectral function being nonzero in $\omega = 0$ is correct, we also calculate $A_{LL,\uparrow\uparrow}(\omega = 0)$ for different values of η. The results are plotted in fig. D.1. Here we clearly see that when increasing the value of η, both the height of the unexpected peak and the value of the normal component of the spectral function $A_{LL\uparrow\uparrow}(\omega = 0)$ increase, and furthermore they have a similar functional dependence on η. Conversely, the height of the expected delta peak is inversely proportional to η in a double-logarithmic coordinate system, which is consistent with the fact that it arises from a Lorentzian (or more specifically, the convolution of two Lorentzians which is also a Lorentzian), which has a height of $1/\pi\eta$. Based on these considerations we conclude that the peak at $\omega = E_{\pm\sigma}$ is indeed a numerical artefact which is due to the fact that we are calculating a convolution of two functions of which one is not exactly zero in $\omega = 0$ due to the use of a finite η. Hence the features we see in the numerical calculation of $\mathrm{Re}\, Y(\omega)$ are in accordance with what we expected from the analytical calculations.

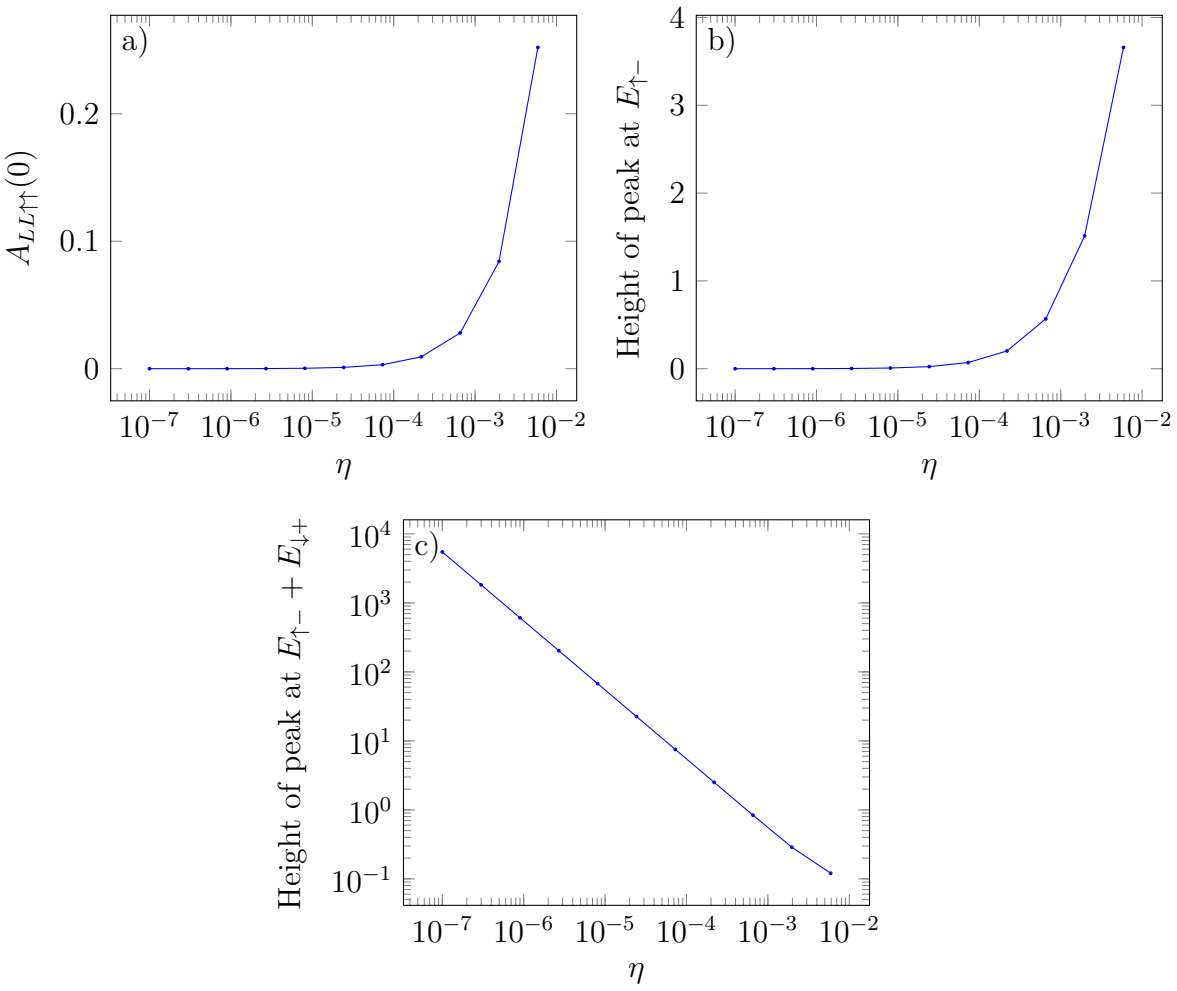

Figure D.1: Change in various quantites as η is varied. **a)** Value of the $A_{LL,\uparrow\uparrow}-$component of the spectral function in $\omega = 0$. **b)** Height of unexpected peak at the position of the smallest bound state energy. **c)** Height of $\delta-$peak in the admittance predicted by the analytical calculation.